DOE-ET-53088-190 IFSR#190

HIGH ENERGY PLASMA ACCELERATORS

T. Tajima*
Institute for Fusion Studies
The University of Texas at Austin
Austin, Texas 78712

*also Dept. of Physics

May 1985

HIGH ENERGY PLASMA ACCELERATORS

T. Tajima
Department of Physics and Institute for Fusion Studies
The University of Texas, Austin, Texas 78712

TABLE OF CONTENTS

ABSTRACT

Colinear intense laser beams ω_0, k_0 and ω_1, k_1 shone on a plasma with frequency separation equal to the electron plasma frequency ω_{pe} are capable of creating a coherent large longitudinal electric field $E_L = mc\,\omega_{pe}/e$ of the order of 1GeV/cm for a plasma density of 10^{18} cm^{-3} through the laser beat excitation of plasma oscillations. Accompanying favorable and deleterious physical effects using this process for a high energy beat-wave accelerator are discussed: the longitudinal dephasing, pump depletion, the transverse laser diffraction, plasma turbulence effects,

self-steepening, self-focusing, etc. The basic equation, the driven nonlinear Schrödinger equation, is derived to describe this system. Advanced accelerator concepts to overcome some of these problems are proposed, including the plasma fiber accelerator of various variations. An advanced laser architecture suitable for the beat-wave accelerator is suggested. Accelerator physics issues such as the luminosity are discussed. Applications of the present process to the current drive in a plasma and to the excitation of collective oscillations within nuclei are also discussed.

I. INTRODUCTION

It is becoming clearer that extrapolation of the present high energy accelerator is not enough to meet today's challenge (Salam, 1983) of ultra-high energies. Apart from cosmical acceleration (Fermi, 1949; McMillan, 1950; Kolomenskii et al., 1963; Tajima and Sakai, 1985), we may be able to make some statements with regard to terrestrial acceleration of particles to very high energies. Supposing that we try to achieve energies of 100 to 1000 TeV within a reasonable physical size (i.e., for example, within a state), we realize that the necessary electric (magnetic) field to accelerate (contain) particles is so large that under the present technology no metallic surface would withstand such a huge electric field and no cost-effective magnets are available for such an intense magnetic field. For example, an electric field of 0.1 GeV/cm (rf or dc) corresponds to 1 eV/Å and thus severely modifies the electron wavefunction within the atom, leading to sparking, breakdown, etc. Besides this difficulty, the surface heating contributes another cause of breakdown with high field. Another point in considering an accelerator for very high energies immediately becomes evident. Since the particles accelerated are at such a high energy that they travel with a velocity very close to the speed of light c, the phase velocity of the accelerating structure (electrostatic or electromagnetic) must also be very close to the speed of light c.

Besides these fundamental physics requirements, we have to consider available technologies for achieving high energies. In looking at various electromagnetic power generation techniques, we

find that the most intense fields are delivered by the laser technology at present, although this does not preclude other technologies in the future. [There have been many ideas using lasers for acceleration, including those of Palmer (1972); Willis (1975, 1977), Hora et al., (1982) etc.; see also Channel (1982)] For example, millimeter wavelengths may be provided by the free-electron laser or gyrotron-type maser. The tendency toward a much shorter wavelength of accelerating structure than the present microwave technology is due to the available high field values in the shorter electromagnetic wave generation techniques. Very roughly speaking, it seems that various available state-of-the-art technologies of short wavelength electromagnetics tend to progress in line with the boundary characterized that the field amplitude squared times the wavelength squared (i.e., the power) is invariant. Shorter wavelengths may also be favored if we have to deal with a tiny structure or bunch of fields and particles, because the design of finer structure design of fields is possible with shorter wavelengths. This becomes clearer when we consider the luminosity of the particle beams. From Heisenberg's uncertainty principle, $\Delta E \Delta t \gtrsim \hbar$, the cross-section σ of particle reaction at $\Delta E \to \infty$ is proportional to E_{cm}^{-2}, where E_{cm} is the energy of the particle at the center-of-the-mass. Because of this, the cross-section becomes smaller and smaller at higher energy. This means that the luminosity has to increase as E_{cm}^{2} in order to keep the number of events in unit time constant. This puts a very stringent condition on the accelerator concept at high energies. As the individual partaicle energy goes up with the total energy

and the luminosity kept constant, we have to have less particles packed in tiny beams which have to be narrowly focused. This again points to the laser technology.

A particle in an electromagnetic field of small amplitude is accelerated perpendicular to the direction of this electromagnetic wave $\underset{\sim}{k}$ and executes oscillations along the electric field direction $\underset{\sim}{E}$. No net acceleration, therefore, is achieved (Kaw et al., 1973; Kibble, 1966; Schmidt et al., 1973). This holds true even if the electromagnetic field amplitude is large and there is magnetic acceleration (see Fig. 1). The magnetic acceleration with the electric acceleration makes the particle execute a figure-eight orbit with no net acceleration. A spatially or temporally localized packet of electromagnetic waves cannot cancel all the oscillatory motion and thus leaves a net acceleration (Chan, 1971; Lai, 1980), but the amount of acceleration remains small. It is important to note, however that the figure-eight orbit has a component of longitudinal motion (see Fig. 1b). The case of ultra-relativistic waves in this connection is discussed in Section IV.

In the present article we review basic principles of the laser driven beat-wave accelerator (Tajima and Dawson, 1979b) only to an extent necessary to introduce new and more advanced concepts and developments. In this sense the paper does not intend to cover all the related literatures of plasma collective accelerators, but rather focus on or around the author's activities that led to the important recent developments. This includes the basic beat-wave accelerator concept, in-depth analysis of it, and new advanced

concepts stemming from this, various considerations of accelerator physics, laser physics, plasma physics, and high energy physics issues that arise in this concept. The weaving theme of the present paper is the process of collective excitation of eigenmodes of a nonlinear physical system by a drive such as beat of laser beams, be it for the excitation of a plasma wave for acceleration, for the current drive for tokamak plasmas, or for the excitation of nuclear collective oscillations such as quark-gluon plasma oscillations.

There have been many attempts to gain net acceleration by electromagnetic waves, which may be categorized into two types: the virtual photon approach and the real photon approach. Most of the conventional accelerators including (proposed) collective accelerators are in the first category. Consider Fig. 2a. In order to obtain an electric field component parallel to the wave propagation $k_{\parallel}$, some (metal) reflector is placed. The wave has $E_{\parallel}$ component, but unfortunately the phase velocity of the wave is larger than the speed of light $\omega/k_{\parallel} > \omega/k = c$. Thus no coupling. One may confine the electromagnetic field by two conductors in a waveguide (Fig. 2b) instead of the semi-infinite case in Fig. 2a. The characteristics of wave phase velocity of a waveguide are well-known (see Fig. 2c). The phase velocity is always larger than c: $v_{ph} = c\left(1 - (\omega_c/\omega)^2\right)^{-1/2}$ where ω_c is the cutoff frequency for the waveguide. An accelerator such as SLAC's alleviates this problem by implementing a periodic structure in the waveguide (irises). A periodically rippled waveguide introduces the so-called Brillouin effect into the phase velocity

characteristics. The Brillouin diagram for the frequency vs wavenumber in the ripple waveguide is shown in Fig. 2d. Here sections of phase velocity less than c are realized. There are other ways to make phase velocity less than c, such as dielectric coating. All these techniques may be collectively called a technique for slow-wave structure. Particles can now surf on such field crests and obtain net acceleration. The intensity of the fields is limited by materials considerations such as electric breakdowns. Almost invariably, the localized high electric field results at and near the slow-wave structure, making the breakdown easier there. We suggest that it may be possible to create a slow-wave structure in the form of a plasma waveguide (or plasma "optical fiber"). A narrow waveguide with rippled surface accentuated either by a plasma or by plasma and magnetic fields (see Fig. 3) provides a slow-wave structure. In this slow-wave structure the particles may be able to surf on the electromagnetic wave.

When we utilize the real photon in a plasma, there is no physical limitation due to materials considerations. The characteristics of the phase velocity of the real photon in a plasma are similar to those in a waveguide (see Fig. 2e). The phase velocity of the electromagnetic wave in a plasma is $v_{ph} = c(1 - (\omega_p/\omega)^2)^{-1/2}$, always larger than c in an underdense plasma, indicating again the difficulty of directly coupling the wave to accelerate electrons. Here ω_p is the plasma frequency. It is possible, however, to couple the electromagnetic waves nonlinearly to the plasma if the amplitudes of the electromagnetic

waves are sufficiently large. We have discussed (Tajima and Dawson, 1979a, 1979b, 1981) a laser electron accelerator scheme based on exciting a large-amplitude Langmuir wave created either by a strong photon wavepacket with a very short spatial pulse length as a photon wake or by two beating photons. We concluded (Tajima and Dawson, 1981) that using two photon beams is much more effective in acceleration than using a very short photon pulse. We focus primarily on the two-beam case, although the physics involved in the case of the short wavepacket has much in common with this case. This statement, however, may change with the introduction of idea of the photon wake accelerator [see Sec. II and Fig. 9(b)].

The basic mechanism of particle acceleration is as follows. The two injected laser beams induce plasmons (or a Langmuir wave) through the forward Raman scattering process. This may be regarded as optical mixing. The resultant large-amplitude plasma wave with phase velocity very close to the speed of light grows and is sustained by the laser lights. It grows until the amplitude becomes relativistic, i.e., the quivering velocity of the electrostatic field becomes c (or of the order of c) so that the wave begins trapping electrons in the tail of distribution. When the injected electromagnetic waves are nonrelativistic i.e., their quivering velocities are less than c, the electrostatic wave saturates before this mechanism sets in. A detail will be discussed in Sec. VI. If the quivering velocity of the electrostatic wave reaches c, the bulk electrons begin to be trapped. Since the plasma is underdense, the phase velocity of the electrostatic wave is very close to c. Since the energy

dependence of the accelerated electron velocity is nonlinear, the detrapping time of electrons is long. This is a significant advantage of linear acceleration of this type compared with that in a circular machine. In a circular machine such as a buncher, the energy dependence of the electron angular velocity is approximately linear (Vomvoridis et al., 1983). Thus the detrapping time is much shorter for the latter.

II. PLASMA BEAT-WAVE ACCELERATOR

The plasma beat-wave accelerator concept using an intense laser potentially meets the afore-mentioned challenge and requirements for acceleration of particles to ultra-high energies. Two laser beams of frequency and wavenumber ω_0, k_0 and ω_1, k_1, whose frequency separation $\omega_0 - \omega_1$ is equal to the plasma frequency ω_p, are capable of inducing a large-amplitude electrostatic plasma wave through the Raman process. This electrostatic plasma wave amplitude eventually reaches a value of $E_L \simeq m\omega_p c/e$ as a result of the Raman instability if the laser amplitude E_1 is a noise or the pump amplitude $E_1 < m\omega_1 c/e$. The electrostatic wave amplitude quickly reaches a value of $E_L \simeq m\omega_p c/e$ when E_0 and E_1 are $\sim m\omega_0 c/e$. This is because of the ponderomotive force (see Fig. 4)

$$\nabla(e^2 \underset{\sim}{E}_0 \cdot \underset{\sim}{E}_1/m\omega_0\omega_1) = eE_L(x) = e(m\omega_p c/e)e^{ik_p x} \qquad (1)$$

is equivalent to having the longitudinal electric field E_L of size $m\omega_p c/e$ in the latter case.

Consider two large-amplitude traveling electromagnetic waves, (ω_0, k_0) and (ω_1, k_1), injected in an underdense plasma, which induce a plasma wave $(\omega_p, k_0 - k_1)$ through the beating of two electromagnetic waves if the frequency separation of the two electromagnetic waves is equal to the plasma frequency:

$$\omega_0 - \omega_1 = \omega_p \ , \tag{2}$$

$$k_0 - k_1 = k_p \ , \tag{3}$$

where k_p is the wavenumber of the plasma wave. The beat of the two electromagnetic waves gives rise to a nonlinear ponderomotive force, Eq. (1), which sets off the plasma oscillations (Tajima and Dawson, 1979a, 1979b). This process may also be regarded as a nonlinear optical mixing (Kroll et al., 1964) as well as a forward Raman scattering (Joshi et al., 1981; Shen et al., 1985; Tajima et al., 1979b). It may be possible to achieve the objective through the forward Raman instability (Joshi et al., 1981), i.e., the second electromagnetic wave (ω_1, k_1) grows from a thermal noise. Rosenbluth et al. have discussed plasma heating via the beat of the electromagnetic wave (Rosenbluth and Liu, 1972; Cohen et al., 1972). It is important that the plasma be sufficiently underdense so that ω_0 is much larger than ω_p (see Fig. 5). This will ensure that the phase velocity of the plasma wave v_p is very close to the speed of light:

$$v_p = \frac{\omega_p}{k_p} = \frac{\omega_0 - \omega_1}{k_0 - k_1} \ . \tag{4}$$

In the limit of $\omega_p/\omega_0 \ll 1$, Eq. (4) yields

$$v_p = \frac{\omega_p}{k_p} = \lim_{\omega_p/\omega_0 \to 0} \frac{\omega_0 - \omega_1}{k_0 - k_1} = v_g^{EM} = c\left(1 - \frac{\omega_p^2}{\omega_0^2}\right)^{1/2}, \quad (5)$$

the relation we used previously (Tajima and Dawson, 1979b).

Suppose that ω_0 is not very much larger than ω_p, then the phase velocity of the plasma wave is much less than c. The resultant plasma wave can quickly trap electrons and saturates. In the course of interaction the nonlinear effects may change the phase velocity of the plasma wave. Thus, in the case of ω_p/ω_0 not small, the interaction of light waves and plasma is strong, and the light waves suffer strong feedback from the plasma. (The light waves may be called "plastic" or "soft" in this case.) The electron ring accelerator by Veksler (1956), the Cerenkov-plasmon accelerator (Budker 1956), and the beam front accelerator (Poukey and Rostoker, 1971; Tajima and Mako, 1978; Mako and Tajima, 1984), for example, may be classified as using the soft photon approach.

The present mechanism calls for a highly underdense plasma $\omega_p/\omega_0 \ll 1$, which guarantees that laser beams reinforce the plasma wave structure. Such reinforced accelerating structure is necessary, because the acceleration to multi-TeV energies should take a large distance without too many adverse effects or interruption of acceleration. As we shall see later, the ratio of the energy density of the electrostatic plasma wave to that of the electromagnetic wave is $\sim(\omega_p/\omega_0)^2$ as a result of the Manley-Rowe (1956) relation, i.e., the light wave dominated. Therefore, the

plasma wave remains reinforced or "regulated" by the two beating laser beams $\omega_0 = k_0 c/\sqrt{1-\omega_p^2/\omega_0^2} \sim k_0 c$, $\omega_1 = k_1 c/\sqrt{1-\omega_p^2/\omega_1^2} \simeq k_1 c$. (The light waves may be called "hard" in our case.) Since the phase velocity v_p is very close to c for $\omega_p/\omega_0 \ll 1$, the electron trapping and, therefore, saturation, occur only when the electrostatic wave grows up to an amplitude so large that it becomes relativistic. The other important consequence of $\omega_p/\omega_0 \ll 1$ is that particles will be in phase with the plasma wave for a long time and achieve a large amount of acceleration, because, again, the phase velocity $v_p \sim c$ and the particles would not exceed v_p easily.

Let us consider the energy gain of an electron trapped in the electrostatic wave with phase velocity $v_p = \omega_p/k_p$. We go to the rest frame of the photon-induced longitudinal wave (plasma wave). Since the wave has the approximate phase velocity given in Eq. (5), $\beta = v_p/c$ and $\gamma = \omega_0/\omega_p$. Note that this frame is also the rest frame for the photons in the plasma: in this frame the photons have no momentum and the photon wavenumber is zero. The Lorentz transformations of the momentum four-vectors for the photons and the plasmons (the plasma wave) are

$$\begin{pmatrix} \gamma & i\beta\gamma \\ -i\beta\gamma & \gamma \end{pmatrix} \begin{pmatrix} k_0 \\ i\omega_0/c \end{pmatrix} = \begin{pmatrix} 0 \\ i\omega_p/c \end{pmatrix}, \tag{6}$$

$$\begin{pmatrix} \gamma & i\beta\gamma \\ -i\beta\gamma & \gamma \end{pmatrix} \begin{pmatrix} k_p \\ i\omega_p/c \end{pmatrix} = \begin{pmatrix} k_p/\gamma \\ 0 \end{pmatrix}, \tag{7}$$

where the right-hand side refers to the rest frame quantities with respect to the plasma wave ($k_p^{wave} = k_p/\gamma$), k_0 is the photon wavenumber in the laboratory frame, and the well-known dispersion relation for the photon in a plasma $\omega_0 = (\omega_p^2 + k_0^2c^2)^{1/2}$ was used. Equation (6) is reminiscent of the relation between the meson and the massless (vacuum) photon (Yukawa, 1935). Eq. (6) indicates that the photon in the plasma (dressed photon) has rest mass ω_p/c, because the electromagnetic interaction shielded by plasma electrons can reach only the collisionless skin depth c/ω_p in the plasma. This is just as the nuclear force reaches the inverse of the meson mass, and Yukawa (1935) predicted the meson energy as $\omega = (c^2/a^2 + k^2c^2)^{1/2}$, where a is the nuclear interaction radius. Compare:

<Meson> (interaction length a)	<Vacuum Photon> (interaction length ∞)
$\omega = \left(\frac{c^2}{a^2} + k^2c^2\right)^{1/2}$	$\omega = kc$

<Photon in Plasmas> (interaction length c/ω_p)	<Vacuum Photon> (interaction length ∞)
$\omega = \left(\omega_p^2 + k^2c^2\right)^{1/2}$	$\omega = kc$.

At the same time, the Lorentz transformation gives the longitudinal electric field associated with the plasmon as invariant ($E_L^{wave} = E_L$). We note here that the plasma frequency really plays the role of the rest mass in the sense that the plasma frequency ω_p is invariant under the Lorentz transformation. One way to look at this is to Lorentz-transform the plasma density $n' = \gamma n$ and the electron mass $m' = \gamma m$. In doing so, the plasma frequency $\omega_p = (4\pi e^2 n/m)^{1/2} = (4\pi e^2 n'/m')^{1/2}$ remains invariant.

The electrostatic wave amplitude can be evaluated in a few different (independent) ways yielding the same result. Previously (Tajima and Dawson, 1979b) we used an argument resorting to the wave breaking limit. Here let us discuss it in terms of the available electron density. When most of electrons are bunched as a result of the beat electromagnetic waves, we may estimate the electrostatic field by assuming that most of the electrons give rise to this field:

$$\nabla \cdot \underline{E} = -4\pi en \quad \text{or} \quad -k_p E_L = -4\pi en \qquad (8)$$

where n is the electron density. The maximum electrostatic field is, therefore,

$$E_L = m\omega_p c/e \qquad (9)$$

We may derive the maximum electrostatic field, Eq. (9), by another method. As we shall discuss in Section III, the electrostatic wave saturates only when the trapping width of the wave becomes wide enough to begin trapping the tail of electrons. This condition may be written as

$$v_p - v_e \lesssim v_{tr} = \left(\frac{eE_L}{m\omega_p} v_p\right)^{1/2}, \qquad (10)$$

where v_e is the electron thermal velocity. If we neglect v_e in comparison with v_p and approximate v_p by c, then Eq. (10) yields Eq. (9). Yet another method for obtaining Eq. (9) was discussed in association with the ponderomotive force, Eq. (1).

The condition (9) is valid even if the trapped electrons are highly accelerated as long as the bulk of electrons remain nonrelativistic. However, when the bulk of electrons obtain kinetic energy, say perpendicular energy, then the formula needs corrections (Sullivan et al., 1981; Tang et al., 1984). When the effects of relativistic mass change or heating of electrons are taken into account, mismatching of conditions (2) and (3) arises, and we need more detailed study on the attainable electric field in

this case Rosenbluth and Liu (1972) and more recently Tang et al. (1984) and Horton and Tajima (1985a) studied this problem. The nonlinear saturation due to the relativistic mass and subsequent detuning gives the saturated electric field at $\Delta\omega = \omega_0 - \omega_1 = \omega_p$ as

$$E_L = \frac{m\omega_p c}{e} \left(\frac{16}{3} \frac{eE_0}{m\omega_0 c} \frac{eE_1}{m\omega_1 c}\right)^{1/3} . \tag{11}$$

The electric potential due to the plasma wave evaluated in the laboratory frame is

$$e\varphi = e\int_0^{\lambda} E_L dx = e \frac{m\omega_p c}{e} \left(\frac{c}{\omega_p}\right) = mc^2 . \tag{12}$$

Going to the wave frame, we obtain the potential in the wave frame

$$e\varphi^{wave} = \gamma e\varphi = \gamma mc^2 . \tag{13}$$

This energy in the wave frame corresponds to the laboratory energy by the Lorentz transformation

$$\begin{pmatrix} \gamma & -i\beta\gamma \\ i\beta\gamma & \gamma \end{pmatrix} \begin{pmatrix} \gamma\beta mc \\ i\gamma mc^2 \end{pmatrix} = \begin{pmatrix} 2\gamma^2\beta mc \\ imc\gamma^2(1 + \beta^2) \end{pmatrix}, \tag{14}$$

where the right-hand side refers to the laboratory frame

quantities. Thus we obtain the maximum energy electrons can achieve by the plasma wave trapping as

$$W^{max} = \gamma^{max} mc^2 = 2\gamma^2 mc^2 = 2\left(\frac{\omega_0}{\omega_p}\right)^2 mc^2 \quad (15)$$

The time to reach energies of Eq. (15) may be given by

$$t_a \simeq W^{max}/ceE_L = 2\left(\frac{\omega_0}{\omega_p}\right)^2/\omega_p \quad (16)$$

and the length of acceleration to reach the Eq. (15) energy as

$$\ell_a \simeq 2\omega_0^2 c/\omega_p^3 \quad (17)$$

For a glass laser of 1-μ wavelength shone on a plasma of density 10^{18} (10^{19}) cm^{-3}, it would require under the present mechanism a power of $< 10^{18}$ (10^{18}) W/cm^2 to accelerate electrons to energies W^{max} of 10^9 (10^8) eV over a distance of 1 (0.03) cm with a longitudinal field E_L of 10^9 (3×10^9) V/cm. For a CO_2 laser of 10-μ wavelength, these numbers scale accordingly.

To demonstrate the present mechanism for electron acceleration, we have carried out computer simulations employing a $1\frac{2}{2}$ - D (one spatial and three velocity and field dimensions) fully self-consistent relativistic electromagnetic code (Lin et al., 1974). Two parallel electromagnetic waves (ω_0, k_0) and (ω_1, k_1) are imposed on an initially uniform thermal electron plasma. The direction of the photon propagation as well as the allowed spatial

variation is taken as the x-direction. The system length is $L_x = 1024\Delta$, the speed of light $c = 10\omega_p\Delta$, the photon wavenumber $k_0 = 2\pi \times 68/1024\Delta$, the number of electrons 10240, and the particle size 1Δ with a Gaussian shape, and the ions are fixed and uniform, where Δ is the grid spacing. The thermal velocity $v_e = 1\omega_p\Delta$. The photon frequencies are taken as $\omega_0 = 4.29\omega_p$ and $\omega_1 = 3.29\omega_p$, while the amplitudes are $v_i \equiv eE_i/m\omega_i = c$ ($i = 0$ or 1).

Figure 6 shows the phase space of electrons accelerated by the beat plasma wave $k_p \simeq \omega_p/c$. High energy electrons are seen in every ridge of each length of the resonantly excited electron plasma wave. The horizontally stretched arms in Fig. 6a are separated by a length $\lambda = 2\pi/k_p$. The maximum electron energy was $85mc^2$ in this case, higher than the value given by Eq. (15). One reason for this discrepancy may be that we now have two intense electromagnetic waves so that magnetic acceleration associated with $v_0 \times B_1$ and $v_1 \times B_0$ also begins to play a role. The distribution function $f(p_\parallel)$ or $f(\gamma_\parallel)$ is shown in Fig. 6b, exhibiting strong main body heating as well as a high energy tail. The electrostatic field profile in space at $t = 77\omega^{-1}$ (an early time) is shown in Fig. 7b. The field amplitude already reached $E_x \simeq E_L = m\omega_p c/e$. One can also see its coherent field pattern. The observed wavelength is $2\pi/k_p = 2\pi/(k_0 - k_1)$.

The second case is that of injection of a wavepacket of a single photon (ω_0, k_0), whose packet length $L_t = \lambda/2 = \pi c/\omega_p$, as discussed previously (Tajima and Dawson, 1979a, 1979b). The photon packet of half the plasma wavelength acts just like a hammer to resonantly excite the plasma wave. The plasma wave will be excited

in the wake of the photon "bullet". If the photon "bullets" are repeated at a right interval, such as at every $2\pi n\omega_p^{-1}$ time where n is an integer, the growth of the plasma wave as a wake of photon bullets should be much more effective. To produce such a syncopated laser beam, a fast rotating (or other type of) mirror or shutter/filter may be employed. This idea of inducing wake plasmons by the photon packet is somewhat similar to the idea of inducing Cherenkov plasma waves by a relativistic electron beam pulse proposed by Budker (1956). An extension of this idea and that of Budker's has been considered by Chen et al. (1985) and by Ruth et al. (1985). Using the same code with parameters $L_x = 512\Delta$, $c = 5v_e$, photon wavenumber $k_0 = 2\pi/15\Delta$, number of electrons 5120, $eE_0/m\omega_0 = eB_0/m\omega_0 = c$, $L_t = \pi c/\omega_p$, $p_0 = eE_0/\omega_0$, and $\omega_0 = (\omega_p^2 + k_0^2c^2)^{1/2}$, we start the system with electromagnetic pulse in the plasma with initial conditions $E_y = E_0 \sin k_0(x - x_0)$, $B_z = B_0 \sin k_0(x - x_0)$. $p_y = p_{thermal} + p_0 \cos k_0(x - x_0)$, for the period of $x = [50\Delta, 81.4\Delta]$ and $x_0 = 50\Delta$. With the assignment, the wavepacket has a spectrum in k with a peak around $k = k_0$ and $\omega = (\omega_p^2 + k_0^2c^2)^{1/2}$, and propagates in the forward x-direction approximately retaining the original polarization. Figure 8 shows an early stage of the system development. The phase-space plot (p_y vs. x in Fig. 8b) indicates a strong modulation in the p_y distribution within the photon packet location. The kink structure extends beyond the packet ending. Figure 8a shows p_x vs. x. The intense longitudinal momentum oscillations are clearly appearing, beginning at the photon packet and extending to its initial starting point. This is the wake plasma wave set off by the photon

packet seen in Fig. 8b. As in Fig. 7, the long stretching arm-like phase-space pattern (Fig. 8a) appears with its momentum keeping increasing. The wake plasmon structure is also apparent in the longitudinal fields (Fig. 8c). A schematic mechanism of charge separation due to the photon wavepacket is shown in Fig. 9. In this case the electrostatic field reaches values around $E_L \sim 0.6\ mc\omega_p/e$. This value as well as $E_L \sim 0.7 m\omega_p c/e$ for the Fig. 7 case should be compared with theoretical values of Eqs. (9) and (11). In Fig. 10 we plot the maximum electron energy observed in our simulations as a function of $(\omega_0/\omega_p)^2$. The prediction Eq. (14) is drawn as a solid line to compare with the simulation values. Agreements are reasonable.

III. FORWARD RAMAN INSTABILITY AND WAVE STEEPENING

We study the spectral distribution of photons and plasmons in time during the process of inducing the plasma beat-wave. This casts light on underlying nonlinear processes of the electromagnetic waves and the electrostatic waves. From the simulation run with two photons (ω_0, k_0) and (ω_1, k_1) that we discussed in Section II we observe in Fig. 11 a clear-cut energy cascade via multiple Raman forward scattering. Some of the statistical properties of this cascade are discussed in Section VIA. The original waves with equal amplitude $E_i = mc\omega_i/e$ ($i = 0$ or 1) cascade toward smaller k as seen in Figs. 11a and 11b. A smaller amount of energy is up-converted. The spectrum is sharply peaked at a particular discrete wavenumber $k_n = k_0 - nk_p$ where n is an integer. The spectral intensity $S(k,\omega)$ for the electrostatic

component shows an overwhelming peak at $k = k_p$ and no significant energy in any frequency at the backscatter wavenumbers. This strongly suggests that all possible backscattering processes are suppressed or saturated at a very low level in our present problem. An example is shown in Fig. 12 with parameters being $v_{os}^{(i)}/c = 0.5(i=1,2)$, $c = 9.99$, $L_x = 1024$, $v_e = 0.3$, $k_1 = 2\pi\times 68/1024\Delta$, and $k_2 = 2\pi\times 51/1024\Delta$. Ions are immobile. Figure 12 shows $|E_L(k;\ t=60\omega_p^{-1})|^2$ vs. the wavenumber k. Around time $t = 60\omega_p^{-1}$ the electrostatic energy peaked. In Fig. 12 we plotted this in ℓn–ℓn scales: it seems to fit $|E(k)|^2 \sim \exp(-\beta n k_p)$, where n is the harmonic number. This implies that a simple explanation of higher harmonics of plasma waves by wave steepening via conversion of the sinusoidal oscillations in the Lagrangian frame to the Eulerian frame may be responsible for the higher harmonic generation, because this conversion (Jackson, 1960) produces higher harmonic contentes whose amplitude is proportional to $(\omega_p\xi_0/c)^n$ in the regime $(\omega_p\xi_0/c) << 1$, where ξ_0 is the amplitude of the displacement $\xi_0 = E_{L0}/(4\pi ne)$. This is because the finite amplitude wave steepens in the Eulerian frame (in the laboratory frame). According to O'Neill et al. (1971), however, when the trapping of electrons begin, the exponential spectrum ceases to exist, but instead a power law dependence begins to manifest itself. In our simulation certainly a formation of relativistic electron tongues is observed but not the O'Neil et al., type nonrelativistic trapping. The electrostatic spectral density $S(k,\omega)$ shows peaks at $k = k_p$, $\omega = \omega_p$ as well as $k = nk_p$, $\omega = n'\omega_p$ $(n' \leqslant n)$. More details will be reported later elsewhere (Tajima and Sudan, 1985). All

these observations confirm that the downward photon cascade is due to the multiple forward Raman scattering.

A similar downward photon cascade is observed in the case with a photon packet of one laser wave (ω_0, k_0). Figure 13 shows the wavenumber spectrum of the electromagnetic pulse at successive times. The original smooth-shaped spectrum evolves into a multipeak structure with a roughly equal, but slightly increasing, separation in wavenumber as k approaches k_p. This again indicates that the photon (ω_0, k_0) decays into (ω_1, k_1), (ω_2, k_2), ... by successive or multiple forward Raman instability.

The reason why the backscattering is suppressed but the forward scattering is very prominent is the following: when the backscattering plasma wave is excited, enhanced Landau damping (Dawson and Shanny, 1968; Leboeuf and Tajima, 1979a, 1979b) or electron trapping by this plasma wave saturates the plasma wave at a low level, thus limiting the backscattering to a small value. The wavenumber k_b of the plasma wave produced by the backscattering process in the case of $\omega_p/\omega_0 << 1$ is $k_b = 2k_0$. The phase velocity of the backscattering plasma wave is

$$v_p = \frac{\omega_p}{2k_0} = \frac{c}{2}\frac{\omega_p}{\omega_0} \qquad (18)$$

Trapping of electrons by this wave begins happening when the trapping width v_{tr} becomes wide enough to reach the tail of the thermal electron distribution. An approximate trapping width may be written as

$$v_{tr} = \left(\frac{e\varphi^b}{m}\right)^{1/2} = \left(\frac{eE_L^b}{m\omega_p} v_p\right)^{1/2} , \tag{19}$$

where the superscripts b refer to the backscattering electrostatic wave. See Fig. 14. [Sometimes v_{tr} is defined as $\sqrt{2}$ times the value of Eq. (19)]. The formula is nonrelativistic, but is sufficient for the present purpose. Also recall the discussion given after Eq. (11). The condition that a large number of electrons are trapped is given (Dawson and Shanny, 1968) by

$$v_p - v_{tr} \leq 2v_e = 2(T_e/m)^{1/2} . \tag{20}$$

The maximum electrostatic wave amplitude is obtained for a cold plasma by setting $v_e = 0$:

$$\frac{eE_L^b}{m\omega_p} = \frac{c}{4}\frac{\omega_p}{\omega_0} . \tag{21}$$

In the cases of both Fig. 11 and Fig. 13 we did not detect a large peak of electrostatic spectrum $S(k,\omega)$ at $k = 2k_0$ that is a signature of backscattering plasmons. Thus the forward Raman process appears to be the last parametric process to saturate in a hot underdense plasma. In fact it can be argued that it will saturate only when the original electromagnetic wave has completely cascaded by multiple forward Raman process to waves near $\omega \sim \omega_p$. In this case most of the electromagnetic energy may be extracted

from the laser lights to electrostatic wave energy and eventually to kinetic energy. The idealized efficiency, therefore, may be given by $\eta = 1 - (\omega_p/\omega_0)^2$.

An experimental observation of the forward Raman instability and associated electron acceleration and heating has recently been done (Joshi et al., 1981) in conjunction with the present concept and physical discussion. A CO_2 laser is shone on an underdense plasma producing electrons of energy up to 1.4 MeV. The laser power density is such that $eE_0/m\omega_0 c \sim 0.3$ and the frequencies are $\omega_p/\omega_0 \sim 0.46$. The plasma was created by the laser light shone on 130-Å-thick carbon foil producing the initial plasma temperature of ~20 keV. In the experiment the laser emits only one beam so that the beat has to grow from the noise. It is, therefore, in general, possible to have other competing processes such as side scatter, backscatter, and two-plasmon decay simultaneously taking place. In spite of these competing processes, lower quivering velocity of the laser, and lower ω_0/ω_p, the experiment shows (Joshi et al., 1981) high energy electrons in the forward direction.

Simulations are carried out in order to see the wave spectrum and to compare the distribution function of electrons with the experiment. Using a similar setup as before, we set the plasma parameters the same as in the experiment (Joshi et al., 1981): $T_e \sim 20$ keV; uniform plasma, $\omega_p/\omega_0 \sim 0.46$; and the propagating electromagnetic wave having $eE_0/m\omega_0 c \sim 0.3$. The electron parallel distribution function $f(p_\parallel)$ along with the electrostatic wave spectra are displayed in Fig. 14. The temperature and the maximum electron energy observed in the simulation distributions are

similar to the experimentally measured values. For example, simulations show the forward electron maximum energy as 1.3 MeV and temperature as 100 keV in comparison with the experimental values of 1.4 MeV and 90 ~ 100 keV, respectively. In the backward direction, simulations show the electron maximum energy as 0.9 MeV and temperature as 60 keV compared with the experimental values of 0.8 MeV and 40 ~ 50 keV. The electrostatic wave spectrum, Fig. 15b, shows that the backscattering mode k_b (which grows initially) is swamped by other modes with a smaller wavenumber, the most intense of which is the plasma wave associated with forward scattering k_p. In addition, there are some wavenumbers which are less than k_p. Thus the heated electron distributions obtained by experiment and by simulations agree well with most of the electron heating due to the forward Raman instability, but not so much due to the backward process. In the present case the phase velocity of the backscattering plasma wave $\omega_p/k_b \sim 1.6v_e$. Thus this wave is heavily Landau damped to begin with, and, as it grows in amplitude, more and more electrons will be trapped by it, and the damping will grow. In view of Eq. (20), therefore, the experimental as well as the simulation results are reasonably well understood.

Recently Joshi (1985) reported an experiment done by his group in which CO_2 laser beams of wavelengths 9.6 and 10.6μ were shone with intensities such that $(v_{os}/c)_{10.6} \simeq 0.03$ and $(v_{os}/c)_{9.6} \simeq 0.015$ on a plasma of density $\sim 10^{17} cm^{-3}$. They have detected the creation of beat-wave, its wave frequency, wavenumber spectrum, and cascades in frequencies in agreement with the theoretical prediction (Tajima and Dawson, 1979b). The measured

longitudinal electric field was ≃1GeV/m confirmed from the Thomson scattering measurement of electron density fluctuations for the fast wave.

IV. ULTRARELATIVISTIC WAVES AND RELATIVISTIC GAS DYNAMICS

As the laser beam becomes more intense, the accelerated electrons become more numerous and they are more energetic. When the laser beam is ultrarelativistic (i.e., $eE_0/m\omega_0 c > 1$) and the laser wavepacket is localized, such a wavepacket exerts a large ponderomotive force on the plasma and can create a local vacuum (Ashour-Abdalla et al., 1981). The intense electromagnetic wave pulse pushes the plasma forward and expands the region of plasma-plowed area (vacuum or very low density plasma). Since the expanding electromagnetic pulse acts like a piston that reflects incoming particles, we can evaluate how much momentum transfer takes place during the process. Equating the electromagnetic pressure (piston pressure) to the momentum exchange by electrons which are pushed by the piston, we obtain

$$P = \frac{E_0^2}{8\pi} = nv_g p \simeq nv_g \gamma mc \ , \tag{22}$$

where v_g is the velocity of the electromagnetic wave front. From Eq. (22), the particle energy γ^{ave} is calculated as

$$\gamma^{ave} \simeq \left(\frac{c}{v_g}\right)\left(\frac{\omega_0}{\omega_p}\right)^2\left(\frac{eE_0}{m\omega_0 c}\right)^2 , \tag{23}$$

which agrees with Eq. (15) in scaling when $eE_0/m\omega_0 c = 1$. This provides one more method to derive the fundamental scaling Eq. (15).

Simulations have been performed to study this parametric dependence. Again the same type of setups as for the pulsed photon wavepacket in Sec. II and the same code are used. Parameters we use are $L_x = 10240$, $v_e = 1\ \omega_{pe}\Delta$, the initial photon wavenumber $k_0 = 2\pi/10\Delta$, $c = 5\ \omega_{pe}\Delta$, 1024Δ electrons and ions each, and $eE_0/m\omega_0 c$ is varied from 1 to 20. The packet length is chosen to be $L_t \simeq \pi c/\omega_p$. In these runs we set the ion mass equal to the electron mass with the intention of simulating highly relativistic plasmas. The obtained energy scaling is displayed in Fig. 16, showing $\gamma^{max} \propto \nu^2 = (eE_0/m\omega_0 c)^2$. The coefficient of the proportionality is also reasonably fitted with Eq. (23). In a similar study Sullivan and Godfrey (1981) also investigated the accelerated electron energy dependence on the laser field strength. When the laser intensity exceeds $eE_0/m\omega_0 = 1$, there results intense plasma heating in addition to the afore-mentioned acceleration. Heating is more intense when the mass ratio of ions to electrons becomes larger than unity. Therefore, unless a clever way to exploit the ultra-relativistic laser beam is found, too intense laser beams ($eE_0/m\omega_0 c > 1$) are rather detrimental to our purpose in terms of efficiency.

When a continuous relativistic wave is imposed upon the plasma (Leboeuf et al., 1982), the relativistic wave can generate a wind of net plasma flow in the forward direction. As we discussed in Sec. I, this does not happen when the wave amplitude is high but

non-relativistic. When the wave amplitude becomes relativistic, however, the wave severely modifies the plasma (see Figs. 1c and 17). The wave is no longer sinusoidal (Kennel and Pellat, 1976); it resembles a sawtooth in the profile of wave fields. Such a nonlinear (self-consistent) wave can carry particles with the wave. It turns out that the particle flux is as large as $\Gamma \simeq 2n_0c$ in the ultra-relativistic wave (Leboeuf et al., 1982), where n_0 is the average density of plasma electrons in the laboratory frame.

In such a relativistic and nonlinear case we learn that the group velocity of the sawtooth wave structure is the speed of the relativistic phonon phase velocity. In Fig. 17 we observe that the wave structure has a speed of $c/\sqrt{3}$. Since in the ultra-relativistic plasma the charge separation effect is less important, the phonon freedom becomes more evident. Because the energy of a relativistic particle is $\varepsilon = pc$ (Synge, 1957; Landau and Lifshitz, 1959), the pressure P of the relativistic gas is, from Eq. (22),

$$P = \frac{1}{3} n\varepsilon = \frac{1}{3} U , \qquad (24)$$

where U is the internal energy density. The sound speed c_s in a gas governed by Eq. (24) is obtained via a formula $(\partial P/\partial \rho)^{1/2}$, or

$$c_s = c \left(\frac{\partial P}{\partial U}\right)^{1/2} = \frac{c}{\sqrt{3}} . \qquad (25)$$

However, the wind generation by the relativistic wave <u>per se</u> seems

an inefficient process for high energy acceleration. The case of beat of ultra-relativistic waves has not been examined yet, since we do not know an analytic form (Decoster, 1978) of the waves for the case to start out.

A still speculative concept of the relativistic forward Brillouin scattering process in place of the forward Raman process is discussed. In this we use two laser lights with (ω_0, k_0) and (ω_1, k_1) obeying $\omega_0 - \omega_1 = \omega_{pi}$ and $\omega_{pi} = (4\pi ne^2/M)^{1/2}$. According to Eq. (1), the ponderomotive potential will force charge separation. The two intense laser beams will create electrostatic oscillations at the ion plasma frequency, which are forced oscillations (quasi-mode) in the limit of the "sound" velocity put to be the speed of light c with wavelength c/ω_{pi}. An advantage of this scheme would be that the frequency separation of two lasers and the resonant ion plasma frequency are so much smaller than the laser frequency that the phase velocity of the accelerating structure becomes very close to c. (This objective may be achieved by the Raman process by reducing ω_p/ω_0, but this leads to lower plasma density and lower accelerating field strength, in conflict with our original desire.) From our simulation we find that $E_L \sim m\omega_p c/e$. And, therefore, $e\varphi \sim (Mm)^{1/2}\ c^2$. The amplification of energy by the Lorentz transformation $2\gamma^2$ may now be given with $\gamma = \omega_0/\omega_{pi}$ as $W^{max} \lesssim 2\ (\omega_0/\omega_{pi})^2 (M/m)^{1/2}\ mc^2$.

In practice the above energy is hard to obtain. There are several complications: modes different from k_0-k_1 are excited and the electrostatic field profile is not as coherent as in the Raman process. This is perhaps due to the fact that the beat-wave is not

a natural mode of oscillation of the system. Discussion here therefore should be taken as speculative and treated with restraint. One of our preliminary studies by computer simulation is shown in Fig. 18. The parameters in the simulation are: $v_e = 1\omega_p\Delta$, $k_0 = 2\pi \times 77/1024\Delta$, $k_i = 2\pi \times 73/1024\Delta$, $M/m = 25$, $v_i = eE_i/m\omega_i = \sqrt{5}c$ for $i = 0$ and 1, $c = 9\omega_p\Delta$, $L_x = 1024\Delta$, and numbers of electrons and ions are 10240 each, and $\omega_0 - \omega_1$ is kept to be ω_{pi}. A large amount of high energy electrons in phase space are seen in this simulation.

The electrostatic wave spectrum S(k) shows a predominant peak at mode 4, which corresponds to the beat mode $\omega_{pi} = \omega_0 - \omega_1$ at an early time ($t = 60\omega_p^{-1}$; not shown here). At $t = 260\omega_p^{-1}$, the predominant mode of E_L is still at mode 4 with the magnetic wave spectrum largely intact even at this time (see Fig. 19). Later developments of acceleration and plasma responses are also shown in Fig. 19. Figure 20 shows the dispersion relations for the electrostatic branches obtained in this run. We see three major branches: the first is the relativistic electrostatic plasma oscillation $\omega \simeq (\omega_{pe}^2/\langle\gamma_\parallel\rangle + k^2c^2)^{1/2}$, the second is $\omega \sim \min(kc/\sqrt{3}, \omega_{pi})$, and the third is $\omega \sim 0$ (or purely imaginary). From our measurement, the time-averaged relativistic factors $\langle\gamma_\parallel\rangle \simeq 7.2$ and $\langle\gamma_\perp\rangle \simeq 7.5$ over a $400\omega_{pe}^{-1}$ period. Recall the equation of state for relativistic gases Eq. (24). This leads to the effective plasma frequency for $k = 0$ being $\omega \sim [\omega_{pe}^2/\langle\gamma_\parallel\rangle^3 + \omega_{pi}^2]^{1/2} \sim 0.3\omega_{pe}$. The second branch might be related to the ω_{pi} relativistic phonon branch discussed in this section. The slope of $c/\sqrt{3}$ is written in for comparison. As discussed by Synge (1957) and Leboeuf et al.

(1982), the relativistic phonon speed may vary depending on the wave profile. Thus the value of $c/\sqrt{3}$ is only for comparison. The third branch corresponds to $\omega \sim 0$ and the purely imaginary frequency. This is because the ponderomotive potential-forced mode is not the natural mode and therefore decays with a finite lifetime, corresponding to a virtual "particle." In our run we generally find that the third branch contains the largest energy.

In order to provide an eigenmode instead of a virtual mode (quasi-mode), we may impose a vertical magnetic field. When plasma electrons are sufficiently magnetized, the plasma eigenmode with the wavenumber in the direction perpendicular to the magnetic field assumes eigenfrequency of the electrostatic lower hybrid wave. The eigenfrequency is $\omega \simeq \omega_{pi}$ where the angle of propagation $\vartheta = \tan^{-1} k_{\parallel}/k$ is less than the square root of the electron-to-ion mass ratio $(m/M)^{1/2}$. In this mode electrons are essentially insulated by the vertical magnetic field. The electrostatic field will be shorted out before $E_L = B_v$, where B_v is the vertical magnetic field. In this case we should have $e\varphi \leq (\Omega_e/\omega_{pi})mc^2$ and $\gamma^{max} \leq 2(\omega/\omega_{pi})^2(\Omega_e/\omega_{pi})mc^2$. Such an accelerator concept has a benefit of less staging and less pump depletion, while the accelerating grading is less. This type of acceleration may be applicable to protons and muons.

V. PLASMA FIBER ACCELERATOR

We have introduced the concept of a laser accelerator using two parallel intense laser beams and a resultant beat plasma wave. We discussed various characteristics of this scheme and

demonstrated it via computer simulations and to a certain degree via experiments. Here in the present section we discuss more about the way to accelerate particles to high energies without losing the regular structure of the field. This is important since in a very high energy accelerator it is likely that any material may not be able to withstand the very strong accelerating field, and the system has to regulate itself; in the present case the plasma and the laser beams have to regulate themselves. A large regular electric field of 10^9 V/cm range propagating with phase velocity very close to c is certainly attractive for accelerating particles. One possible way to obtain this is to preaccelerate particles to moderately to highly relativistic energies and then to inject them onto this field. See Fig. 21. In order to accelerate to multi-TeV energies one is likely to need many modules of such an accelerator, since laser focus problems, and others, may arise. See Sec. VII. In this case it may be a technical challenge to produce particle clumps in phase with the positive electric field in (or electrons) all those modules. Even if we assume that we can accelerate particles almost all the time, with a field of 10^9 V/cm it would take 10^5cm to reach an energy of 100 TeV.

It is therefore of considerable interest and concern to see whether intense laser light can be propagated over a long distance without deteriorating the laser beam quality too much. If the laser light deteriorates too quickly or refracts over a short distance, we have to reshape the laser light or to inject a fresh laser light. This would amount to a complicated engineering headache and to much higher power consumption for lasers.

We address here a few crucial questions associated with acceleration of particles to high energies with the present concept. The first problem is <u>transverse</u> deterioration: the defocusing of the laser light due to the laser optics as well as to the plasma nonlinear effects on the laser light. We discuss the self-trapping effect in Sec. V.A. The second problem is the <u>longitudinal</u> deterioration of acceleration: the dephasing between the accelerating electrostatic plasma wave and the particles being accelerated. We introduce the method of density mismatching in Sec. V.B. This approach is intended to overcome the longitudinal dephasing. We then introduce a concept of the plasma fiber accelerator to cope with problems of both transverse and longitudinal detuning in Sec V.C.

A. Self-Trapping of the Laser Beam

Let us consider the self-trapping problem. For general reference see Akhmanov et al. (1968). The laser light has a focal length associated with it, the Rayleigh length (see Fig. 22a). This length $z_R = \pi w_0^2/\lambda_\ell$ with λ_ℓ being the laser wavelength and w_0 the focal waist would have to be of the laser acceleration length in order to achieve the energy gain of $2(\omega_0/\omega_p)^2 mc^2$:

$$\ell_a \lesssim 2z_R \ , \tag{26}$$

where $\ell_a = 2(\omega_0/\omega_p)^2 c/\omega_p$. Outside this area, the laser power would go too low and would diverge.

Fortunately, when the laser light is sufficiently intense, self-trapping of the light beam can take place at a certain threshold laser power (Felber, 1980). When the laser power is at the threshold, the laser beam propagates without defocusing, overcoming the natural tendency of spreading over the Rayleigh length. When the laser power exceeds the threshold, the laser beam propagates with its envelope resembling a sausage, without divergence of the beam (see Fig. 22b), still satisfactory to our purpose. Felber gives the self-trapping condition for a laser beam as

$$\left(\frac{eE_0}{mc^2 k_0}\right)^2 > \frac{4mc^2}{mc^2+2T}\left(\frac{c}{a_0\omega_p}\right)^2, \qquad (27)$$

where T the electron temperature, a_0 the light beam cross-section radius, and k_0 the laser wavenumber. The trapping condition Eq. (27) is not very difficult for an itense laser beam to fulfill. According to Felber, a self-consistent density profile for uniform plasma fiber can be obtained. The equations describing the propagation of a circularly polarized wave with planar phase fronts are

$$\left[\frac{d^2}{dr^2} + \frac{1}{r}\frac{d}{dr} + \frac{1}{a^2} + \frac{\omega_{p0}^2}{c^2(1+\nu_0^2)^{1/2}} - \frac{\omega_p^2}{c^2(1+\nu^2)^{1/2}}\right]\nu = 0 \ , \qquad (28)$$

where $\omega_p^2 = \omega_{p\infty}^2 \exp\left\{-\frac{mc^2}{2kT}\left[(1+\nu^2)^{1/2} - 1\right]\right\}$,

$$\omega^2 = \omega_{p0}^2 + (k^2 + \frac{1}{a^2})c^2 ,$$

$$\nu = eA/mc^2 ,$$

and A is the vector potential, $\omega_{p0}^2 = 4\pi ne^2/m$ is the nonrelativistic plasma frequency, and a is the constant radius. If $\omega_p^2 \ll c^2/a^2$, then Eq. (28) reduces to a Bessel equation with solution $A = A_0 J_0(r/a)$.

Another possibly damaging instability is filamentation instability (Felber and Chernin, 1981), which develops perpendicular to the beam propagation direction and is due to either the photon pressure or the plasma temperature effect. This instability makes the originally uniform beam profile into a spiky nonuniform one, leading to possible difficulty in accelerating uniformly and enhanced emittance. The mechanism of this instability and the conditions for avoiding it have been studied (Felber and Chernin, 1981). It is possible to have the above mentioned self-trapping and to avoid filamentation instability at the same time if we choose a certain domain of laser power, beam radius, plasma density, plasma temperature, etc. See Fig. 23. This corresponds to the regime with enough beam intensity and enough beam radius.

To check the self-trapping the Los Alamos group (1984) carried out two-dimensional electromagnetic simulations. The laser beams are shown to self-focus. At the same time the electron current generted in the direction of the acceleration created a large

poloidal magnetic field. Self-trapping by the mechanism of the electron relativistic mass variation has been calculated by Schmidt and Horton (1985). Their result is

$$\frac{v_{0s}}{c} > \sqrt{2}\, c/(a_0\omega_p) \ , \tag{29}$$

which is essentially in agreement with Felber's result.

B. Phase Adjustment Between the Particles and the Plasma Wave

The problem of the deterioration of the matching of particles and wave phases and a possible cure for it are discussed in this and subsequent subsections. In the original laser beat-wave accelerator the dephasing between the accelerating electrostatic plasma wave and the particles being accelerated takes place as the electrons are being trapped in the plasma wave and accelerated. In a half cycle of the trapping oscillation the particle moves, changing its phase from retarded to advanced relative to the wave. In the ultra-high energy accelerator under consideration, the particle enters into the electrostatic wave with a retarded phase, quickly overtaking the wave, because the particle of concern to us already has a velocity extremely close to the speed of light. The particle velocity relative to that of the wave is

$$\Delta v \simeq c - v_{ph} \cong \frac{1}{2}\left(\frac{\omega_p}{\omega_0}\right)^2 c \ , \tag{30}$$

where $v_{ph} = c\left[1 - (\omega_0/\omega_p)^2\right]^{1/2}$ the phase velocity of the plasma

wave. The dephasing can take place over a half wavelength. Therefore, the dephasing time is obtained as

$$\tau_d \simeq \frac{\lambda/2}{\Delta v} = 2\pi\left(\frac{\omega_0}{\omega_p}\right)^2 \frac{1}{\omega_p} , \tag{31}$$

where λ is the wavelength of this plasma wave. This dephasing time is very similar to (and essentially the same as) the acceleration time $t_a = 2(\omega_0/\omega_p)^2/\omega_p$ according to Eq. (16).

On the other hand, the time for ions to be accelerated by energy $Mc^2\Delta\gamma$ is given as

$$\tau_a \simeq \frac{\Delta\gamma Mc^2}{eE_L c} \cong \frac{\Delta\gamma Mc^2}{\gamma_\perp^{1/2} m\omega_p c^2} = \frac{\Delta\gamma}{\gamma_\perp^{1/2}} \left(\frac{M}{m}\right) \frac{1}{\omega_p} , \tag{32}$$

where M is the ion mass. Since the electron perpendicular temperature cannot be extremely high, $\gamma_\perp^{1/2}$ is of order unity (perhaps $< 2 \sim 3$). The energy gain within the dephasing time, therefore, is

$$\Delta\gamma \lesssim 2\pi \left(\frac{m}{M}\right) \left(\frac{\omega_0}{\omega_p}\right)^2 \gamma_\perp^{1/2} . \tag{33}$$

This indicates that if one wants to accelerate up to 100 TeV with $(\omega_0/\omega_p)^2 \sim 10^5$, one would need 10^3 rephasing operations between accelerating ions and the wave. This requires to have 10^3 modules of tiny plasma tubes with optics for intense lasers. When we accelerate electrons, we also need rephasing. In this case, we

only have to replace ion mass M by electron mass m in Eqs. (31) and (32). Again, if we want to accelerate electrons up to 100 TeV, we would need 10^3 rephasings if $(\omega_0/\omega_p)^2 \sim 10^5$ is taken.

An elementary method for reduction of the dephasing is to apply longitudinal spatial modulations of the plasma density either by segmenting resonant regions $[\omega_0 - \omega_1 = \omega_p(x)]$ and non-resonant regions $[\omega_0 - \omega_1 \neq \omega_p(x)]$ (see Fig. 24) or by smoothly changing the density of the plasma. An optimal profile of such a scheme has to be determined.

In order to cope with the longitudinal dephasing problems, a few further ideas have been proposed, including the surfatron (Katsouleas et al., 1983) and the plasma fiber accelerator (Tajima, 1983). We discuss the idea of the plasma fiber accelerator in some detail here.

C. The Plasma Fiber Accelerator

The idea of the plasma fiber accelerator (Tajima, 1983; Mima et al., 1985) is to tackle simultaneously two problems: (i) the longitudinal phase mismatch between the plasma wave and the particles; (ii) the tendency of laser light to spread in the transverse direction. It is crucial to overcome these difficulties in order to scale the scheme to ultra-high energies. The plasma wave excited by the beat of two laser lights has a phase velocity equal to the group velocity of the electromagnetic waves in the plasma according to Eq. (5). Since the phase velocity of the plasma wave is less than the speed of light, the plasma wave will be outrun by high energy particles during the dephasing time

$\tau_d = 2\pi(\omega_0/\omega_p)^2\omega_p^{-1}$. The particles that are trapped by the plasma wave gain energy by $2(\omega_0/\omega_p)^2 mc^2$, calculated by using the wave-breaking limit electric field $E_L = mc\omega_{p/e}$.

We shall show that the plasma fiber under appropriate conditions possesses a property to overcome this difficulty. The duct structure, in which the plasma density is low inside and the density is so high outside that the electromagnetic wave is evanescent, enables it to sustain a beat-wave phase velocity equal to any prescribed velocity including the speed of light. In addition to this benefit the plasma fiber confines the light, overcoming the natural tendency toward transverse spreading. Thus the idea of the plasma fiber plays a central role in improving the laser beat-wave accelerator in two of the most important points. It is to be noted that the optical fiber waveguide is one of very active and important areas of optics in recent years (Marcuse, 1974; Clarricoats, 1976; Adams, 1981). It is known that the fiber structure can well sustain the shape and the amplitude of light pulses over 10^7 cm, used as an efficient communication method. The fiber may have favorable properties such as sustaining optical solitons under certain conditions (Hasegawa and Kodama, 1981; Hasegawa, 1984). In the usual dielectric optical fiber the index of refraction is small toward the outside so that the light beam is trapped in the duct. In the present problem, of course, the plasma dielectric constant is less than unity so that the plasma density has to rise toward the outside. This cavitated structure of fiber type is often a natural ocurrence of plasmas with intense light shone (Amherd et al., 1974; Hoffman et al., 1978).

A way to match the phase of the accelerating field with high energy particles is to inject particles oblique to the electric field direction (Fig. 25). In order to phase-lock, the angle ϑ between the particle momentum and the electric field is given by

$$\cos\vartheta = \left(1 - \frac{\omega_p^2}{\omega_0^2}\right)^{1/2} . \tag{34}$$

Although we match the parallel phase, we have now introduced an extraneous perpendicular acceleration, which bends the particle orbit To correct this situation, it was proposed (Katsouleas and Dawson, 1983) that a static vertical magnetic field be imposed. The magnetic field is such that

$$\frac{B}{E} = \sin\vartheta = \frac{\omega_p}{\omega_0} , \tag{35}$$

for relativistic particles where B is out of the board in Fig. 25(c).

An alternative approach is to conduct the laser lights in a plasma duct where the plasma density in the middle is low and the edge density high (see Fig. 25b) (Tajima 1983; Mima et al., 1985). We choose the outside density so high that the electromagnetic waves are evanescent there and therefore they are trapped within the duct structure (plasma fiber). By choosing a right width of the duct we can show that the beat-wave velocity matches the speed of light. Let us choose flat densities n inside the duct and

n_1 outside of it with duct width d. We demand frequency matching among the two lasers and the plasma wave:

$$\omega_0 - \omega_1 = \omega_p \quad . \tag{36}$$

Further, we demand that the parallel velocity of the two lasers, which is equal to the parallel phase velocity of the plasma wave, be the speed of light (to be precise, this speed should be the particle velocity).

$$v_{gr\parallel}^{EM} \equiv \frac{\omega_0 - \omega_1}{k_{\parallel 0} - k_{\parallel 1}} = v_{ph\parallel} = c \quad , \tag{37}$$

where $$k_{\parallel j} = \left[\frac{\omega_j^2}{c^2} - \frac{\omega_p^2(r)}{c^2} - \left(\frac{\pi}{d}\right)^2 n_j^2\right]^{1/2} \tag{38}$$

and j=0 or 1 and we choose $n_0 = n_1 + 1$, where n_j are the number of transverse nodes. In a slab model with the y-direction parallel to the laser injection direction the electromagnetic fields may take the transverse magnetic or the transverse electric forms. The transverse electric case, for example, has the E_z, B_x, and B_y fields. If the plasma density abruptly changes from the duct plasma density to a very large value with the duct width d for simplicity, the electromagnetic field inside the duct may be approximated by the wave-guide modes:

$$E_{zj} = E_{zj}^0 \sin(k_{xj}x)\cos(k_{yj}y - \omega_j t) \quad , \tag{39}$$

$$B_{yj} = -\frac{ck_{xj}}{\omega_j} E^0_{zj} \cos(k_{xj}x)\sin(k_{yj}y-\omega_{tj}t) \ , \qquad (40)$$

$$B_{xj} = \frac{ck_{yj}}{\omega_j} E^0_{zj} \sin(k_{xj}x)\cos(k_{yj}y-\omega_j t) \ , \qquad (41)$$

where $k_{xj} = \pi n_j/d$ with j=0 or 1. The dispersion relation of the electromagnetic waves is $\omega_j = [\omega_p^2 + (k_{xj}^2 + k_{yj}^2)c^2]^{1/2}$, where ω_p^2 is determined by the plasma density inside the duct. The condition Eq. (36) yields the following relation

$$d^{-2} = \{-[AB+4(ED'+E'D)] \pm \sqrt{[AB+4(ED'+E'D)]^2-(B^2-4DD')(A^2-4EE')}\}$$
$$\times (A^2-4EE')^{-1} \ , \qquad (42)$$

where

$$A = E + E' \ ,$$

$$B = 1 - D - D' \ ,$$

$$D = \left(\frac{\omega_0}{\omega_p}\right)^2 - 1 \ ,$$

$$D' = \left(\frac{\omega_1}{\omega_p}\right)^2 - 1 \ ,$$

$$E = \left(\frac{\pi n_0 c}{\omega_p}\right)^2 \ ,$$

$$E' = \left(\frac{\pi n_1 c}{\omega_p}\right)^2 \ .$$

By choosing $n_0 = 2$ and $n_1 = 1$, and using $(\omega_0/\omega_p)^2 >> 1$ and $(\omega_1/\omega_p)^2 >> 1$, we arrive at the following condition for the duct width

$$d \simeq \sqrt{3}\,\frac{\pi c}{\omega_p}\left(\frac{\omega_0}{\omega_p}\right)^{1/2} . \tag{43}$$

If the density outside density n′ satisfied the condition

$$n' \geq n + \frac{9\pi m c^2}{4e^2 d^2} , \tag{44}$$

the electromagnetic waves are evanescent outside the plasma fiber. The plasma wave phase front is straight, i.e., $\varphi(z,r) \sim A(r)\cos(k_{\parallel p} z - \omega_p t)$ (see Fig. 25b).

In Fig. 26 we show the condition for the duct with Eq. (43) as a function of the ratio of the laser frequency to the plasma frequency: Eq. (43) is a good approximation. An example of simulation runs with the transverse electric field with a flat wave amplitude within the duct is discussed. The prescribed density profile of duct structure in the x-direction is shown in Fig. 27. The original light wavenumbers are $k_0 = 2\pi\times 20/128$ and $k_1 = 2\pi\times 15/128$, the speed of light $c = 4.09\omega_{p0}\Delta$, the quivering velocities of the light waves $v_{osj} = c$ (j=1 and 2), $d = 35\Delta$, $v_t = 0.5\omega_{p0}\Delta$, where ω_{p0} is the plasma frequency in the duct. The electrostatic potential of the beat plasma wave is shown in Fig. 28. Phase space of electrons in the y-direction shows trapped electrons by the beat plasma wave. The measurement of phase

velocity is exhibited in Fig. 29, which shows the phase velocity of the plasma wave is kept very close to $v_{ph} = 4.0\omega_p\Delta$ whereas $c = 4.09\omega_p\Delta$).

The above-mentioned role of the plasma fiber leads to a generalization of the plasma fiber accelerator. The original beat-wave accelerator was invented to create a slow wave out of the fast electromagnetic waves in a plasma via the nonlinear beat-wave coupling. However, it may be possible to impose a slow wave structure in a more "traditional" way employing the ripple structure (irises) on the fiber surface (Tajima, 1983) (see Fig. 3). The index of refraction of the plasma may be given as

$$n^2(r,z) = 1 - \omega_p^2(r,z)/\omega[\omega \pm \omega_{ce}(r,z)] , \qquad (45)$$

where $\omega_{ce} = eB_z/mc$ and the z-dependence refers to the ripple structure. Stated in a simplistic way, the duct structure makes the laser electric field possess the parallel component, while the ripple structure makes the electromagnetic wave be a slow wave. If the relation

$$\frac{\omega}{k+\Delta k} = c \qquad (46)$$

is satisfied, the slow wave is in phase with high energy particles, where Δk is the ripple wavenumber (Mima et al., 1985). Then the particles may be accelerated resonantly. A possibility of self-induced trapping is illustrated in Fig. 22. If the laser power is large enough, the self trapping (Felber, 1980) may produce

the above mentioned favorable fiber structure in a plasma. The electric field component perpendicular to the particle propagation can be canceled by an imposed magnetic field as discussed through Eq. (35). This latter variation of the plasma fiber accelerator utilizes the laser electric field directly as an accelerating field, and therefore it is not necessary to have a plasma inside the plasma fiber as a special case. In this last scheme we no longer rely on the beat-wave.

There exists an experimental evidence that the plasma fiber structure helps the laser driven acceleration process (Mima, 1985). The experimentalists of the Osaka group injected two CO_2 laser beams of 10.6μ and 9.6μ into a preformed plasma fiber structure of different lengths (1mm and 3mm). They found that the energy spectrum of accelerated electrons became harder for a longer plasma fiber.

VI. PLASMA NOISE

It is expected that imperfections in plasma density profile, plasma noise, and plasma turbulence tend to detune the necessary conditions for laser acceleration. These imperfections may be present before the laser injection due to external reasons such as noises caused by plasma generation. These imperfect conditions may also be generated as a result of laser injection caused by, for example, parasite plasma instabilities.

A. Multiscattering and Plasma Wave Incoherency

In addition to these causes of noise, the multiscattering of photons can give rise to incoherent plasma waves. Consider Fig. 5. Since the phase velocity of the plasma wave determined by Eq. (5) changes as a function of the photon frequency, there is a difference between the phase velocities in each stage of the cascade of photons: ω_0 and ω_1 producing ω_2, ω_1 and ω_2 producing ω_3, and so on. This difference in phase velocity is

$$\Delta v_{ph} \cong c\left(1 - \frac{\omega_p^2}{\omega_0^2}\right)^{1/2} - c\left(1 - \frac{\omega_p^2}{\omega_1^2}\right)^{1/2} \simeq c\left(\frac{\omega_p}{\omega_0}\right)^3 . \tag{47}$$

It takes a time

$$t_c \simeq \frac{c}{\omega_p} \frac{1}{\Delta v_{ph}} \sim \left(\frac{\omega_0}{\omega_p}\right)^3 \frac{1}{\omega_p} \tag{48}$$

for the plasma waves to become incoherent. This effect may explain the simulation result by Kindel and Forslund (1983) in which they observed that the beat plasma wave becomes incoherent after a sufficiently long period of time. The incoherent wave pattern begins at a certain distance behind the front of the laser light.

As a model problem to investigate one aspect of various problems of noise and incoherency, let us pick the problem of multiscattering and stochasticity due to many waves by ignoring all particle dynamics and even the phase velocity mismatching effect [Tajima, Schmidt and Pellat (1985b)]. This highly idealized model

may have some relevance if the wave begins to cascade without too strong accompanying electron heatings and the phase velocity mismatch is negligibly small. A case close to this situation but not quite the same may be found in Fig. 11. Once we thus isolate the photon–plasmon coupling process from the rest of the possible interactions such as the wave–particle interaction, the system may be described by mode–mode coupling equations. One example of such coupling equations is

$$\frac{\partial a_0}{\partial t} = -a_1 a_p \ ,$$

$$\frac{\partial a_1}{\partial t} = a_0 a_p^* - a_2 a_p \ ,$$

$$\frac{\partial a_i}{\partial t} = a_{i-1} a_p^* - a_{i+1} a_p \ ,$$

$$\frac{\partial a_q}{\partial t} = a_{q-1} a_p^* \ ,$$

$$\frac{\partial a_p}{\partial t} = a_0 a_q^* + a_1 a_2^* + \cdots + a_{q-1} a_q^* \ . \tag{49}$$

Here a_1 is the (complex) amplitude of photon 1 and wave i designates lower frequency photons. a_p is the amplitude of the plasmon. The amplitude of the photon with lowest possible

frequency here is a_q. We assume that no frequency up-conversion takes place.

To Eqs. (45) belong two invariants:

$$N = \sum_{k=0}^{q} |a_k|^2 , \tag{50}$$

$$H = \sum_{k=0}^{q} k|a_k|^2 - |a_p|^2 = 0 . \tag{51}$$

Equation (50) corresponds to the quantum number (action) and its conservation; Eq. (51) corresponds to the energy (after multiplying by $\hbar\omega_p$) and its conservation. As is well known (Sagdeev and Galeev, 1969), a three-wave (two photons and one plasmon) coupling case of Eqs. (49) is completely integrable via elliptic integrals and produces a periodic solution. The case with four waves (three photons and one plasmon) is still periodic, as seen in Fig. 30. We see aperiodic behaviors when the number of waves is equal to or greater than 5 (Fig. 31). As we allow a larger number of waves, the behavior becomes more chaotic. There simply are not enough constraints (Eqs. 50 and 51) to keep the system integrable for these cases (see Fig. 32).

It may become reasonable to treat the problem in a statistical way when the system behaves completely chaotically. One plausible ansatz then would be the assumption of ergodicity in phase space spanned by 2(q+2) dimensional wave-amplitudes (real and imaginary as independent dimensions), whose elemental volume is $da_{0r}da_{0i}da_{1r}da_{1i}\cdots da_{qr}da_{qi}da_{pr}da_{pi}$. The dynamics of Eqs. (49) is

described by a trajectory of a point (for one sample) in 2(q+2)D phase space. From Eqs. (49) the phase volume conserves:

$$\frac{\partial}{\partial a_k}\frac{d}{dt}a_k = 0 \ . \tag{52}$$

The surface of phase space is cut out by two constraints Eqs. (50) and (51). The ergodicity ansatz dictates that the points will wander in any location of this restricted phase space with equal likelihood.

The statistical mechanical argument will lead us to predict the most probably state among all the possible phase space configurations. With the aid of Lagrange multipliers a quantity R is defined

$$R = \sum_{k=0}^{q} \ell n|a_k|^2 + C - \lambda\Big(\sum_{k=0}^{q}|a_k|^2 - N\Big) - \mu\Big(\sum_{k=0}^{\infty} k|a_k|^2 - P\Big) \ , \tag{53}$$

where $P = |a_p|^2$. The most probable state is obtained by maximizing R with respect to variations of a_k. By letting $\partial R/\partial|a_k|^2 = 0$, we find

$$|a_k|^2 = \frac{1}{\lambda + \mu k} \ . \tag{54}$$

The Lagrange multipliers are determined by

$$\sum_{k=0}^{q} \frac{1}{\lambda + \mu k} = N \ , \tag{55}$$

$$\sum_{k=0}^{q} \frac{k}{\lambda + \mu k} = P \quad . \tag{56}$$

From Eqs. (55) and (56) we find $P = (q+1-\lambda N)/\mu$. In order to find the most probable state for P, we should maximize R with respect to P, which yields

$$q + 1 - \lambda N = 0 \quad , \tag{57}$$

thus $$\mu = 0 \quad . \tag{58}$$

Substituting Eqs. (57) and (58) into Eqs. (54) and (55), we find

$$|a_k|^2 = \frac{N}{q+1} \quad , \tag{59}$$

$$P = |a_p|^2 = \frac{q}{2} N \quad . \tag{60}$$

This is simply the law of equipartition. The entropy

$$S = \sum_{k=0}^{q} - |a_k|^2 \ln |a_k|^2 \tag{61}$$

tends to the value $S = -[N/(q+1)] \ln [N/(q+1)]$ as an asymptotic value. These theoretical predictions are reasonably satisfied when the number of waves is sufficiently large. The case in Fig. 32 has 20 waves. As we can see in Fig. 32, the waves quickly become chaotic. The obtained average amplitude for each wave is close to

the value Eq. (59). The entropy also tends to a steady-state value.

B. Imperfect Beat-Wave Condition Due to Plasma Inhomogeneity

Once a noise appears in the plasma density, it will contribute to make the beat-wave condition imperfect. This has been under study (Horton and Tajima, 1985a). Consider two laser fields (0 and 1) with frequency and wavenumber (ω_0, k_0) and (ω_1, k_1): $E_{y0} \sin(k_0 x - \omega_0 t)$, $E_{y1} \sin(k_1 x - \omega_1 t)$. The longitudinal displacement (in the x-direction) ξ_x is related to the longitudinal electric field through Poisson's equation

$$E_x = 4\pi n_0(x) e \xi_x \quad . \tag{62}$$

The equation of motion for electrons is

$$\frac{d\underset{\sim}{v}}{dt} = -\frac{e}{m}\left(\underset{\sim}{E} + \frac{\underset{\sim}{v}}{c} \times \underset{\sim}{B}_z\right) , \tag{63}$$

where B_z is the laser field. Equation (63) can be cast into

$$\frac{d^2}{dt^2}\xi_x = -\frac{4\pi n_0(x) e^2}{m}\xi_x - \frac{e}{mc}\left(\dot{\xi}_y^1 B_z^2 + \dot{\xi}_y^2 B_z^1\right) , \tag{64}$$

where superscripts 0 and 1 refer to lasers 0 and 1. The derivative of displacements is

$$\dot{\xi}_{y0} = -\frac{eE_{y0}}{m\omega_0}\cos(\bar{k}_0 x - \omega_0 t) \ , \qquad (65)$$

$$\dot{\xi}_{y1} = -\frac{eE_{y1}}{m\omega_1}\cos(\bar{k}_1 x - \omega_1 t) \ , \qquad (66)$$

where $\bar{k}_0$, $\bar{k}_1$ are the averages of k_0 and k_1, and

$$\Delta k_0 = k_0 - \bar{k}_0 \simeq \left(\frac{\omega_{p0}}{\omega_0}\right)\frac{\Delta\omega_p(x)}{c} \ .$$

Let us write the displacement as

$$\xi_x(x_0,t) = A(t,x)\sin[k_p x_0 - \omega_p(x)t + \varphi] \ . \qquad (67)$$

The nonlinear term on the right-hand side (RHS) of Eq. (66) is rewritten in terms of Eq. (67) as

$$\text{RHS} = \left(-\frac{e}{mc}\right) \times \left\{-\frac{e}{2m\omega_0}E_0(x)\left[e^{i[k_0(x)x-\omega_0 t]}\right.\right.$$

$$\left. + e^{-i[k_0(x)x-\omega_0 t]}\right]B_1(x)\sin[k_1(x)x - \omega_1 t] - \frac{e}{2m\omega_1}E_1(x)$$

$$\left.\times \left[e^{[ik_1(x)-\omega_1 t]} + e^{-i[k_1(x)x-\omega_1 t]}\right]B_0(x)\sin[k_0(x)x - \omega_0 t]\right\} \ , \qquad (68)$$

where $B_{0_1} = [\frac{k_0(x)c}{\omega_{0_1}}]E_{0_1}$. (69)

Thus we have

$$RHS = \frac{1}{2}\frac{e^2}{m^2}\frac{E_0E_1}{\omega_0\omega_1}\{k_1(x)\cos[k_0(x)x - \omega_0 t]\sin[k_0(x)x - \omega_1 t]$$

$$+ k_0(x)\cos[k_1(x)x - \omega_1 t]\sin[k_0(x)x - \omega_0 t]\} \quad . \tag{70}$$

We write $k_0(x) = k_1(x) + \Delta k(x)$. We now time-average Eq. (66) or Eq. (70) over $1/\omega_0$ or longer, but less than $1/\Delta\omega$, obtaining

$$\langle[RHS]\rangle = \frac{1}{2}\frac{e^2}{m^2}\frac{E^0E^1}{\omega_0\omega_1}\frac{\Delta k}{4i}\langle[e^{i[k_0(x)-k_1(x)-(\omega_0-\omega_1)t]} - c.c.]\rangle \quad . \tag{71}$$

Here note that the phase factor can be expanded in terms of the Bessel function

$$e^{i(\Delta k(x)x-\Delta\omega t)} = e^{-i\Delta\omega t}e^{i\Delta k(x_0+\xi_x)}$$

$$\simeq e^{i(\Delta kx_0-\Delta\omega t)}\sum_{\ell} J_\ell(\Delta kA(t))e^{i\ell[k_\Delta(x)x_0-\omega_p(x)t]+i\ell\varphi} \quad . \tag{72}$$

Going back to the fluid description, the equation of motion of electrons is expressed as

$$nm\left(\frac{\partial v}{\partial t} + v\cdot\nabla v\right) = -\nabla p + n_e E + n_e\left(E_t + \frac{v}{c}\times B\right) \quad . \tag{73}$$

Using the previous result [Eq. (72)], we have

$$-i\omega n_0 m v_x = -\gamma v_e^2 m \frac{\partial n_1}{\partial x} + n_0 e E_x$$

$$= \frac{1}{4i} \frac{e^2 n_0}{m} \Delta k \frac{E_0 E_1}{\omega_0 \omega_1} e^{i\Delta k x_0 - \varphi} J_0(\Delta k A) \quad , \tag{74}$$

where only the $\ell=0$ term is taken. Poisson's equation and the continuity equation yield

$$-i\omega E_x = -4\pi n_0 e v_x \quad , \tag{75}$$

and

$$-i\omega \frac{\partial n_1}{\partial x} = \frac{\partial^2}{\partial x^2} \left(n_0(x) v_x\right) \quad . \tag{76}$$

We have then from Eq. (74)

$$-i\omega n_0 m v_x = \frac{\gamma v_e^2 m}{i\omega} \frac{\partial^2}{\partial x^2} \left[n_0(x) v_x\right] + \frac{4\pi n_0^2 e^2 v_x}{i\omega}$$

$$+ \frac{1}{4i} \frac{n_0 e^2}{m} \Delta k(x) \frac{E_1 E_2}{\omega_1 \omega_2} e^{i\Delta k x - \varphi} J_0(\Delta k A) \quad . \tag{77}$$

Multiplying by $i\omega/n_0 m$, we get

$$(\omega_p(x)^2-\omega^2)v_x - \frac{\gamma v_e^2}{n_0}\frac{\partial^2}{\partial x^2}[n_0(x)v_x] = \frac{1}{4}\omega\left(\frac{e}{m}\right)^2 \Delta k \frac{E_0E_1}{\omega_0\omega_1} e^{i(\Delta kx-\varphi)} J \quad (78)$$

By recalling $n_0 v_x = \frac{i\omega}{4\pi e} E_x$, we have

$$(\omega_p^2(x) - \omega^2)E_x - \gamma v_e^2 \frac{\partial^2}{\partial x^2} E_x$$

$$= \frac{\pi e n_0}{i} \left(\frac{e}{m}\right)^2 \Delta k \frac{E_0E_1^*}{\omega_0\omega_1} e^{i(\Delta kx\varphi)} J_0 . \quad (79)$$

This may be rewritten as

$$\frac{\partial^2}{\partial t^2} E_x + [\omega_p^2(x) - \gamma v_e^2 \frac{\partial^2}{\partial x^2}]E_x$$

$$= \frac{\pi e n_0}{i} \left(\frac{e}{m}\right)^2 \Delta k \frac{E_0E_1^*}{\omega_0\omega_1} e^{i(\Delta kx-\varphi)} J_0 \cdot e^{-i\Delta\omega t} . \quad (80)$$

Or in short we have

$$[\frac{\partial^2}{\partial t^2} - \gamma v_e^2 \frac{\partial^2}{\partial x^2} + \omega_p^2]E_x = S(x,t) , \quad (81)$$

where the right-hand side is a source term due to the beat-wave effect. This is the main equation we want to consider.

If the source term is generated by the beat of two EM waves and we assume that the source term $S(x,t)$ dependence is by $S(x-v_g t)\cos(\Delta kx-\Delta\omega t)$, then we can simplify Eq. (81). Let us also assume

$$\frac{\Delta\omega}{\Delta k} \equiv v_{ph}^{ES} = v_{gr}^{EM} \ , \tag{82}$$

which is equivalent to Eq. (5) for the uniform case. That is to assume that the inhomogeneous structure moves together with the EM wavepacket.

In the frame of laser pulse, we rewrite the variables from (x,t) to (x',t') as

$$x' \equiv x - vt \ , \tag{83}$$

$$t' = t \ , \tag{84}$$

where $v = v_{gr} = v_{ph}$. Then Eq. (81) becomes

$$\left[\left(\frac{\partial}{\partial t'} - v_p \frac{\partial}{\partial x'}\right)^2 - \gamma v_e^2 \frac{\partial^2}{\partial x'^2} + \omega_p^2(x' + v_p t', t')\right] E(x', t')$$

$$= S(x')\cos\left[\Delta k v_p - \Delta\omega)t' + \Delta kx'\right] = S(x')\cos(\Delta kx') \ . \tag{85}$$

An assumption that $\omega_p^2(x'+v_p t', t')$ goes like $\omega_p^2(x')$ is now made. This means that the density ripple is moving with v_{ph}. A limiting case is analyzed. Equation (85) can be approximated as

$$[v_p^2\partial_x^2 + \omega_p^2(x')]E(x') = S(x')\cos(\Delta kx') \quad , \tag{86}$$

because $v_e^2 \ll c^2$ and t' independence are assumed. To check the known simple case when the plasma is uniform and the profile of the laser pulse is a square case, let us further take

$$\omega_p^2(x') = \omega_{p0}^2 \quad ,$$

$$S(x') = S_0[\Theta(x) - \Theta(x-L)] \quad ,$$

$$\Delta k v_p = \omega_{p0} \quad .$$

An exact solution to Eq. (86) is obtained:

$$E(x') \begin{cases} = -\dfrac{m\omega_{p0}}{e} S_0 \dfrac{\Delta kx'}{2(\Delta kv_p)^2} \sin(\Delta kx') & (0 \leqslant x' \leqslant L) \quad , \quad (87a) \\ = -\dfrac{m\omega_{p0}}{e} S_0 \dfrac{\Delta kL}{2(\Delta kv_p)^2} \sin(\Delta kx') & (x' \geqslant L) \quad . \quad (87b) \end{cases}$$

Equation (87) indicates the secular growth of $E(x')$ due to the beat resonance, and then $E(x')$ saturates when the source term is gone.

Let us now discuss a more general case. Here $\omega_p(x')$, $S(x')$ do have x'-dependence. We use x as x' from now on,

$$[v_p^2\partial_x^2 + \omega_p^2(x)]E_x(x) = S(x)\cos(\Delta kx) \quad . \tag{88}$$

Define linearly independent functions of a homogeneous differential equation

$$\left[\partial_x^2 + \frac{\omega_p^2(x)}{v_p^2}\right]\begin{pmatrix} E_c(x) \\ E_s(x) \end{pmatrix} = 0 \ , \tag{89}$$

such that

$$E_c(x) \propto \left[\frac{k_{L0}}{k_L(x)}\right]^{1/2} \cos\left(\int_0^x k_L(x')dx'\right) \ , \tag{90}$$

$$E_s(x) \propto \left[\frac{k_{L0}}{k_L(x)}\right]^{1/2} \sin\left(\int_0^x k_L(x')dx'\right) \ , \tag{91}$$

with $k_L^2(x) \equiv \frac{\omega_p^2(x)}{v_p^2}$. $E_c(x)$ and $E_s(x)$ are the WKB solution of the homogeneous equation (89). The solution of the inhomogeneous equation now becomes

$$E(x) = \int_0^x dx' \ \frac{S(x')\cos(\Delta k x')}{v_p^2 W(E_c(x'),E_s(x'))} \left[E_c(x')E_s(x) - E_s(x')E_c(x)\right] \ , \tag{92}$$

where the Wronskian is defined as

$$W(E_c,E_s) \equiv E_c \frac{dE_s}{dx} - E_s \frac{dE_s}{dx}$$

$$\simeq k_L(x)\frac{\cos^2\int k_L dx}{(k_L(x)/k_{L0})} + k_L(x)\frac{\sin^2\int k_L dx}{(k_L(x)/k_{L0})} \simeq k_{L0} \quad . \qquad (93)$$

Thus, Eq. (92) is written as

$$E(x) = E_s(x)\int_0^x dx' \frac{S(x')\cos(\Delta k x')}{v_p^2 k_{L0}} E_c(x')$$

$$- E_c(x)\int_0^x dx' \frac{S(x')\cos(\Delta k x')}{v_p^2 k_{L0}} E_s(x')$$

$$\simeq E_s(x)\int_0^x dx' \frac{1}{v_p^2 k_{L0}} S(x')\cos(\Delta k x')\left[\frac{k_{L0}}{k_L(x')}\right]^{1/2}\cos\left(\int_0^{x'} k_L(x'')dx''\right)$$

$$\simeq \frac{1}{2}\frac{E_s(x)}{v_p^2 k_{L0}^{1/2}}\int_0^x dx' \frac{S(x')}{(k_L(x'))^{1/2}}\cos\left[\int_0^{x'}(k_L(x'') - \Delta k)dx'\right] \quad . \qquad (94)$$

We have now

$$E_x(x) \propto \int_0^x dx' S(x')\cos\left[\int_0^{x'}(k_L(x'') - \Delta k)dx''\right]$$

$$\simeq S(x_r)\left[\frac{2\pi}{dk_L/dx}(x_r)\right]^{1/2}\cos\left[\int_0^{x_r}(k_L(x') - \Delta k)dx' + \frac{\pi}{4}\right] \quad . \qquad (95)$$

We have to evaluate the integral in the argument of cos in Eq. (95).

In the first case the density is assumed to be linear near x_r:

$$\int_{x_r}^{x} (k_L(x') - (\Delta k))dx' = \left.\frac{dk_L}{dx}\right|_{x_r} \cdot \frac{(x - x_r)^2}{2} , \qquad (96)$$

where x_r is the resonance point. Equation (95) is evaluated by replacing $\int dx'$ by L. Then we have

$$E_x(x) \propto \left(\frac{2\pi}{dk_L/dx}\right)^{1/2} \simeq \left(\frac{4\pi}{k_L} L_n\right)^{1/2} = (2\lambda_L L_n)^{1/2} , \qquad (97)$$

where $\lambda_L = 2\pi/k_L$ is the wavelength of the plasma wave and L_n is the characteristic length over which the plasma frequency rises significantly ($\simeq$ the density scale length). In this case finally we have

$$E_x(x) \simeq S_0 \frac{E_s(x)}{2k_L v_p^2} \left(\frac{4\pi L_n}{k_L}\right)^{1/2} \cos\left[\int_0^{x_r} (k_L - \Delta k)dx + \frac{\pi}{4}\right] . \qquad (98)$$

As a second case, we consider a case when the density varies stochastically. The density variation δn affects k_L as $k_L = \bar{k}_L + \delta k_L$. We assume Gaussian variation of δk_L or $\delta\omega_p$ or δn: i.e., $\delta k_L = \delta\omega_p/v_p$ varies Gaussian statistics. Under this assumption, we have $\langle\delta k_L\rangle = 0$, $\langle\delta k_L^2\rangle \neq 0$. Equation (94) is averaged over random fluctuations of the density:

$$E_x(x) \simeq \frac{E_s(x)}{2\bar{k}_L v_p^2} \int_0^x dx' \, S(x') \cos\left[\int_0^{x'} (k_L(x'') - \Delta k)dx''\right] \qquad (99)$$

and the average becomes

$$\langle E_x(x)\rangle \propto \langle \cos\left[\int_0^x (k_L(x') - \Delta k)dx'\right]\rangle \ . \qquad (100)$$

Now let us take an example of a Gaussian average:

$$\langle \cos(\varphi + \delta\varphi)\rangle = \frac{1}{2}\langle e^{i\varphi + i\delta\varphi} + e^{-i\varphi - i\delta\varphi}\rangle = e^{-\langle\delta\varphi^2\rangle/2}\cos\varphi \ , \qquad (101)$$

$$\text{and} \quad \langle\delta\varphi^2\rangle = \left\langle \int_0^x k_L(x')dx' \int_0^x k_L(x'')dx''\right\rangle \simeq x\, L_k\langle\delta k_L^2\rangle \ , \qquad (102)$$

where L_k is the autocorrelation length for k_L. Thus we obtain

$$\langle E(x)\rangle \simeq \frac{E_s(x)}{2\langle k_L\rangle v_p^2}\int_0^x dx'\, S(x')e^{-\frac{x'}{2}L_k\langle\delta k_L^2\rangle}$$

$$\simeq \frac{E_s(x)}{\langle k_L\rangle v_p^2 L_k\langle\delta k_L^2\rangle}\left[1 - e^{-\frac{x}{2}L_k\langle\delta k_L^2\rangle}\right] \ . \qquad (103)$$

$$\text{Here} \quad L_k\langle\delta k_L^2\rangle = \int_{-\infty}^{\infty} dx\langle\delta k_L(x)\delta k_L(x)\rangle \ . \qquad (104)$$

We have now learned that the amplitude $E_x(x)$ originally given by Eq. (87) is reduced because of the plasma density variations by the following

Case I Reduction by a factor of $\frac{(\lambda_L L_n)^{1/2}}{L}$

Case II Reduction by a factor of $\sim (LL_k\langle\delta k_L^2\rangle/2)^{-1}$.

Here $L_k\langle\delta k_L^2\rangle$ may also be written as $(\omega_p^2/4c^2)\langle\delta n^2/n_0^2\rangle$. Whether the nonlinear saturation Eq. (11) comes in first or not depends on the relative importance of the system nonlinearities and of the plasma noise.

Let us discuss the co-moving plasma noise effects on the beat-wave growth (Horton and Tajima, 1985b) in a relativistically covariant fashion. The noise in the plasma density is characterized by the dimensionless variance $\sigma = \langle\delta n^2\rangle/n^2$ and the correlation length L_c defined by the autocorrelation function of the density along the trajectory of the laser pulse. The strength of the laser fields is given by the dimensionless quiver velocities $a_j = eE_j/m_e c\omega_j$. The ideal growth rate of the plasma wave is given by $\lambda = a_0 a_1/4$ in units of the number of plasma wave oscillations. The relativistic extension of Eq. (64) is given by

$$\frac{\partial}{\partial t}\left(\gamma_{\dot\xi}\frac{\partial\xi}{\partial t}\right) = \gamma_{\dot\xi}^3\frac{\partial^2\xi}{\partial t^2} = \frac{-e}{m_e}E_x + \frac{-e}{m_e c}\left(v_y^{(0)}B_z^{(1)} + v_y^{(1)}B_z^{(0)}\right) \quad (105)$$

where $\gamma_{\dot\xi} = (1-\dot\xi^2/c^2)^{-1/2}$. Neglecting the high frequency $\omega_1+\omega_2$ oscillations and substituting in Eq. (105) for E_x from Eq. (62), we obtain

$$\gamma_\xi^3 \frac{\partial^2 \xi}{\partial t^2} + \omega_p^2 \xi = 2\Delta\omega c\lambda S(x-v_p t)\sin[k_p(x-v_p t)+\Delta\varphi] \qquad (106)$$

for the relativistic plasma oscillations.

Since both the laser pulse envelope $S(x-v_p t)$ and the plasma wave travel with the speed v_p, it is convenient to study the growth of the plasma wave in the Lorentz frame traveling with the laser pulse $x' = \gamma_p(x-v_p t)$ and $t' = \gamma_p(t-v_p x/c^2)$. In this frame the time variation of the plasma wave is slow with $\omega' = \gamma_p(\omega-kv_p) << \omega_p$. Transforming the space-time coordinates in Eq. (105) to the Lorentz frame with parameters v_p and $\gamma_p = (1-v_p^2/c^2)^{-1/2}$ the basic equation for the slowly evolving plasma wave is

$$-2\gamma_p^2 v_p \frac{\partial^2 \xi}{\partial x' \partial t'} + \gamma_p^2 v_p^2 \frac{\partial^2 \xi}{\partial x'^2} + \frac{\omega_p^2}{\gamma_\xi^3}\xi = \frac{2\Delta\omega c\lambda}{\gamma_\xi^3} S(x')\sin(k_w x'+\Delta\varphi) \qquad (107)$$

where the wavenumber in the wave frame is $k_w = k_p^{wave} = k_p/\gamma_p$.

The ideal solution of equation in the weakly relativistic limit is given analytically by Rosenbluth and Liu (1972) in terms of an envelope approximation. Writing the field as

$$\frac{\omega_p \xi(x't')}{c} = \frac{1}{2}\hat{\xi}(x't')e^{ik_w x'} + \frac{1}{2}\hat{\xi}^*(x't')e^{-ik_w x'}, \qquad (108)$$

making the expansion $\gamma_\xi^{-3} = 1-3/2\ \dot{\xi}^2/c^2$ and calculating the secular part of $\ddot{\xi}\xi$ leads to the envelope equation for the resonant system

$$-\frac{2i\gamma_p}{\omega_p}\left(\frac{\partial\hat{\xi}}{\partial t'}+v_p\frac{\partial\hat{\xi}}{\partial x'}\right)+\left(\frac{\delta n(x't')}{n}-\frac{3}{8}|\hat{\xi}|^2\right)\hat{\xi}=-2i\lambda\hat{S}(x') \quad , \quad (109)$$

where $S(x')$ is the envelope of the intensity of the laser beam. We note that Eq. (109) is a driven nonlinear Schrödinger-type equation with δn acting as a potential.

For $\delta n = \text{const}$ and $S(-x') = \Theta(-x')$ Eq. (109) reduces to the ideal equation

$$-2i\frac{\partial\hat{\xi}}{\partial\vartheta}-\frac{3}{8}|\hat{\xi}|^2\hat{\xi}+\frac{\delta n}{n}\hat{\xi}=-2i\lambda \quad (110)$$

with $\vartheta = \omega_p t = -\omega_p x'/\gamma_p v_p$. The integral of Eq. (110) is given by the three wave Hamiltonian with the action variable $I = |\hat{\xi}|^2$ and the angle variable $\psi = \arg(\hat{\xi})$

$$H(I,\psi) = -\frac{\delta n}{2n}I+\frac{3}{32}I^2-2\lambda I^{1/2}\sin\psi \quad (111)$$

The equations of motion are

$$\frac{dI}{d\vartheta}=-\frac{\partial H}{\partial\psi}=2I^{1/2}\lambda\cos\psi$$

$$\frac{d\psi}{d\vartheta}=\frac{\partial H}{\partial I}=-\frac{\delta n}{2n}+\frac{3}{16}I-\lambda I^{-1/2}\sin\psi \quad (112)$$

The maximum amplitude of the ideal solution follows from $H = \text{const} = 0$ so that $I_{max}^{3/2} = 64\,\lambda/3$ or

$$\max\left(\frac{\omega_p \xi}{c}\right) = I_{max}^{1/2} = 4\left(\frac{\lambda}{3}\right)^{1/3} \quad . \tag{113}$$

This is a reproduction of formula Eq. (11) and agrees with Rosenbluth and Liu (1972) and with Tang et al. (1984). The time to reach the maximum amplitude is

$$\Delta\vartheta = \omega_p T \equiv \int_0^{I_{max}} dI/\dot{I} \cong 3.89\lambda^{-2/3} \quad . \tag{114}$$

The effect of the scattering of the plasma wave by inhomogeneities in the plasma density $\delta n(xt)$ has been calculated using renormalized mode coupling theory. The theory (Horton and Tajima, 1985a) predicts an equation for the evolution of the ensemble average $<\xi>$ displacement which is governed by a renormalized Langmuir wave propagator $L(k\omega) = -\omega^2+\omega_p^2+\Delta\omega_k^2-i\omega\nu_k$. The frequency shift $\Delta\omega_k$ and the effective damping ν_k due to the scattering of the plasma density fluctuations is given in terms of the fluctuation spectrum $<|\delta n(k\omega)|^2>$ through the usual nonlinear-integral propagator equation. The theory is too complicated to review here. Instead, we describe some of the predictions of the theory.

For weak density fluctuations the scattering from $\delta n(k\omega)$ causes a diffusion of the plasma wave phase away from the mean resonant phase $<\vartheta> = <\omega_p^2>^{1/2}x/v_p$. The most dangerous noise in terms of reducing the amplitude of the accelerating electric field and in terms of changing the particle orbits by resonant interaction with noise is that moving with the laser pulse so that $\omega' = \gamma_p(\omega-kv_p) = 0$ and $k' = \gamma_p(k-v_p\omega/c^2) = k/\gamma_p$. The correlation

function for two points moving with the laser pulse $\langle \delta n(x_1,t_1)\delta n(x_2,t_2)\rangle$ defines the correlation length $L_c = 1/\Delta k$ or $L_c' = 1/\Delta k' = \gamma_p L_c$ in the wave frame and the laboratory frame respectively. For $x > L_c$ the changes in the wavenumber $\delta k = (\omega_p/2v_p)\delta n/n$ are uncorrelated. The mean phase of the plasma wave increases as $\langle\vartheta\rangle = \omega_p x/v_p$ and the actual phase $\vartheta(x)$ diffuses away from the mean phase as

$$\langle(\vartheta(x)-\langle\vartheta\rangle)^2\rangle = D\ x \tag{115}$$

for $|x| \gg L_c$ where

$$D = \langle\delta k^2\rangle L_c = \frac{\omega_p^2}{4v_p^2}\,\sigma L_c \tag{116}$$

The effective length for stochastization of the phase L_{eff} is

$$L_{eff} = \frac{1}{D} = \frac{4v_p^2}{\omega_p^2}\,\frac{1}{L_c\sigma} \tag{117}$$

After a distance L_{eff} the phase of the plasma wave is completely uncertain. For the maximum ideal amplitude to be reached before the the phase becomes uncertain, the condition

$$L_{eff}^{-1} = D = \frac{\omega_p^2}{4v_p^2}\,\sigma L_c < 0.26\,\frac{\omega_p}{c}\,\lambda^{2/3} \tag{118}$$

must be satisfied.

For higher levels of fluctuations $\sigma > \sigma_c = 4v_p^2/\omega_p^2 L_c^2$ the phase stochastization length L_{eff} becomes equal to the correlation length L_c and the plasma wave oscillation is formed in its own local density fluctuations. In this regime the growth of the plasma wave occurs over the correlation distance L_c and the amplitude of the plasma wave is limited to

$$\max(\xi) = \lambda L_c \quad . \tag{119}$$

We briefly discuss the conditions for wave growth as follows. The energy density in the plasma waves is $W \cong mnc^2|\hat{\xi}|^2$. If this is much greater than a threshold, the modulational instability develops when the plasma wave couples to the ion acoustic waves. It may be important to limit the downstream turbulence by requiring growth to the ideal amplitude limit before an ion plasma period. This requirement can be written as $\lambda > 8.2(m_e/m_e)^{3/4} \simeq 0.029$ or $a_1 > 5.7(m_e/m_i)^{3/8} \sim 0.2$–$0.3$. For such strong laser fields the plasma oscillation is strongly nonlinear and has a broad resonance in the amplitude versus the driving frequency parameter $\Delta\omega/\omega_p$ as shown in Figure 33. The nonlinear broadening of the resonance has the disadvantage of limiting the increase of the accelerating field to the one–third power of the laser intensity. It has, however, the advantageous effect of increasing the width of resonant growth of the plasma wave by $\delta\omega/\omega_p \simeq \lambda^{2/3}$. In the presence of sufficiently strong plasma fluctuations moving with the phase velocity of the plasma wave the diffusion of the phase of the

plasma wave limits the effective length of wave growth to $L_{eff} = 1/D$ which is less than the ideal growth length $4c/\omega_p \lambda^{2/3}$ for $L_c \simeq c/\omega_p$, $\sigma << \lambda^{2/3}$. In this regime the maximum useful amplitude of the plasma wave is given by $\xi = \lambda L_{eff}$ and decreases inversely with increasing intensity of the noise.

We note that although the effect of transient noise propagating through the laser pulse is less effective in limiting the amplitude of the plasma wave than the resonant noise considered here, the transient noise has a frequency $\omega' = \gamma_p(\omega - kv_p)$ which can resonate with the phase locking frequency of the accelerating particles and cause them to be lost from the regions of accelerating phase in the ponderamotive buckets.

We note that the considerations given here can be applied to the conventional beat wave accelerator (Tajima and Dawson, 1979b), the surfatron (Katsouleas and Dawson, 1983) or the above-mentioned plasma fiber accelerating system (Tajima, 1983).

The emittance growth of the particle beam due to the turbulence in the tail of the beat-wave train may be a problem for ultra-high energy accelerators because of their very stringent (Richter, 1985) emittance requirements in higher energies. A possible cure is to inject laser beams in a different spot of a fresh plasma at a different repetition of particle beam injection in order to avoid the interference of the plasma turbulence on the beat-wave growth process we discussed in the above and the enhancement of emittance of the particle beam. Fortunately, the group velocity of the plasma wave out of the beat-wave excitation region is small, i.e., $v_{gr} = 3(k_\perp \lambda_{De}) v_e$, where $k_\perp$ is the

perpendicular plasma wavenumber. Therefore, the contaminated plasma wave does not quickly propagate so that the next shot does not have to be aim very far out of the area shone by laser beams away from the previous shot spot. In addition there is a tendency of plasma waves to spatially coalesce and collapse together (Nishikawa et al., 1975).

VII. LASER STAGING FOR BEAT-WAVE ACCELERATOR

The phase velocity of the beat plasma wave Eq. (5) is less than c, which introduces a phase slippage between the plasma wave and high energy particles in a matter of the longitudinal dephasing time given by Eq. (31). In addition there remains a question of the pump depletion of laser beams. According to Horton (1985) the pump depletion length L_{pd} is expressed as

$$L_{pd} = L_{\ell p} \frac{1}{\hat{\xi}^2} \times \left(\frac{E_0^2}{4\pi mnc^2}\right) , \tag{120}$$

where $\hat{\xi} = \omega_p \xi / c$ and $L_{\ell p}$ is the laser pulse length. The relativistically detuned saturation level for $\hat{\xi}$ is given by Eq. (113) as $\hat{\xi}^2 = 16(\lambda/3)^{2/3}$. This yields the condition

$$L_{pd} = \frac{3^{2/3}}{4} \lambda^{1/3} \left(\frac{\omega_0}{\omega_p}\right)^2 L_{\ell p} . \tag{121}$$

On the other hand, the laser pulse length $L_{\ell p}$ should be taken

larger than the beat-wave growth length, which is evaluated by using Eq. (114) and $\lambda = a_0 a_1/4$ as

$$\frac{L_{\ell p}}{c} \geqslant T = \frac{L_{sat}}{c} = \frac{3.9}{\omega_p} \lambda^{-2/3} . \tag{122}$$

Employing Eq. (122) in Eq. (120), we obtain

$$\tau_{pd} = \frac{L_{pd}}{c} \geqslant 3^{2/3} \lambda^{-1/3} \left(\frac{\omega_0}{\omega_p}\right)^2 \frac{1}{\omega_p} . \tag{123}$$

If the laser pulse length is taken equal to the beat-wave growth length for reasons of efficiency, avoiding noisy plasma and others, τ_{pd} is equal to the right-hand side in Eq. (123). In this case the pump depletion time is not much different from the longitudinal dephasing time Eq. (31) and the acceleration time Eq. (16). It is thus important to devise a method of supplying fresh laser power over the pump depletion length L_{pd} or that of amplifying the laser beam while it is used for acceleration (in situ amplification). In this section we (Tajima, Witte, and Singer, 1985) introduce a concept of laser staging for the beat-wave accelerator.

In order to cope with the pump depletion and/or the longitudinal dephasing, we inject fresh laser beams at a certain interval of length over L_{pd} given by Eq. (123). In order to ease the difficulty to compensate the consumed laser power used for acceleration, distributed amplifiers amplify the master laser beam at the site of the acceleration. In order to cope with the matching the phase in different acceleration modules, all modules

share one master oscillator. In order to adjust the optical path difference, we introduce path adjusters. Figure 24 shows the schematic description of our laser staging concept. [We have come to realize that after we finished this research a similar concept had been reported by Pellegrini (1982) for far field accelerators.] This architecture of the beat-wave accelerator consists of the following features: (i) distributed laser staging optically connected by the master oscillator; (ii) optical delay lines synchronizing the timing and phase of each laser stage; (iii) appropriate mirror and filter systems; (iv) optical guides (plasma fiber) as discussed in Sec. V to trap laser beams created by acoustic transducers or other mechanisms. If necessary, additional collector devices may be added to collect any unused portion of laser power and to convert it for reuse.

The individual accelerator module should stack up in tandem until the desired energy of particles is reached. Each module is separated by a distance of the laser pump depletion length plus the mirror focal length. As we have noted in the above, under the circumstance of most typical operations of the beat-wave accelerator the longitudinal dephasing length is close to the pump depletion length. Therefore, this concept of laser staging conveniently satisfies both requirements for the module repetition length arising from the pump depletion and from the dephasing simultaneously.

Although more research is due in the future, excimer lasers seem favorable lasers for staging in situ for several reasons (Tajima et al., 1985) including possible high efficiency, possible

high repetition rate, reasonable gain, fairly short wavelength etc. One example is a XeCl laser.

VIII. LUMINOSITY

As discussed in the Introduction, an ultra-high energy accelerator must be able to deliver increasingly larger luminosity because the cross-section of collision events becomes diminishingly small ($\sigma \propto E_{cm}^{-2}$). See Fig. 35. In order to meet this demand we face many difficulties. One obvious difficulty is the total energy that needs to be supplied to the accelerator. In short, in order to increase the luminosity, more particles are desired and at the same time individual particles now have to carry more energy, which contradicts with the upper limit for available power. In order to avert this dilemma, we have to pose tough conditions on other requirements.

The luminosity for two colliding beams with one interaction region may be written as

$$\mathscr{L} = \frac{N^2 f}{\pi a_\perp^2} , \qquad (124)$$

where N is the number of particles in one beam, f the frequency of the beams, and $a_\perp$ the radius of the focused beam at collision. In order to alleviate unreasonable demands for laser energy to meet both the high luminosity and the high energy requirements, from Eq. (124) we are forced to have a high repetition rate (large f) or small beam focal size (small $a_\perp$) or both. The repetition rate of

the beam bunch is determined by (i) the overall laser pulse repetition rate and (ii) the number of plasma wave ridges per laser pulse. The first is governed by the laser capability of recovery, and let us take the number of pulses per second as 10 for the sake of the argument here. The second is determined by the laser pulse length and the wavelength of the plasma wave. For example, if the laser pulse is 0.5 nsec and $\omega_0/\omega_p = 33$ (plasma density $9 \times 10^{15}/cm^3$ for a CO_2 laser), the number f is $\sim 3 \times 10^4$/sec. If the same numbers are used with a KrF laser, f is $\sim 8 \times 10^5$/sec.

With the repetition rate f roughly determined, the only parameter we can work with is the focal size of the particle beam (beam radius $a_\perp$). In particle beam optics it is well known that the hot beam or high emittance beam is difficult to focus on a small spot. It is detrimental, therefore, to have hot (in the perpendicular temperature) electrons (or ions).

It is known (Hollebeek, 1981; Keil et al., 1979; Rees, 1984) that the colliding beam machine will have two mechanisms of a fundamental physical nature that potentially determine the maximum luminosity attainable. They are the beam disruption and the beamstrahlung. Both are fundamental arising from the plasma properties at the collision point. The physical phenomenon that shows up in the highly focused collider beams is the beam-beam (two-stream) instability. This is the beam disruption. Thus the beam disruption is primarily an electrostatic phenomenon. On the other hand the beamstrahlung is a collective synchrotron radiation process when the counterstreaming beams pinch by self-magnetic fields if two beams have opposite charge. Thus the beamstrahlung

is primarily an electromagnetic phenomenon. Beam disruption is indicated by the disruption parameter D exceeding a value of the order of unity. The condition for avoiding disruption (Hollebeek 1981) is

$$D \equiv \frac{r_e \ell_b N}{\gamma a_\perp^2} \lesssim 1\text{~}10 \ , \tag{125}$$

where r_e is the classical electron radius (e^2/mc^2), and ℓ_b is the particle beam length. Equation (125) can be looked upon a condition to determine the bunch length ℓ_b if the upper maximum for D is taken:

$$\ell_b \simeq (1\text{-}10)\ \pi a_\perp^2 \gamma D/(r_e N) \ . \tag{126}$$

Equation (126) shows that if the beam length is small, the radius of the beam can be small without disruption. The disruption parameter D can be rewritten as

$$D = \frac{1}{4}\frac{\ell_b^2 \omega_b^2}{c^2} = \frac{1}{4}\left(\frac{\tau_s}{\tau_b}\right)^2 \ , \tag{127}$$

where $\omega_b = (4Ne^2/\gamma m a_\perp^2 \ell_b)^{1/2}$ the beam plasma frequency, $\tau_s = \ell_b/c$ the beam streaming (transit) time, and $\tau_b = \omega_b^{-1}$ the beam plasma time. The particle beam power P is expressed as

$$P = fN\gamma mc^2 \ . \tag{128}$$

In terms of the particle physics requirements on γ and $\mathscr{L}$ and the realizability requirement on power P, we eliminate the number of particles N from Eq. (124) to obtain

$$\pi f a_\perp^2 = \frac{P^2}{\mathscr{L}(\gamma mc^2)^2} \quad . \tag{129}$$

If the repetition rate f is given by the other realizability requirement from laser technology, the required colliding cross-section is given as

$$\pi a_\perp^2 = \frac{P^2}{f\mathscr{L}(\gamma mc^2)^2} \quad . \tag{130}$$

With f given by laser requirements we have the number of particles in a bunch as

$$N = \frac{P}{f\gamma mc^2} \quad . \tag{131}$$

For a hadron (or a muon) collider, it is likely that the disruption effect is a more important factor than the beamstrahlung that determines the maximum luminosity. The disruption-limited luminosity is expressed by substituting D in Eq. (125) into Eq. (124):

$$\mathscr{L} = \frac{\pi n_b^2 \ell_b^2 r^4 f}{a_\perp^2} = \frac{PD}{\pi e^2 \ell_b} \quad , \tag{132}$$

where n_b is the beam particle density before focus in the laboratory frame, and r is the beam radius before focus. With condition Eq. (125), the luminosity, Eq. (132), is expressed as

$$\mathscr{L} \lesssim 10\pi n_b r^2 f\gamma r_e^{-1} \quad . \tag{133}$$

If we assume $n_b \sim 10^{-1} n_p$, the plasma density, $\mathscr{L} \lesssim \pi n_p f^2 f\gamma r_e^{-1}$. This indicates that the luminosity increases as n_p and f increase. As is clear from our earlier discussion, the plasma density $n_p \propto \lambda_\ell^{-2}$ when ω_0/ω_p is fixed, where λ_ℓ is the laser wavelength. This way the luminosity goes like λ_ℓ^{-2}. In the hadron machine (and also in the muon machine) the synchrotron radiation is down by a factor of $(M/m)^4$ from that for an electron counterpart, where M/m is the ratio of hadron (or muon) to electron mass. Thus, even in an ultra-high energy regime the beamstrahlung is unlikely to limit the luminosity in a hadron (or muon) collider.

The muon-muon or muon-hadron collider (Neuffer 1983)is unique. The nature almost duplicates itself with the electronic construct being almost identical to the munonic (and tau) construct, although there exists a significant mass difference, which makes it possible for the muon accelerator to adopt strong magnetic fields. In addition, according to Glashow, muonic collision provides much larger cross-section for the creation of the hypothetical Higgs' particle. With its long life time, the "heavy" lepton, muon, collider should play a much more important role in the future ultra-high energy accelerator, possessing two of the best worlds: (i) collisions of structureless particles as a lepton

makes experiments easy; (iii) the heavy mass of the muon makes the synchrotron and beamstrahlung not as much important to concern as for electron colliders.

On the other hand, in the electron collider, beamstrahlung looms as the most troublesome process at the focus. Although the beamstrahlung enhances the luminosity to a certain degree by its pinching effect (Hollebeek, 1981) on one hand, it will destroy the beam and also loses lepton energy off synchrotron radiation. The beamstrahlung-limited luminosity may be derived as follows. The beamstrahlung parameter δ is defined as the ratio of the energy loss of the beam due to synchrotron radiation to the initial beam energy

$$\delta = \frac{\Delta\varepsilon}{\gamma mc^2} . \tag{134}$$

Using the magnetic acceleration $dp/dt = eB_\theta$ and Ampere's law $B_\theta = 2eN/a\ell$ where ℓ is the focal length, we have

$$\delta = \frac{2e^4B^2\gamma^2}{3m^2c^3}\left(\frac{\ell}{c}\right) = \frac{8}{3}\gamma r_e^3 N^2\left(\frac{\ell}{a_\perp^2 \ell_b^2}\right) . \tag{135}$$

At this point one should check whether δ is sufficiently less than unity or not in Eq. (135). If δ turns out to be unacceptable for particle physics point of view, one should go back to change the originally given parameters. It is also possible to write the luminosity in terms of the beamstrahlung parameter δ. Eliminating N^2 in Eq. (124) by using Eq. (135), we obtain

$$\mathscr{L} = \frac{3}{8\pi}\left(\frac{\ell_b^2/\ell}{r_e^3}\right)\left(\frac{f}{\gamma}\right)\delta \quad . \tag{136}$$

Experimentalists might want to limit $\delta < 10^{-2}$. Thus, given δ, the luminosity becomes independent of the focal size and the number of beam particles. The expression Eq. (138) is also independent of the laser wavelength. The condition for an acceptable beamstrahlung parameter for experiments determines the number of beam particles as

$$N^2 = \left(\frac{a_\perp^2 \ell_b}{r_e^3}\right)\left(\frac{\delta}{\gamma}\right) \quad . \tag{137}$$

As the energy of the beam goes up, we have to reduce the beam focal size in order to keep the luminosity Eq. (124) and the total energy of acceleration $\varepsilon \cong NE\eta$ constant, where E is the energy of an individual particle and η the acceleration efficiency. It is quite a technical challenge to reduce $a_\perp$. At the same time there arise a number of physics questions associated with this. Some of them have already been discussed, namely the beamstrahlung and disruption. Let us first look at synchrotron radiation power loss.

$$P = \frac{2}{3}\frac{e^2}{m^2c^3}\gamma^2\left(\frac{dp}{dt}\right)^2 = \frac{2}{3}\frac{e^4B^2}{m^2c^3}\gamma^2 = \frac{2}{3}\omega_c^2 r_e\, mc\gamma^2 \quad , \tag{138}$$

where $dp/dt \simeq eB_\theta$ and $\omega_c = eB/mc$. A possible way to reduce the

synchrotron loss by self-pinch is to apply a longitudinal magnetic field (see Fig. 36). Here the longitudinal magnetic field B_t may be either the external field or the enhanced external field by the compression of trapped external fields upon pinch. To stabilize beamstrahlung by B_t, we need

$$v_\perp B_t \cong v_\parallel B_\theta \ , \tag{139}$$

where $v_\perp$ is the electron velocity perpendicular to the propagation due to B_θ and $v_\parallel$ the parallel velocity. According to Eq. (135),

$$\beta_\perp = \frac{v_\perp}{c} = \frac{(3/2)^{1/2}}{\gamma} \left(\frac{\delta}{\gamma}\right)^{1/2} \left(\frac{\ell}{r_e}\right)^{1/2} \ , \tag{140}$$

where we used

$$\Delta p_\perp \sim \frac{dp_\perp}{dt} \frac{\ell}{c} \sim \delta^{1/2} \left(\frac{3m^2c^3\ell}{2e^2\gamma^2 c} \gamma mc^2\right)^{1/2} \ .$$

From Eq. (139), we obtain the longitudinal field necessary as

$$B_t = \left(\frac{2\gamma^3 r_e}{3\ell\delta}\right)^{1/2} \frac{2eN}{a_\perp \ell_b} \ , \tag{141}$$

or in terms of the luminosity

$$B_t = \left(\frac{2\pi\gamma^3 r_e a^2}{3\ell\delta f}\right)^{1/2} \frac{2e}{a_\perp \ell_b} \ . \tag{142}$$

For typical parameters the necessary magnetic field seems too high under present technologies. A thought would be to use a spin-polarized electron (positron) beam so that the spin magnetization contributes to the stabilizing influence against the pinching (see Fig. 36c). However, with Bohr's dipole moment $\mu_B = e\hbar/2mc$ a very strong degeneracy of plasma at focus is required under typical parameters.

It is important to make sure, of course, that an energy gain of a particle due to accelerating fields is larger than an energy loss of the particle due to other effects. One of the worries may be that the laser electromagnetic fields may shake electrons (or hadrons) so that they emit and thus lose energy. It is convenient to compare these in the particle frame (and assume that is also the plasma wave phase frame). First the acceleration gain $\Delta\varepsilon = c\Delta p_{\parallel}$ is given by

$$W_a = c\,\frac{dp_{\parallel}}{dt} = ceE_{\parallel} = \alpha' mc^2\omega_p \ , \qquad (143)$$

where $E_{\parallel}$ is invariant and $E_{\parallel} \equiv \alpha' m\omega_p c/e$ is used, where $\alpha' \lesssim 1$. On the other hand, the deceleration loss due to the laser electromagnetic fields in this frame is essentially through synchrotron radiation (radiation loss) and is given by

$$W_d = \frac{2}{3}\,\frac{e^2\gamma^2}{m^2c^3}\left(\frac{dp'}{dt}\right)^2 \ , \qquad (144)$$

where p' is the particle momentum in this frame. The laser fields

and particle momentum are transformed from the laboratory frame (without primes) to this frame (with primes) as

$$E' = \gamma(E - \beta B) = \frac{1}{\gamma} E \ , \tag{145}$$

$$B' = \gamma(B + \beta E) = 0 \ , \tag{146}$$

and

$$p' = \gamma\left(p - \beta \frac{\varepsilon}{c}\right) \ , \tag{147}$$

$$\varepsilon' = \gamma(\varepsilon - \beta c p) \ , \tag{148}$$

where γ and β are the same as in Eq. (14). Important things to note here are that the transverse electric field E′ is reduced by a factor $1/\gamma$ from the laboratory value E and that the laser magnetic field B′ vanishes. Thus the loss is calculated as

$$W_d = \frac{2}{3} \frac{e^4 E_0^2}{m^2 c^3} \ , \tag{149}$$

where E_0 is the laser field in the laboratory frame. The ratio of Eq. (148) to Eq. (143) is

$$\frac{W_d}{W_a} = \frac{4\pi}{3} \frac{\alpha^2}{\alpha'} \frac{r_e}{\lambda_\ell} \frac{\omega_0}{\omega_p} \ , \tag{150}$$

where $E_0 \equiv \alpha m \omega_0 c/e$ and ω_0 is the laser frequency. The ratio Eq. (150) is typically much less than unity, by many orders of magnitude. Because of the closeness of the phase velocity of

plasmons to c, the energy loss due to the laser electromagnetic fields turns out to be very small.

In addition to the disruption and the beamstrahlung at the focal spot of the particle beams, the following problem may restrict the luminosity. As we inject a high energy beam of particles which are accelerated by the plasma electric field, this beam will emit plasma oscillations due to the beam-plasma interaction. This process is analogous to the Cerenkov radiation by fast charged particles in a medium. Here the role of photons in the Cerenkov process is replaced by the plasmon emission. Such a process may be looked upon in terms of Van Kampen's picture (Van Kampen, 1955; Leboeuf and Tajima, 1979a). The beam-plasma instability tries to trap electrons in the induced plasma wave and to slow down electrons if the beam is unimpeded. It would execute trapping oscillations (O'Neill, 1965) in phase space.

In order to avoid this beam electron trapping and the slow-down of the beam, therefore, the electrostatic field created by the beat plasma wave due to the laser ponderomotive force has to exceed the tendency of the trapping effect (Leboeuf and Tajima, 1979b). In other words, the beam has to run away the plasma all the the time by virtue of electrostatic acceleration by the beat plasma wave. The critical field above which the accelerated particle beam (density n_b) does not emit plasma waves and thus no drag is given by Leboeuf and Tajima (1979b) as

$$E_{cr} = \left[4\pi n_b \gamma mc^2 S(1+S)^{-5/2}\right]^{1/2} \qquad (151)$$

where $S = \gamma(n_b/2n_p)^{1/2}$ with n_p the plasma density. This may result in one or both of the following. (i) The higher the beam density n_b is, the stronger the tendency for the beam to slow down. We may have to reduce the ratio of beam to plasma densities n_b/n_p to mitigate the beam–plasma interaction, thereby leading to a lower luminosity. (ii) In order to exceed the "drag force" due to plasmon emission, we may need a higher value of electrostatic field. This may lead to a need for more intense lasers or to a lower value of ω_0/ω_p. Detailed studies are called for here.

IX. EXOTIC PROBLEMS

It is clear that many fundamental physics questions as well as technical questions need to be addressed and solved in order to realize an ultra–high energy accelerator. Some of them are related to the unique nature of the present plasma beat–wave accelerator scheme and some to general problems associated with very high energies. One of the difficulties arising from very high energy accelerators is that of luminosity, as discussed in the previous section. Since reducing the beam focal size is perhaps the only approach to ever–higher energies, unique and exotic physics questions can be encountered in these regimes. In this section we speculate on some of these exotic problems.

One of them is severeness of beamstrahlung. Beamstrahlung has already become an issue in present–day lepton colliders such as SLC. Since the beamstrahlung increases very rapidly as the energy increases, this can become a prohibitive problem, as discussed in the previous section. It might be possible, however, to utilize

such beams (e^-e^+ beams) to efficiently convert the particle energy into high photon energies in turn. See Fig. 37. At the collision point the current-unneutralized and charge-neutralized colliding beams produce an intense magnetic field $B_\theta = 2eN/(a_\perp \ell_b)$ (easily exceeding MG), which leads to explosive pinching of beams. If this process, including collective emission of synchrotron radiation as a result of pinch, can occur in a self-similar fashion so that the entire energy of beams is converting into γ-rays, hopefully in high frequency domains, a possibility of a γ-γ collider arises. A theoretical exploration of such a self-similar explosive solution for the collective beamstrahlung would be interesting. If this does not occur in a collective fashion, we should use the Bethe-Heitler formula for the γ-ray spectrum:

$$\frac{d\sigma}{d\omega} \sim \frac{16}{3}\frac{e^2}{c}\left(\frac{e^2}{mc^2}\right)^2\left(1-\frac{\hbar\omega}{E}+\frac{3\hbar^2\omega^2}{4E^2}\right)\left(\ell n\frac{2EE'}{mc^2\hbar\omega}-\frac{1}{2}\right),$$

where the photon cutoff frequency is $\omega = E/\hbar$ instead of the classical value of $\omega_c = 3\gamma^3 c/\rho$ with ρ being the curvature radius of leptons in B_ϑ and $E = \gamma mc^2$ and E' their energies. Recently this point has been well appreciated (Erber, 1966; Noble and Himel, 1985). According to Schwinger (1954) and Klepikov (1954), the radiated power loss by a constant magnetic field in the strong quantum effect limit is

$$P_{QM} \cong 0.5 \times \frac{2}{3} c\alpha \cdot \frac{mc^2}{\lambda_c} \Upsilon^{2/3}, \quad (\Upsilon >> 1)$$

while the classical synchrotron radiation power loss is $P_{c\ell} = \frac{2}{3}\alpha \frac{mc^2}{\lambda_c}\tau^2$, where $\tau = \gamma B/B_{cr}$, $\lambda_c = \hbar/mc$, $\alpha = e^2/\hbar c = 1/137$, and $B_{cr} = m^2c^3/e\hbar$. Such a $\gamma-\gamma$ collider may have its own virtue for experiments because of certain prohibited processes for lepton-lepton collisions. Ginzburg et al. (1981, 1984) proposed colliding γ-e beams and $\gamma-\gamma$ beams using the inverse compton scattering of laser light by an electron beam. The backscattering of laser light by an electron beam upconverts the frequency, creating a γ beam. They argued that in this way one is possible to have more detailed study of $W^{\pm}$ and Z particles as well as gluons.

In the following we present a speculative idea whose central theme is a direct coupling of the macroscopic beam structure with collective modes of the strong interaction (the quark-gluon subnuclear system where the coupling constant $g^2/\hbar c \sim 1$).

To be concrete, let us have two colliding beams of proton and (anti-)proton or proton and electron. It is important to note that for the incoming proton beam (beam 1) with the relativistic factor $\gamma_1 = 10^5$ the structural length ℓ of the counter-streaming proton or electron beam (beam 2) is Lorentz-contracted by the γ_1 factor in the frame of the incoming proton beam,

$$\ell' = \frac{1}{\gamma_1}\ell \ , \qquad (152)$$

where ℓ' is the structural length in the incoming proton beam frame. If the structural length ℓ, such as the length of density modulation of beam 2, is 10^{-8} cm (= 1 Å), the structural length ℓ' in the frame of the incoming beam 1 is 10^{-13} cm (= 1 fermi) and the

period of modulation is $\ell'/c \approx 10^{-23}$ sec. Thus it is possible to collectively excite the strongly interactive subnuclear system by the modulated (or syncopated) beam. The structural length ℓ of 1 Å may be obtained by the Raman backscattering of an electromagnetic wave or the wiggler magnetic fields through the free electron laser mechanism. When the counterstream beam 2 is protons ($\gamma_2 = 10^5$), we shine CO_2 laser light (wavelength 10 μ) against the counterstreaming proton beam; when beam 2 is electrons ($\gamma_2 = 10^8$), we impose wiggler fields with a periodicity of 1 cm. Because of the Lorentz contraction of the original electromagnetic (or magnetic) wavelength λ, the wavelength of the density modulation λ' becomes, in the frame of beam 2,

$$\ell = \lambda' = \frac{1}{2\gamma_2}\lambda \ . \tag{153}$$

The wavelength should be ~1 cm for electron beams of $\gamma_2 = 10^8$ and ~10 μ for proton beams of $\gamma_2 = 10^5$. In either case the beam density at focus should be in the neighborhood of solid density.

Bjorken (1983) has stated that the leading-order interaction in this problem is the beamstrahlung, and excitation by the bunch is a higher-order interaction. Even if this is the case, if the bunch period ℓ'/c is resonant with the collective period of nuclear matter, such as the gluon plasma period, then collective oscillations might be able to grow secularly in time. One of the problems is that the transverse dimension of the beam is so much larger than the size of the target nucleus that the bunched beam or its photons may be far apart in the transverse dimension. It

should be noted, however, that such investigations may open the door to a possible "nuclear wave accelerator" mediated by macroscopic bunches of particles or photons.

X. BEAT-WAVE CURRENT DRIVE

It is also possible to apply the present beat-wave process to the current drive in a magnetically confined fusion plasma: large currents can be efficinetly driven by the ponderomotive force created by the beating of two electromagnetic waves. The beating waves can be cyclotron waves propagating parallel to the magnetic field or light waves propagating obliquely to the magnetic field.

The ultimate feasibility of tokamak fusion reactors may critically depend on the possibility of maintaining the toroidal current in the plasma in steady-state or quasi steady-state operation. Present devices rely entirely on inductive current generation which is not appropriate for steady-state operation. Various schemes have been proposed for non-inductive current drive using injection of neutral particles (Ohkawa, 1970), rotating magnetic fields (Hugrass, 1982), electromagnetic waves (Fisch, 1978), etc. Of particular relevance is the current drive by radio-frequency waves because the power sources are readily available, the basic theoretical aspects are reasonably understood, and the scheme is attractive from an engineering point of view (Ehst, 1979).

Here we propose a nonlinear mechanism for current drive by electromagnetic waves (Galvao and Tajima, 1985). Two strong electromagnetic waves are made to beat at the characteristic

frequency of an electrostatic plasma mode. Particles trapped in the potential well of the ponderomotive force are accelerated and cause an elongation of the distribution function, generating current. The mechanism is similar to the one we have mentioned in the application to accelerators; but there are differences. In the laser beat-wave accelerator, the electrostatic (plasmon) mode is produced by forward scattering and its velocity is meant to be the speed of light. For successful current drive, the phase velocity of the driven electrostatic mode has to be a few times the thermal velocity of the electrons of the plasma. This can be achieved by backward scattering or even by forward scattering of fast electromagnetic waves under proper conditions. In particular, we consider two possibilities for nonlinear current drive: i) two cyclotron waves propagating parallel to the magnetic field $\vec{B}$ and beating to produce an electrostatic magnetized plasma mode and ii) two laser beams propagating obliquely to $\vec{B}$ and backscattering at the upper hybrid resonance layer. These two processes can be efficient in high magnetic field devices such that $\Omega > \omega_p$, where Ω and ω_p are respectively the gyrofrequency and the plasma frequency of the plasma electrons. In the following we consider explicitly the current generation by the beating of cyclotron waves and also indicate the results for current generation by the laser excitation of the upper hybrid mode.

Consider two strong waves (ω_0, k_0) and (ω_1, k_1) propagating in the direction parallel to $\vec{B}$. We assume that the amplitude of the waves are approximately constant and that the matching conditions $\omega_0 - \omega_1 = \omega$ and $k_0 \pm k_1 = k$ are fulfilled over a certain distance

somewhere in the plasma. Here ω and k are respectively the frequency and wavenumber of an electrostatic plasma mode. The low-frequency plasma oscillations are described by equations similar to Eqs. (73)-(76):

$$\frac{\partial n}{\partial t} + \nabla \cdot (n_0 \vec{v}) = -\nabla \cdot \left[n^{(0)} \vec{v}^{(1)} + n^{(1)} \vec{v}^{(0)} \right] , \qquad (154)$$

$$\frac{\partial \vec{v}}{\partial t} - \frac{e}{m} \nabla \varphi + \Omega \left(\vec{v} \times \frac{\vec{B}}{B} \right) + \gamma \frac{v_e^2}{n_0} \nabla n$$

$$= -\vec{v}^{(0)} \cdot \nabla \vec{v}^{(1)} - \vec{v}^{(1)} \cdot \nabla \vec{v}^{(0)} - \frac{e}{m} \left(\vec{v}^{(0)} \times \vec{B}^{(1)} + \vec{v}^{(1)} \times \vec{B}^{(0)} \right) \qquad (155)$$

and $$\nabla^2 \varphi = 4\pi e n_e , \qquad (156)$$

where $n, \vec{v}$, and φ are respectively the perturbed density, velocity, and electrostatic potential of the low-frequency mode, n_0 is the equilibrium density, v_e is the thermal speed of the electrons, and $n^{(i)}$, $\vec{v}^{(i)}$, and $\vec{B}^{(i)}$, i=0,1, are respectively the perturbed density, velocity, and magnetic field of the high-frequency cyclotron modes. Using the appropriate expressions (Tajima, 1977) for $n^{(i)}$, $\vec{v}^{(i)}$, and $\vec{B}^{(i)}$, i=0,1, it is easy to show that $n^{(i)} \vec{v}^{(j)} = \vec{v}^{(i)} \cdot \nabla \vec{v}^{(j)} = 0$, $i \neq j$. Thus, only the $\vec{v} \times \vec{B}$ term in Eq. (155) provides a nonlinear force. Calculating this term, substituting in Eq. (155), and carrying out the phase average over the high-frequency oscillations, Eqs. (154)-(156) can be reduced to a single equation for the low-frequency density perturbation

$$\frac{\partial^2 n}{\partial t^2} - \gamma v_e^2 \frac{\partial^2 n}{\partial x^2} + \omega_p^2 n = -n_0 \Lambda \sin(kx-\omega t) \ , \qquad (157)$$

where

$$\Lambda = v_{os}^{(0)} v_{os}^{(1)} \left(\frac{k_0}{1 - \frac{\Omega}{\omega_1}} \pm \frac{k_1}{1 - \frac{\Omega}{\omega_0}} \right) k \ , \qquad (158)$$

$v_{os}^{(i)} = \frac{eE^{(i)}}{m\omega_i}$, i=0,1, and $E^{(i)}$ is the amplitude of the corresponding high-frequency wave. Equation (158) is the equation for a harmonic oscillator driven at its resonance frequency. The solution is given by

$$n(t) = n_0 \tilde{\Lambda} t \ \sin(kx-\omega t- \frac{\pi}{2}) \ ; \qquad (159)$$

where $\tilde{\Lambda} = \Lambda/2\omega$ and $\omega^2 = \omega_p^2 + \gamma k^2 v_e^2$. Equation (159) is a generalization of the result obtained by Rosenbluth and Liu (1972) for the beating of light waves and those equations discussed in Sec. VI. As the electrostatic energy increases, particles in the bulk of the distribution function begin to be trapped and the growth is curbed by strong nonlinear Landau damping and nonlinear frequency shift not included in this simple fluid model. The saturation time can be estimated by requiring that the oscillation velocity in the electrostatic potential, $|2e\varphi/m|^{1/2}$, be of the order of the thermal velocity. Using Eqs. (157), (158), and (159),

we find $\tau_s \approx k^2 v_e^2 \omega / \Lambda \omega_p^2$. For $v_{os}^{(0)} = v_{os}^{(1)} = v_{os}$, this reduces to $\tau_s \approx (v_e/v_{os})^2 \omega_p^{-1}$.

To check the results of our fluid model, we have carried out computer simulations employing the same particle code. Two right-hand circularly polarized waves with wave numbers k_0 and k_1 are imposed on an initially uniform thermal plasma. The waves propagate in the x-direction. The plasma parameters are chosen such that $\Omega/\omega_p \simeq 1.6$ and $v_e/c \simeq 0.1$. The frequencies of the two electromagnetic waves are given by $\omega_0/\omega_p = 3.5$ and $\omega_1/\omega_p = 2.4$, such that they are in the upper fast branch of the dispersion curve for cyclotron waves. The system has typically a length $L_x = 512\Delta$, the wave numbers of the electromagnetic waves are given by $k_0 = 2\pi \times 29/512\Delta$ and $k_1 = 2\pi \times 15/512\Delta$. The number of particles in each species is 5120, and the particle size is 1Δ with a Gaussian shape, where Δ is the unit spatial grid distance and is equal to the Debye length. The intensity of the electromagnetic waves is chosen such that $v_{os}/c = 0.01$.

The electron distribution function at $t = 0$ and after a time $t = 22\omega_p^{-1}$ are shown in Figs. 38(a) and 38(b), respectively. In this case, the matching conditions are such that the phase velocity of the electrostatic wave is about $3v_e$. Accordingly, the electron distribution function develops a positive tail leading to current generation. The electrostatic energy density and the driven current density are shown in Figs. 38(c) and 38(d), respectively. The current density is normalized to nev_e. Both the electrostatic energy density and current density tend to nonlinearly saturate after the initial growth. At a time $\tau_s \approx 24\omega_p^{-1}$, the current

density reaches a peak value $j/nev_e \approx 0.2$ and oscillates afterwards. A similar value for j is obtained for $v_{os}/c = 0.1$ at a much shorter time. The value of the saturation time in the numerical simulations is somewhat smaller than the one predicted by our rough model, i.e., $\tau_s \approx (v_e/v_{os})^2\omega_p^{-1} = 100\omega_p^{-1}$. This indicates that the nonlinear frequency shift also plays a role in the saturation mechanism.

After the saturation value of the current density is reached, the source can be turned off and the current be left to collisionally relax until the next pulse. For a plasma with $T_e \approx 5keV(v_e/c \approx 0.1)$ and $n = 10^{14}cm^{-3}$ and for $v_{os}/c = 0.01$, the collision and saturation times are about $50\mu sec$ and $5 \times 10^{-5}\mu sec$, respectively. Thus, steady-state operation can be obtained by a sequence of very short pulses. The width of each pulse cannot always be made of the order of τ_s because the minimum width of the pulse in gyrotrons is limited by the transit time of the electrons in the resonant cavity. For $v_{os}/c = 0.01$, this time is longer than the saturation time τ_s. For smaller values of v_{os}/c, i.e., for smaller intensities of the beating waves, the two times can be made of the same order.

The ratio between the current density and the power density dissipated to drive the current, j/P, is considered to be an important parameter to measure the local efficiency of different schemes for current drive. However, in the beat-wave scheme, the crucial parameter is the intensity of the electromagnetic waves required to induce the nonlinear process. The maximum intensities that are achievable with lasers range from approximately $10^{16}W/cm^2$

for CO_2 to 10^{18} for Nd-Yag lasers. For microwaves, the maximum intensities are limited to approximately $10^8 W/cm^2$ by breakdown problems in the waveguides. In our simulation, we have obtained a saturated current of $j \approx 0.2 n e v_e$ for $v_{os}/c = 0.01$ and $v_e/c = 0.1$. Taking $n = 10^{14} cm^{-3}$, we obtain $j \approx 10 kA/cm^2$. This is much larger than the average value of the current density in actual devices, i.e., $j < 1 kA/cm^2$. The required intensity to obtain such a current is $I \approx 1.4 \times 10^8 (v_{os}/c)^2/\lambda_0^2$, where I is given in W/cm^2 and λ_0 is the wavelength of the electromagnetic waves ($\lambda_0^{(1)} \approx \lambda_0^{(2)} \approx \lambda_0$) in microns. In actual applications, the current pulses can be decreased almost an order of magnitude. This can be done by decreasing the intensity of the electromagnetic waves which also leads to an increase in the saturation time τ_s.

To estimate the average j/P parameter, let us represent the current density by $j = \Delta n e(\omega/k)$, where Δn is the average density increase related to the trapped particles. The power lost by collisional dissipation is given by $P = \Delta n [m(\omega/k)^2/2] \nu$, where ν is the electron-ion collision frequency. Thus,

$$\frac{j/(n_0 e v_e)}{P/(n_0 m v_e^2 \nu)} \approx 2 \frac{v_e}{\omega/k} \quad (160)$$

This is a number of order one, comparable to the value of the j/P parameter for the scheme of current drive by lower hybrid waves (Fisch, 1978; Ehst, 1979).

Finally, let us briefly discuss the possibility of driving currents by the nonlinear excitation of the upper hybrid electrostatic mode. The upper hybrid waves near the center of a tokamak plasma cannot be easily excited by linear conversion of electromagnetic waves propagating inwards because of the evanescent domain between the cut-off and upper hybrid resonance layers. This problem can be alleviated by using the beat of two high-frequency light waves. Consider two laser beams (ω_0,k_0) and (ω_1,k_1) propagating at an angle α with the magnetic field, such that $\cos\alpha << 1$. Because the phase velocity of the light waves is approximately c, the electrostatic mode generated by the beating of the laser beams has also a phase velocity close to c for forward scattering. However, using backscattering, it is possible to obtain a Doppler-shifted phase velocity $(\omega-\Omega)/k\cos\alpha$ close to v_e, in the direction of $\vec{B}_0$. By properly choosing the matching conditions $\omega_0-\omega_1 = \omega_{uh}$ and $k_0+k_1 = k$ and the angle α, it is possible to excite the upper hybrid electrostatic mode with a parallel Doppler-shifted phase velocity of a few times the thermal velocity and drive current. Using a fluid model similar to the one described before, we find that the electrostatic fluctuations increase linearly with time according to Eq. (159), with $\tilde{\Lambda}$ replaced by

$$\tilde{\Lambda}_{uh} = \frac{1}{4}\, v_{os}^{(0)} v_{os}^{(1)} \frac{(\omega^2-\Omega^2\cos^2\alpha)}{\omega^2} \left[\frac{k_0\omega_1^2(\omega_0^2-\Omega^2) + k_1\omega_0^2(\omega_1^2-\Omega^2)}{(\omega_0^2-\Omega^2)(\omega_1^2-\Omega^2)}\right] \frac{k}{\omega}, \quad (161)$$

where ω and k are related by the dispersion relation for (nearly) electrostatic upper hybrid waves (Stix, 1965).

XI. CONCLUSIONS

We have studied the crucial physical problems associated with the laser beat-wave accelerator and its outgrowths. Since the inception of the idea of the laser electron accelerator (Tajima and Dawson, 1979a), many studies have been carried out. It seems that the original idea is still viable, tested and supported by computer simulations (Tajima and Dawson, 1979b; Sullivan and Godfrey, 1981; Kindel and Forslund, 1983; Sullivan and Tajima, 1984), by a preliminary experiment (Joshi et al., 1981), and by a more recent experiment (Joshi, 1985). The concept needs much more study and many more experiments to substantiate, as we pointed out wherever the issues were raised throughout the present paper.

A number of areas of development are called for. The development of powerful lasers for accelerator purposes requires emphasis different from that for fusion research. Although at the moment the gaseous CO_2 laser technology is convenient for the present purpose, shorter-wavelength lasers such as KrF and XeCl lasers may be useful for shorter machine sizes and higher luminosities. Since a high repetition rate and high efficiency for the laser is required, the development of gaseous lasers or excimer lasers may prove to be more appropriate than that of glass lasers. High efficiency for the laser is essential because otherwise the total energy consumption of the accelerator will be quite large. It seems crucial to have a short pulse for the laser in order to

avoid various plasma instabilities and noise effects. In this regard the progress toward femtosecond pulses of CO_2 lasers (Corkum, 1983) is important and more efforts should be pursued.

Although many studies have been carried out for intense laser-plasma interaction, they have been primarily target experiments appropriate for the fusion study. Experiments with a uniform axial density have to be carried out to study the intense laser-plasma interaction in an environment necessary for the present purpose. Theoretical developments on two-dimensional effects such as self-focusing, filamentation, refraction, fiber stability, fiber wall resonance, laser injection, ray dynamics, emittance, etc. have to be pursued. In terms of luminosity, when the beams are extremely narrowly focused, there will be technical questions of whether mechanically we can collide them. In addition, the plasma density at the focus will become so high that the usual gaseous treatment of plasmas for beamstrahlung studies may have to be modified to include high correlation effects in high densities (Ichimaru, 1982). We hope that research developments out of the present concept or a completely different new one eventually make it possible for physicists to push forward the frontier of our knowledge of this physical world.

ACKNOWLEDGMENTS

The author would like to thank J. Bjorken, N. Bloenbergen, J.M. Dawson, F. Felber, W. Horton, R. Huson, C. Joshi, J. Lawson, J. Mulvey, K. Mima, D. Neuffer, B. Richter, M.N. Rosenbluth, A. Salam, A. Sessler, S. Singer, R.N. Sudan, D. Sullivan, M. Tigner, P. Wilson, and W. Willis for stimulating discussions, encouragement and interest. The work was supported by U.S. Department of Energy Contract No. DE-FG05-80-ET53088, National Science Foundation Grant ATM82-14730, and U.S. Department of Energy subcontract No. A-X63-3247M through Los Alamos National Laboratory, and the Texas Accelerator Center.

REFERENCES

AKHMANOV, S.A., SUKHORUKOV, A.P., and KHOKHLOV, R.V. 1968 Sov. Phys. Uspekhi 93, 609.

AMHERD, M.N. and VLASES, G.C. 1974 Appl. Phys. Lett. 24, 93.

ASHOUR-ABDALLA, M., LEBOEUF, J.-N., TAJIMA, T., DAWSON, J.M., and KENNEL, C.F. 1981 Phys. Rev. Lett A23, 1906.

BERNSTEIN, B., and SMITH, I., 1973 IEEE Trans. Nucl. Sci. 3, 214.

BJORKEN, J. 1983 (Fermi Lab), Private communication.

BUDKER, G.I. 1956 Proc. CERN Symp. on High Energy Accelerators and Ion Physics, E. Regenspreif, Ed., Vol. 1, p. 68, European Organization

CHAN, Y.W. 1971 Phys. Lett. 35A, 305.

CHANNEL, P.J. 1982 Laser Acceleration of Particles, AIP Conf. Proc. 91, New York.

CHEN, P., DAWSON, J.M.HUFF, R.W. and KATSOULEAS, T. 1985 Phys. Rev. Lett. 54, 693.

CLARRICOATS, P.J.B. 1976 Progress in Optics vol. XIV, ed. by E. Wolf,

COHEN, B.I., KAUFMAN, A.N., and WATSON, K.M. 1972 Phys. Rev. Lett. 29,581.

CORKUM, P. 1983, Opt. Lett. 8, 514. p. 329.

DAWSON, J.M., SHANNY, R. 1968 Phys. Fluids 11, 1506.

DECOSTER, A. 1978 Phys. Rep. 47, 285.

EHST, D. 1979 Nucl. Fusion 19, 1369.

ERBER, T. 1966 Rev. Mod. Phys. 38, 626.

FELBER, F.S. 1980 Phys. Fluids 23, 1410.

FELBER, F.S., CHERNIN, D.P. 1981 J. Appl. Phys 52, 7052.

FERMI, E. 1949 Phys. Rev. 75, 1169.

FISCH, N.J. 1978 Phys. Rev. Lett. 41, 873.

GALVAO, R.M.O., TAJIMA, T. 1985 to be published.

GINZBURG, I.F., KOTKIN, G.L., DANFIL, S.L., SERBO, V.G., and TELNOV, V.I. 1984 Nucl. Instr. and Meth. 219, 5.

GINZBURG, I.F., KOTKIN, G.L., SERBO, V.G., and TELNOV, V.I. 1981 Pisma ZHETF 34, 514.

HASEGAWA, A. 1984 Optics Lett. 9, 288.

HASEGAWA, A., and KODAMA, Y. 1981 Proc. IEEE 69, 1145.

HOFFMAN, A., LOWENTHAL, D.D., and CRAWFORD, E.A. 1978 Appl. Phys. Lett. 33, 282.

HORA, H., JONES, D.A., CANE, E.L., and LUTHER-DAVIS, B. 1982 in AIP Proc. vol. 91, ed. by P. Channel, p. 112.

HORTON, W., and TAJIMA, T. 1985a to be published in Phys. Rev. A.

HORTON, W., and TAJIMA, T. 1985b to be published in Proc. Laser 1984.

HORTON, W. 1985 private communication.

HUGRASS, W.N. 1982 Heating in Toroidal Plasmas Proc. 3rd Joint Varenna-Grenoble Int. Symposium (Grenoble, Commissionn of the European communities) vol. III, p. 879.

JACKSON, E.A. 1960 Phys. Fluids 5, 831.

JOSHI, C., TAJIMA, T., DAWSON, J.M., BALDIS, H.A., and EBRAHIM, N.A. 1981 Phys. Rev. Lett. 47, 1285.

JOSHI, C. 1985, private communication, also to be published in AIP Proceedings.

KATSOULEAS, T., DAWSON, J.M. 1983 Phys. Rev. Lett. 51, 392.

KAW, P.K., KULSRUD, R.M. 1973 Phys. Fluids 16, 321.

KEIL, E. and SKRINSKII, A. 1979 Proc. 2nd ICFA Workshop on Possibilities and Limitations of Accelerators and Detectors, U. Amaldi, Ed., p. 3, CERN.

KENNEL, C.F., and PELLAT, R. 1976 Plasma Phys. 15, 335.

KIBBLE, T.W.B. 1966 Phys. Rev. Lett. 16, 1054.

KINDEL, J., and FORSLUND, D. 1983 Private communication, Los Alamos,

KLEPIKOV, N.P. 1954 ZH. EKSP. TEORET. FYZ., 19.

KOLOMENSKII, A.A., and LEBEDEV, A.N. 1963 Zh. Eksp. Teoret. Fyz. 44, 261 (Sov. Phys. JETP 17, 179).

KROLL, N., RON, A., and ROSTOKER, N. 1964 Phys. Rev. Lett. 13, 83.

LAI, M.N. 1980 Phys. Fluids 23, 2375.

LANDAU, L.D., and LIFSHITZ, E.M. 1959 Fluid Mechanics, p. 502, Pergamon Press, Oxford.

LEBOEUF, J.-N., TAJIMA, T. 1979a Appl. Phys. Lett. 34, 548.

LEBOEUF, J.-N., TAJIMA, T. 1979b Phys. Fluids 22, 1485.

LEBOEUF, J.-N.ASHOUR-ABDALLA, M., TAJIMA, T., KENNELL, C.F., CORONITI, F., and DAWSON, J.M. 1982 Phys. Rev. A25, 1023.

LIN, A.T., DAWSON, J.M., and OKUDA, H. 1974 Phys. Fluids 17, 1995.

MCMILLAN, E.M. 1950 Phys. Rev. 79, 498.

MAKO, F., and TAJIMA, T. 1984 Phys. Fluids 27, 1815.

MANLEY, J.M., and ROWE, H.E. 1956 Proc. IRE 44, 904.

MARCUSE, D. 1974 Theory of Dielectric Optical Waveguides (Academic Press, NY).

MIMA, K., and TAJIMA, T. 1985 to be published.

MIMA, K. 1985 private communication.

NEUFFER, D. 1983 Proc. 12th Inter. Conf. High Energy Accelerators ed. by F. Cole and R. Donaldson (Fermi Nat. Acc. Lab, Batavia, ILL) p. 481.

NISHIKAWA, K., LEE, Y.C., and LIU, C.S. 1975 Comments Plas. Phys. 2, 63.

NOBLE and Himel 1985 Private Communication.

OHKAWA, T. 1970 Nucl. Fusion 10, 185.

O'NEILL, T.M. 1965 Phys. Fluids 8, 2255.

O'NEILL, T.M., WINFREY, J.H., and MALMBERG, J.H. 1971 Phys. Fluids 14, 1204.

PALMER, R.B. 1972 J. Appl. Phys. 43, 3014.

PELLEGRINI, C. 1982 Laser Acceleration of Particles, AIP Conf. Prof. 91, New York, ed. by P.J. Channel, p. 138. The author came to realize the existence of this reference at the last stage of writing the present article.

POUKEY, J.W. and ROSTOKER, N. 1971 Plasma Physics 13, 897.

REESE, J. 1984 presentation at CAS-ECFA-INFN Workshop on the Generation of High Fields for Particle Acceleration to Very High Energy (Frascati).

RICHTER, B. 1985 to be published in AIP Proceedings.

ROSENBLUTH, M.N. and LIU, C.S. 1972 Phys. Rev. Lett. 29, 701.

RUTH, R.D., CHAO, A.W., MORTON, P.L. and WILSON, P.B. 1985 to be published in Particle Accelerators.

SAGDEEV, R.Z. and GALEEV, A.A. 1969 Nonlinear Plasma Theory, p. 19, Benjamin, New York.

SALAM, A. 1983 Proc. ECFA-RAL Meeting on the Challenge of Ultra-High Energies, p. 1, Rutherford Appleton Laboratory, Chilton.

SCHMIDT, G. and WILCOX, T. 1973 Phys. Rev. Lett. 31, 1380.

SCHWINGER, J. 1954 Proc. Nat. Acad. Sci. 40, 132.

SHEN, Y.R. and BLOEMBERGEN, N. 1965 Phys. Rev. 137, A1787.

STIX, T.H. 1965 Phy. Rev. Lett. 15, 878.

SULLIVAN, D.J. and GODFREY, B.B. 1981 IEEE Trans. Nucl. Sci. NS-28, 3395.

SULLIVAN, D.J. and TAJIMA, T. 1984 Proc. Laser Interaction and Related Phenomena Workshop, H. Hora and G.H. Miley, Eds., Vol. 6, p. 1093, Plenum, New York, 1984.

SYNGE, J.L. 1958 The Relativistic Gas, p. 77, North-Holland Amsterdam.

TAJIMA, T. 1977 Phys. Fluids 20, 61.

TAJIMA, T. and MAKO, F. 1978 Phys. Fluids 21, 1459.

TAJIMA, T. and DAWSON, J.M. 1979a IEEE Trans. Nucl. Sci. NS-26, 4188

TAJIMA, T. and DAWSON, J.M. 1979b Phys. Rev. Lett. 43, 267.

TAJIMA, T. and DAWSON, J.M. 1981 IEEE Trans. Nucl. Sci. NS-28, 3416.

TAJIMA, T. 1983 Proc. 12th Int. Conf. on High-Energy Accelerators, F.T. Cole and R. Donaldson, Eds., p. 470, Fermi National Accelerator Laboratory, Batavia, IL.

TAJIMA, T., WITTE, K., and SINGER, S. 1985 to be published.

TAJIMA, T., SCHMIDT, G., and PELLAT, R. 1985 to be published.

TAJIMA, T. and SUDAN, R.N. 1985 to be published.

TAJIMA, T. and SAKAI, J-I. 1985 to be published.

TANG, C.M., SPRANGLE, P., and SUDAN, R.N. 1984 App. Phys. Lett. 45, 375.

VAN KAMPEN, N.G. 1955 Physica 21, 949.

VEKSLER, V.I. 1956 Proc. CERN Symp. on High-Energy Accelerators and Pion Physics, E. Regenspreif, Ed., Vol. 1, p. 80, European Organization for Nuclear Research, Geneva.

VOMVORIDIS, J., TAJIMA, T., FELBER, F.S., SPIVEY, B., and HUNTER, R.O. 1983 IEEE Trans. Nucl. Sci NS-30, 3466.

WILLIS, W.J. 1975 CERN 75-9 (preprint).

WILLIS, W.J. 1977 Laser Interaction and Related Plasma Phenomena, H.J. Schwartz and H. Hora, Eds. Vol. 4B, p. 991, Plenum, New York.

WILLIS, W.J. (CERN), 1982 Private communication.

YUKAWA, H. 1935 Proc. Phys. Math. Soc. Jpn. 17, 48.

Fig. 1

Particle motion in a propagating plane electromagnetic wave. The wavenumber $\underset{\sim}{k}$ is perpendicular to electric field $\underset{\sim}{E}$ and magnetic field $\underset{\sim}{B}$. No net acceleration along the $\underset{\sim}{k}$-direction is achieved. When the EM wave becomes relativistic (c), there can be net plasma acceleration.

Fig. 2

Virtual photons and photons in a plasma. (a) A plane electromagnetic wave reflects on the metallic surface. There is a field component E $\sin\nu$ parallel to $k_{\parallel}$. In the metal the EM field exponentially decays. (b) If we put two metallic plates together, we get a waveguide. Again a field component parallel to $k_{\parallel}$ exists. (c) The dispersion relation of the EM wave in the waveguide. k is the parallel wavenumber. (d) The dispersion relation of EM waves in the uniform and ripple waveguides. (e) The dispersion relation of the EM wave in a plasma.

Fig. 3

The surrounding plasma waveguide structure (plasma fiber optics) plays a role of a slow-wave structure. If one matches $v_{ph} \sim c$, the wave field component parallel to the laser propagation may be employed to accelerate particles.

Fig. 4

The ponderomotive potential φ due to the photon beat.

Fig. 5

Dispersion relation for the EM waves. Two laser beams beat. The process can be expressed as a forward scattering process of a photon by a plasma.

Fig. 6

Photon beat acceleration by two laser beams (ω_0, k_0) and (ω_1, k_1). (a) The electron phase space (x, p_x) at $t = 240\omega_p^{-1}$. The maximum $\gamma_{\parallel}$ for electrons is 85 in this case. (b) The logarithm of the electron distribution function at $t = 135\omega_p^{-1}$. (c) The electron distribution function at $t = 135\omega_p^{-1}$.

Fig. 7

The electrostatic field E_x vs. x at $t = 77\omega_p^{-1}$. The amplitude of the field E_L already reached $E_L \sim m\omega_p c/e$. $\omega_0/\omega_p = 7.29$, $c = 20$, $L_x = 2048\Delta$. Phase space for electrons at $t = 77\omega_p^{-1}$ is also shown for this case.

Fig. 8

Wake-plasmon excitation by a short laser wavepacket and trapping of electrons. The head of the photon packet has proceeded forward to $x = 310$ at $t = 25\omega_p^{-1}$. $\omega_0/\omega_p = 4.3$. (a) The longitudinal momentum ($p_x = p_{\parallel}$) vs. position of electrons. (b) p_y-x phase space. (c) The longitudinal field $E_L = E_{\parallel}$ vs. position. (d) Particle acceler- ation in time (solid line) and electric field intensity in time (dashed line).

Fig. 9
Schematic diagram for the photon wavepacket creating a wake plasmon behind it (a). The photon wake acceleration by a series of photon bullets (b).

Fig. 10
Maximum electron energy vs. $(\omega_0/\omega_p)^2$ in the short wave- packet case. The dots are from simulations and the solid line is from Eq. (14).

Fig. 11
The electromagnetic energy distribution (spectrum) as a function of mode numbers. Two laser beam pumps k_0 and k_1 are indicated by arrows. (a) $t = 142.5\omega_p^{-1}$, (b) $t = 240\omega_p^{-1}$.

Fig. 12
Plasmon spectrum. The electrostataic wavenumber spectrum is shown. $\ell n|E(k)|^2$ vs. $n = k/k_p$ along with $\ell n\, S(nk_p, n\omega_p)$ vs. $\ell n\, n$ are shown for $v_{os}/c = 0.5$ case.

Fig. 13
Electromagnetic spectral intensity in wavenumber. The arrow with 0 indicates the rough position of the original laser beam wavenumber peak; n indicates $k' = k \pm nk_p$.

Fig. 14
Electron velocity distri- bution function in the direction of the incoming photon propagation. When the backscattering plasma wave has phase velocity v_p, the plasma wave quickly saturates by trapping electrons in the bulk distribution.

Fig. 15
Simulation with a single laser beam with $\omega_p/\omega_0 = 0.46$. (a) Electron momentum distribution function at $t = 250\omega_p^{-1}$. (b) The electrostatic mode spectrum at $t = 100\omega_p^{-1}$. (c) The experimental energy.[17]

Fig. 16
The maximum electron energy vs. laser electric field intensity $(eE_0/m\omega_0 c)^2$ in the case of ultra-relativistic laser beams. The straight line is $\gamma^{max} = 1/2(c/v_g)\,(\omega_0/\omega_p)^2\,\nu^2$.

Fig. 17
Phase space (p_x vs. x) for electrons with the ultrarelativistic EM wave originally given a sawtooth profile.[27] The group velocity of the wave structure is close to $c/\sqrt{3}$.

Fig. 18
Relativistic Brillouin forward scattering process. Two beating lasers ω_0, ω_1 with $\omega_0 - \omega_1 = \omega_{pi}$ are injected into a plasma from the left. Extremely high energy electrons are seen in four bunches whose separation is c/ω_{pi}, much wider than that of the Raman bunch c/ω_p. (a) Electron phase space (p_y vs. x) at $t = 0$. (b) Electromagnetic beat-wave B_z as a function of x at $t = 0$.

(c) Electrostatic (plasma) wave E_x as a function of x at $t = 60\omega_{pe}^{-1}$.
(d) Electron phase space (p_x vs. x) at $t = 20\omega_{pe}^{-1}$.
(e) Distribution function of electrons $f(p_x)$ at $t = 60\omega_{pe}^{-1}$.

Fig. 19
The relativistic Brillouin process. (a) Electron phase space (p_x vs. x) at a later time ($t = 260\omega_{pe}^{-1}$). (b) Electrostatic wave spectrum [$E_x(k)$ correlations]. (c) Electromagnetic wave spectrum [$B_z(k)$ correlations]. (d) and (e) The wave forms E_x and B_z at later time ($t = 260\omega_{pe}^{-1}$). (f) Ion phase space (p_y vs. x) at $t = 260\omega_{pe}^{-1}$. (g) Electron phase space (p_y vs. x) at $t = 260\omega_{pe}^{-1}$. (h) Electron distribution function $f(p_x)$ at later time ($t = 260\omega_{pe}^{-1}$).

Fig. 20
Electrostatic modes excited in the relativistic Brillouin case. $L_x = 1024\Delta$, $c = 9\omega_{pe}$, $E_0 = E_1 = \sqrt{5}m\omega_{pe}c/e$, $M/m = 25$. Crosses are forward propagating modes, while circles are backward propagating modes. The strongest modes are around the number 4 ($k = 2\pi\times4/1024\Delta$), with the zero frequency quasi-modes being the most prominent.

Fig. 21
Schematic phase space diagram with bulk electrons, accelerated tail electrons, and injected preaccelerated ions at the right phase. p_{ph} is the phase momentum of the plasma wave excited by the beating two laser beams. p_b is the injected ion beam momentum. The ion clump separation is c/ω_p.

Fig. 22
(a) The laser light divergence and the Rayleigh length z_R. (b) The self-trapped laser light in a plasma and its density profiles.

Fig. 23
The domain stable for filamentation instability and favorable for self-trapping is indicated by the sign OPERATIVE (T/F) with T for trapping and F for filamentation. The UNSTABLE label indicates the domain for the instabilities of self-trapping and filamentation. The STABLE label does the opposite. The figure is redrawn from Felber et. al.

Fig. 24
Matching the phase velocity of the plasma wave and the particle velocity by insertion of non-resonant plasma layers.

Fig. 25
Matching the plasma wave phase with the particle. (a) Tilting the plasma wave direction. (b) Plasma fiber. (c) Cancel- lation of the perpendicular acceleration by a magnetic field.

Fig. 26
The duct width d for the plasma fiber accelerator condition as a function of the laser frequency ω_1. (The numbers are for some particular example.)

Fig. 27
The density profile of the duct structure in the x-direction (y-integrated) in the simulation.

Fig. 28
The electrostatic potential due to the beat wave created in the fiber structure.

Fig. 29
Measured phase velocity of the beat wave in the fiber.

Fig. 30
Temporal behavior of multicascade with four waves (three photons and one plasmon). (a) Photon 1 amplitude vs. time. (b) Photon 2 amplitude vs. time. (c) Plasmon amplitude vs. time. The initial amplitude was $a_{1r} = 1.0$ and the others zero. The time normalization is according to Eq. (49) and the time axis is from 0 to 100 in this unit.

Fig. 31
Temporal behavior of multicascade with five waves (four photons and one plasmon). (a) Photon 1 amplitude vs. time. (b) Photon 2 amplitude vs. time. (c) Plasmon amplitude vs. time. The initial amplitude and the normalization of time are the same as in Fig. 30.

Fig. 32
Chaotic temporal behavior of multicascade with 20 waves (19 photons and one plasmon). (a) Photon 1 amplitude vs. time. (b) Photon 4 amplitude vs. time. (c) Photon 18 amplitude vs. time. (d) Plasmon amplitude vs. time. (e) Entropy (negative) vs. time. The initial amplitude and the renormalization of time are the same as in Fig. 25.

Fig. 33
The saturated beat-wave amplitude as a function of the beat-wave frequency under the influence of plasma turbulence. The turbulence effects are incorporated through the turbulent damping rate ν. Various levels of turbulence (with ν changed) are compared. The pump amplitude is characterized by $\lambda = 0.1$ for this diagram (see Horton and Tajima, 1985a).

Fig. 34
A conceptual plasma fiber accelerator with laser staging amplification in situ. The separation between the modules is characterized by the sum of the focal length and the pump depletion length. An example of $X_eC\ell$ lasers is taken.

Fig. 35
The asymptotic cross-section of lepton-lepton collisions.

Fig. 36
Self-pinching of colliding beams and possible cures.

Fig. 37

(Collective) beamstrahlung and collisions of γ-γ at the focus of a lepton collider.

Fig. 38

Electron distribution function at t=0 (a) and at $t = 22\omega_p^{-1}$ (b), electrostatic field energy (c), and electronic current density (d). The scale of the horizontal axis in (a) and (b) is in units of the thermal speed of v_t of the electron. The scale of the horizontal axis in (c) and (d) is in units of ω_p^{-1}. The scale of the vertical axis in (d) is in units of $n_0 e v_t$. The broken line in (c) corresponds to the increase in electrostatic energy predicted by the fluids theory.

(a)

$\underset{\sim}{E} \perp \underset{\sim}{k}$

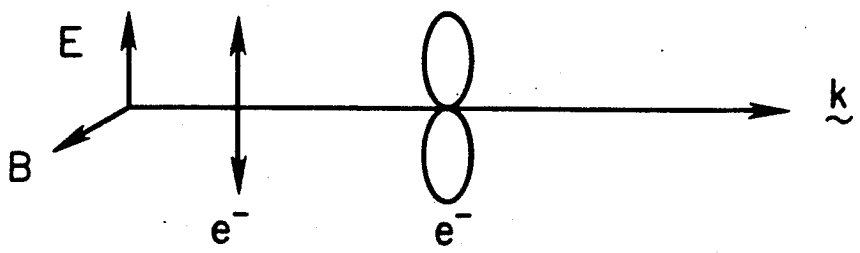

No acceleration

However electron 8-figure motion involves longitudinal oscillations.

(b)

(c)

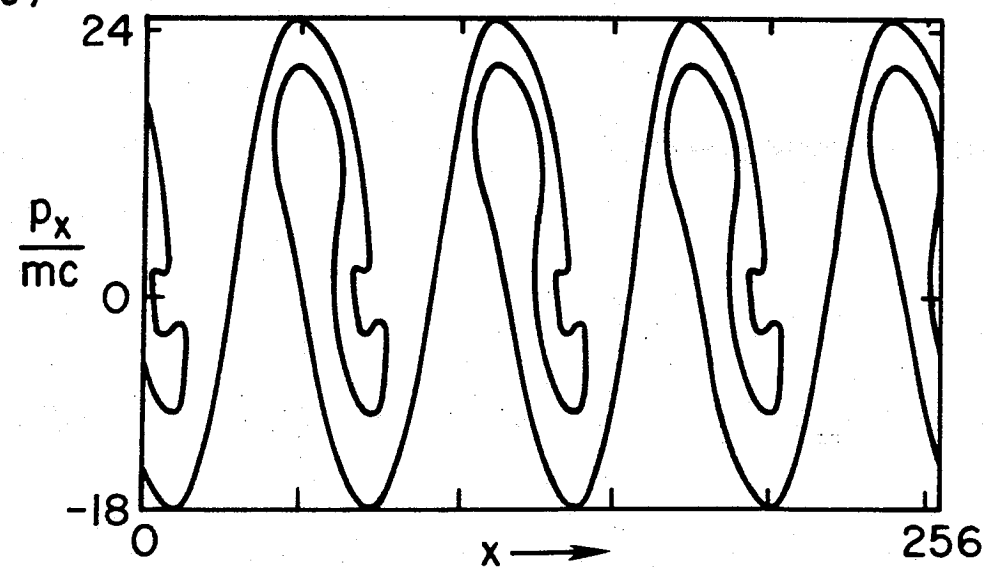

FIG. 1

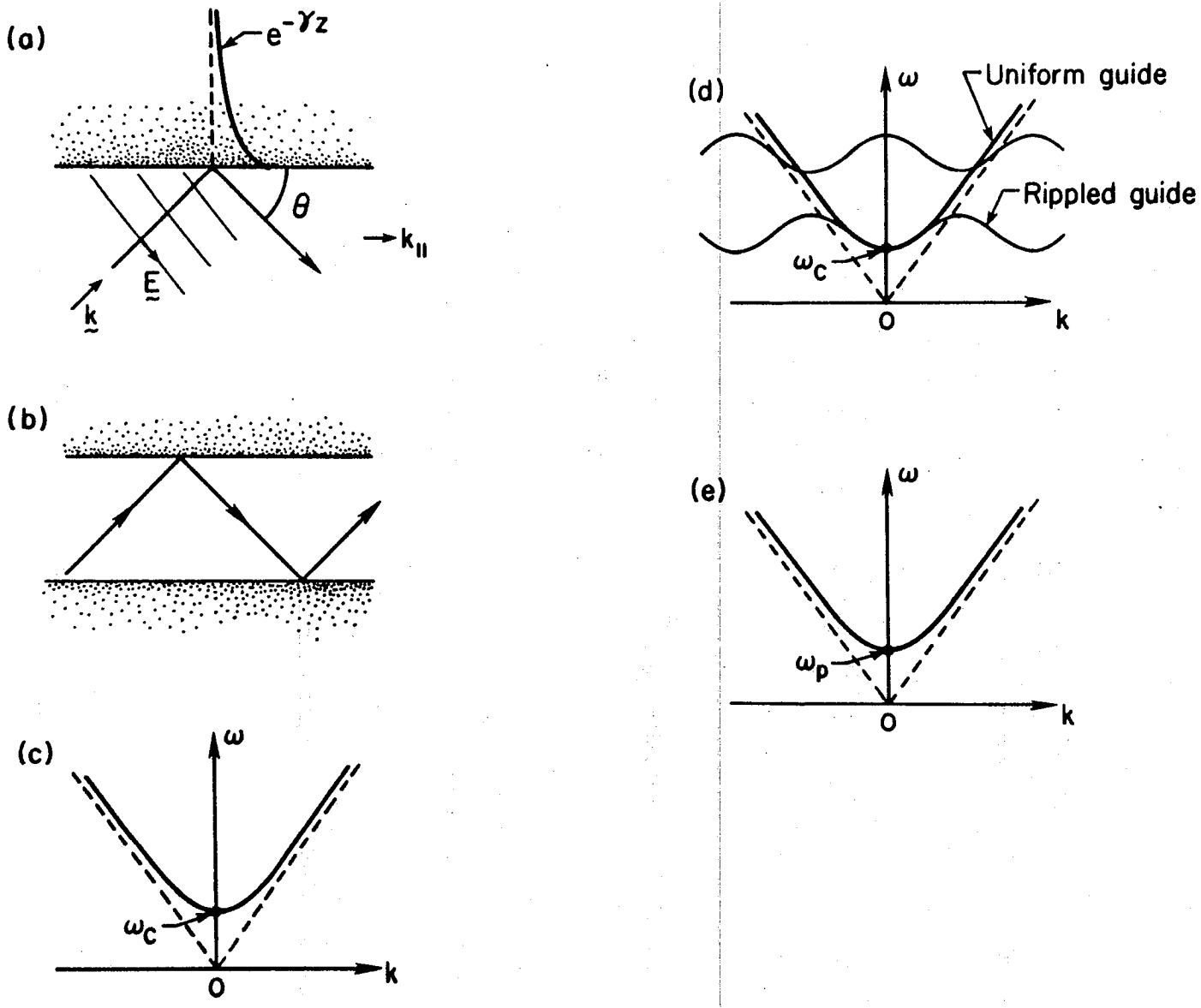
(a)
$e^{-\gamma z}$
θ
$k_{\parallel}$
E
k
(b)
(c)
ω
ω_c
0
k
(d)
ω
Uniform guide
Rippled guide
ω_c
0
k
(e)
ω
ω_p
0
k

FIG. 2

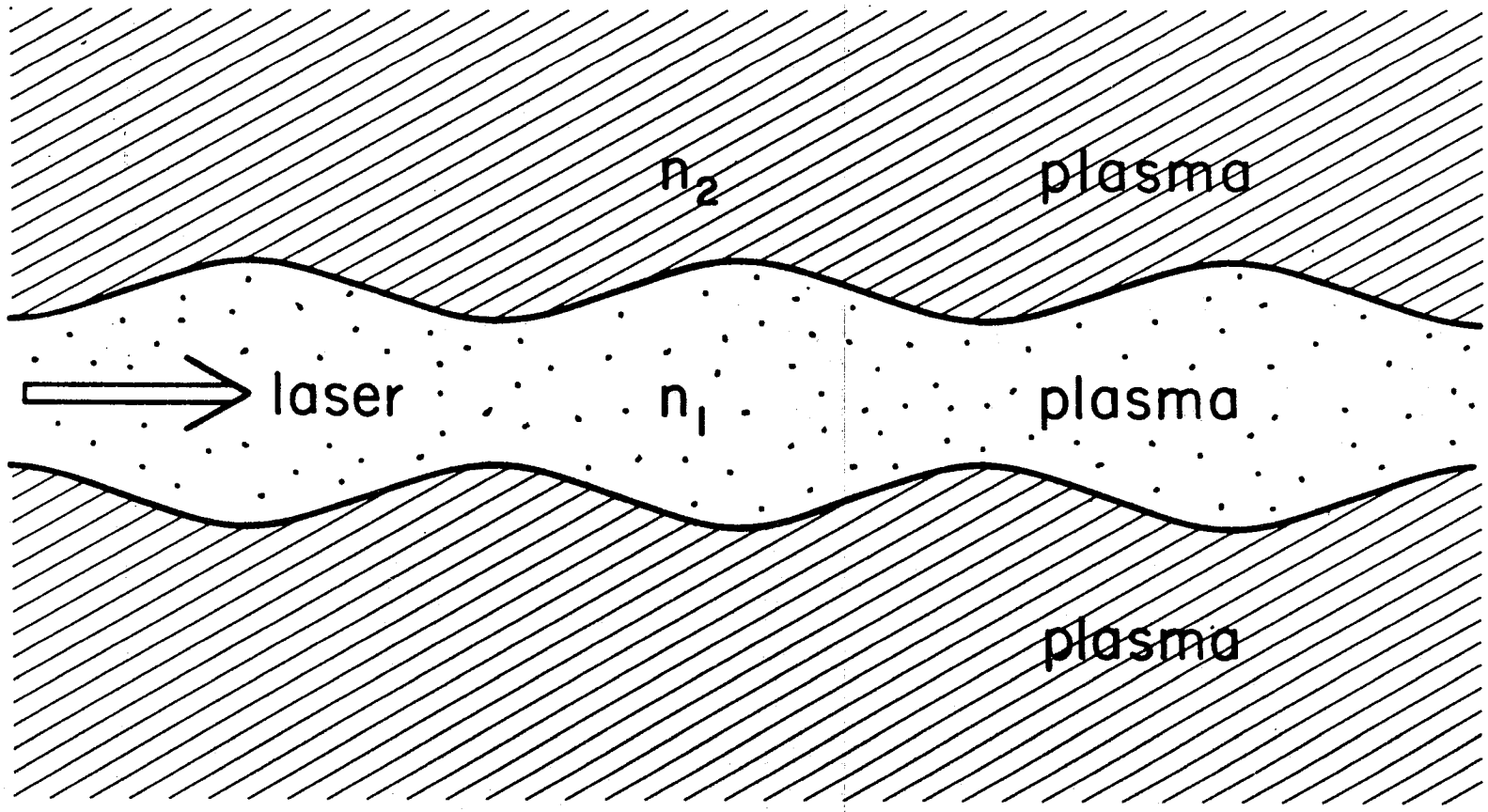

FIG. 3

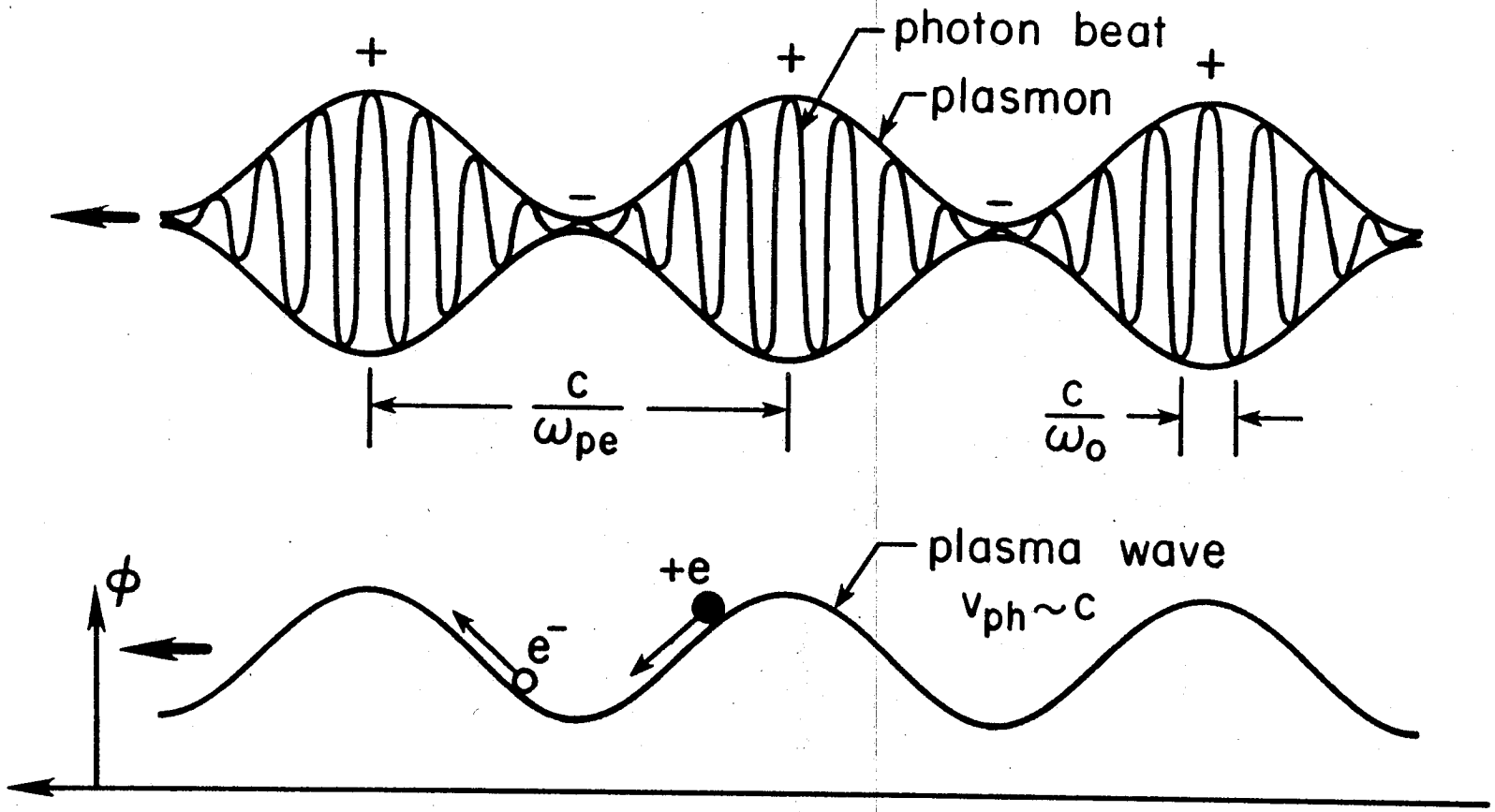

FIG. 4

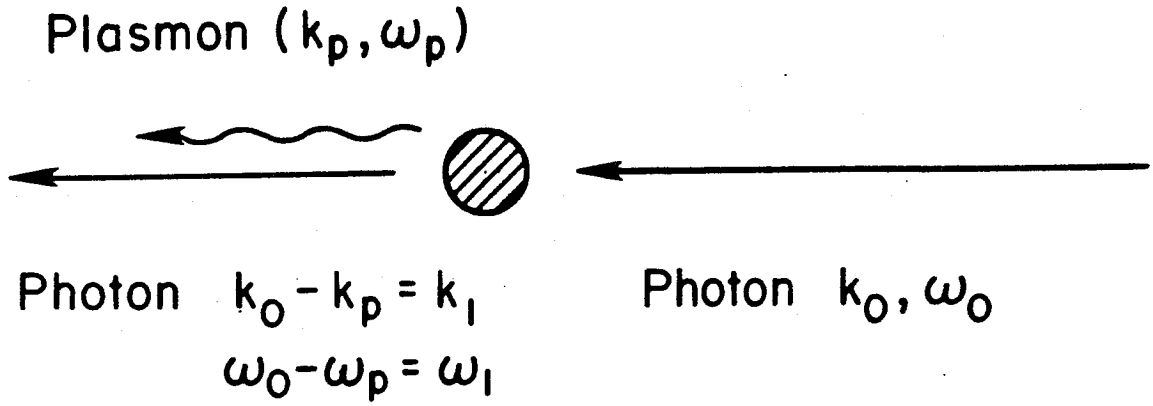
Plasmon (k_p, ω_p)
Photon $k_0 - k_p = k_1$
$\omega_0 - \omega_p = \omega_1$
Photon k_0, ω_0

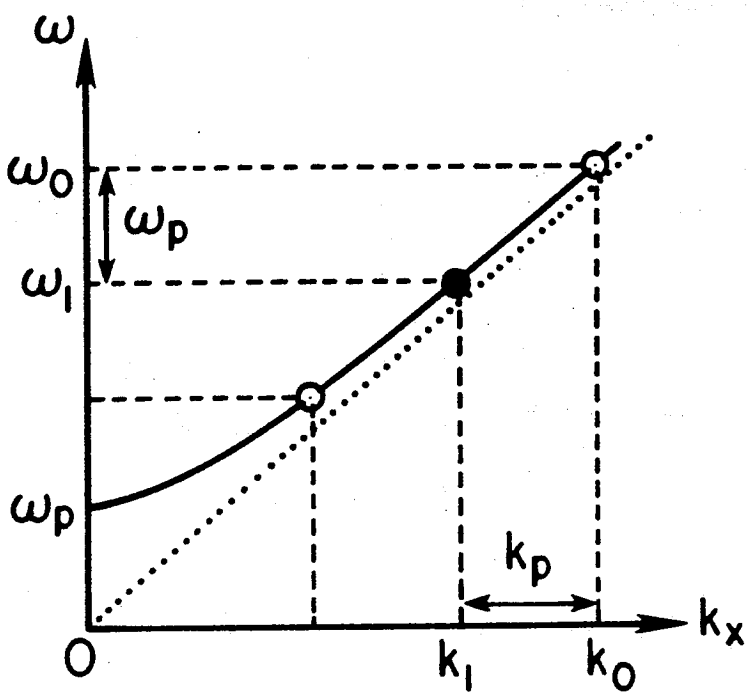
ω
ω_0
ω_p
ω_1
ω_p
k_p
k_x
O
k_1
k_0

FIG. 5

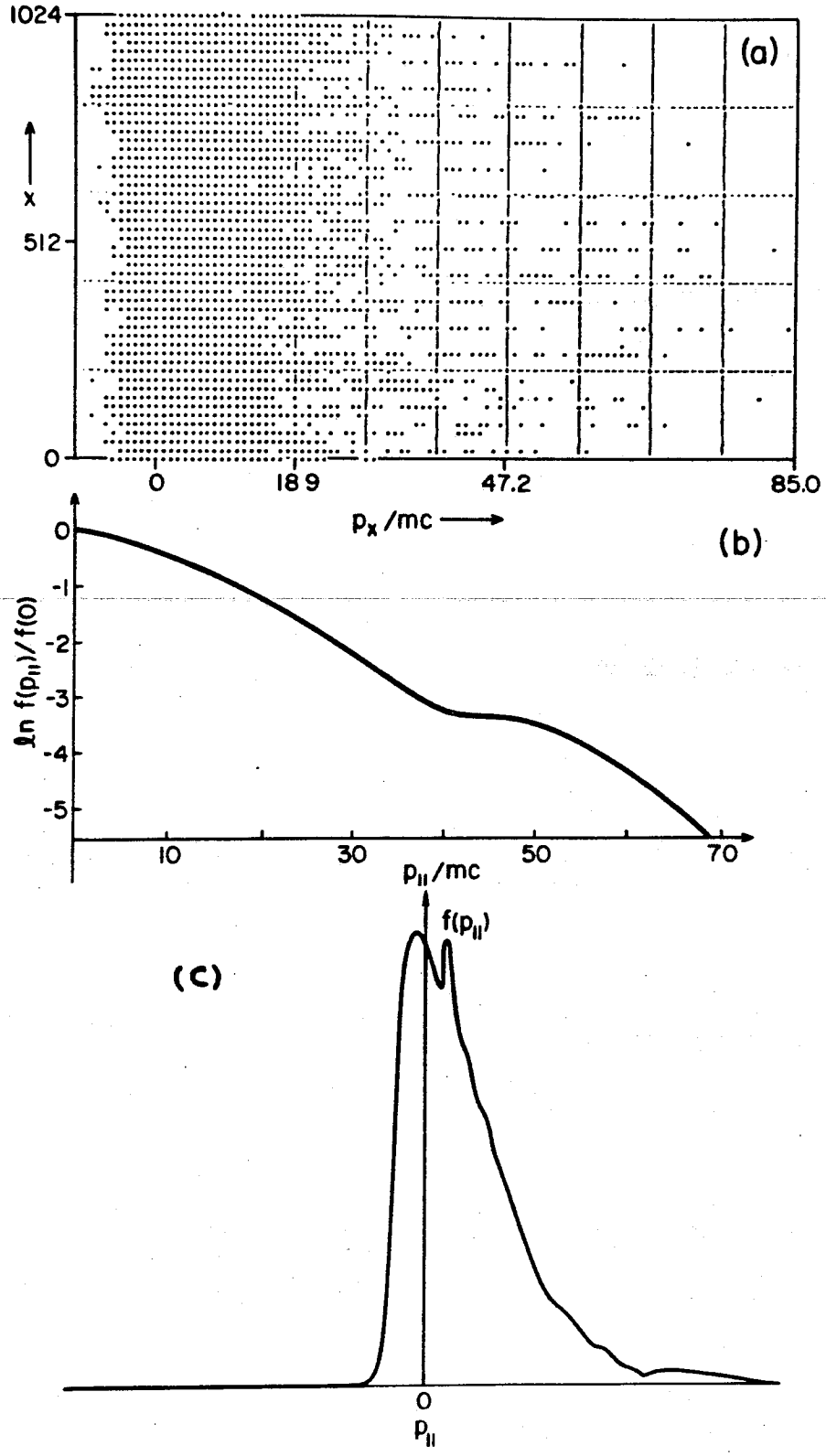
1024
512
0
x
(a)
0
18 9
47.2
85.0
p_x/mc
(b)
0
-1
-2
-3
-4
-5
ln $f(p_{||})/f(0)$
10
30
50
70
$p_{||}/mc$
(c)
$f(p_{||})$
0
$p_{||}$

FIG. 6

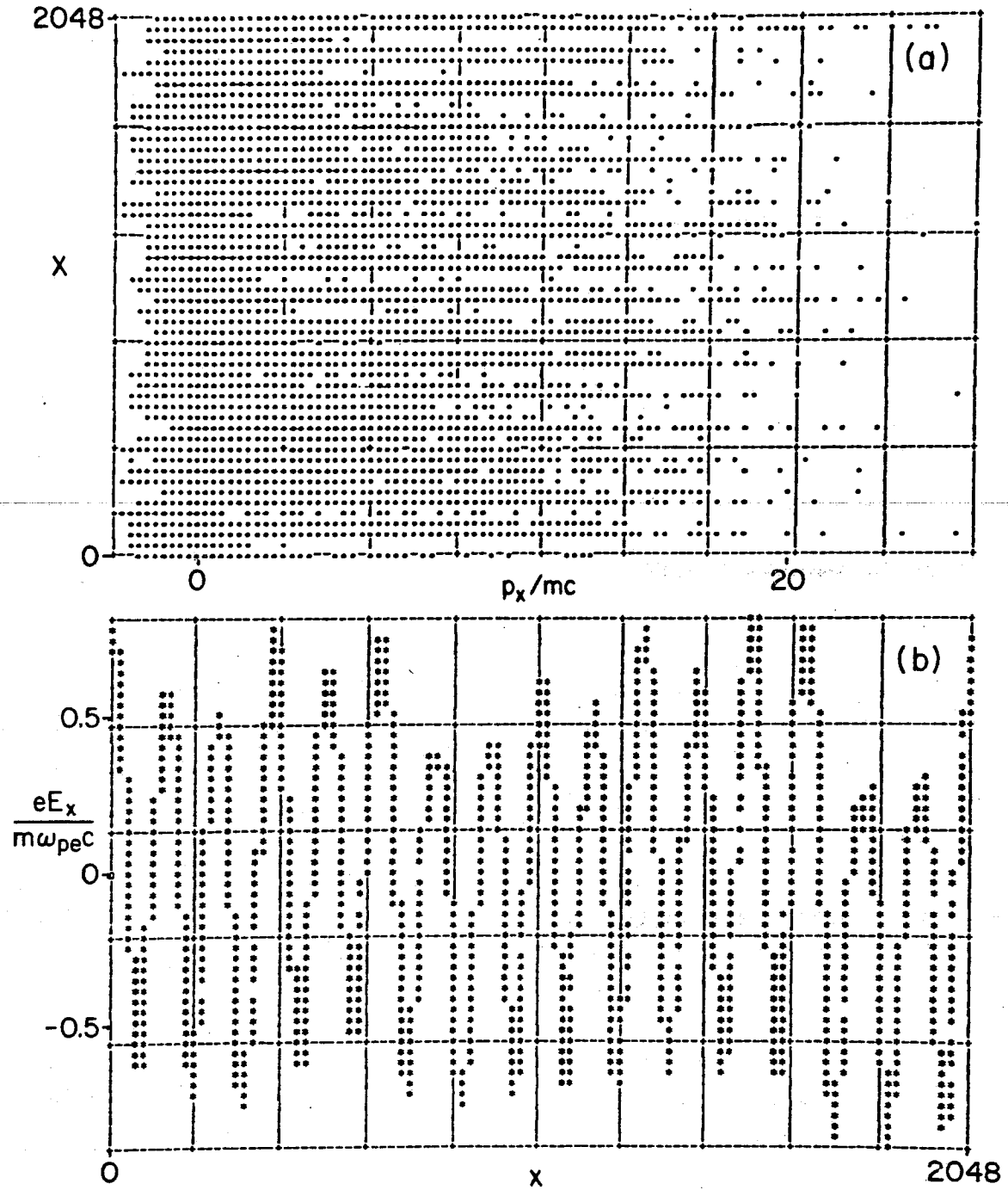

FIG. 7

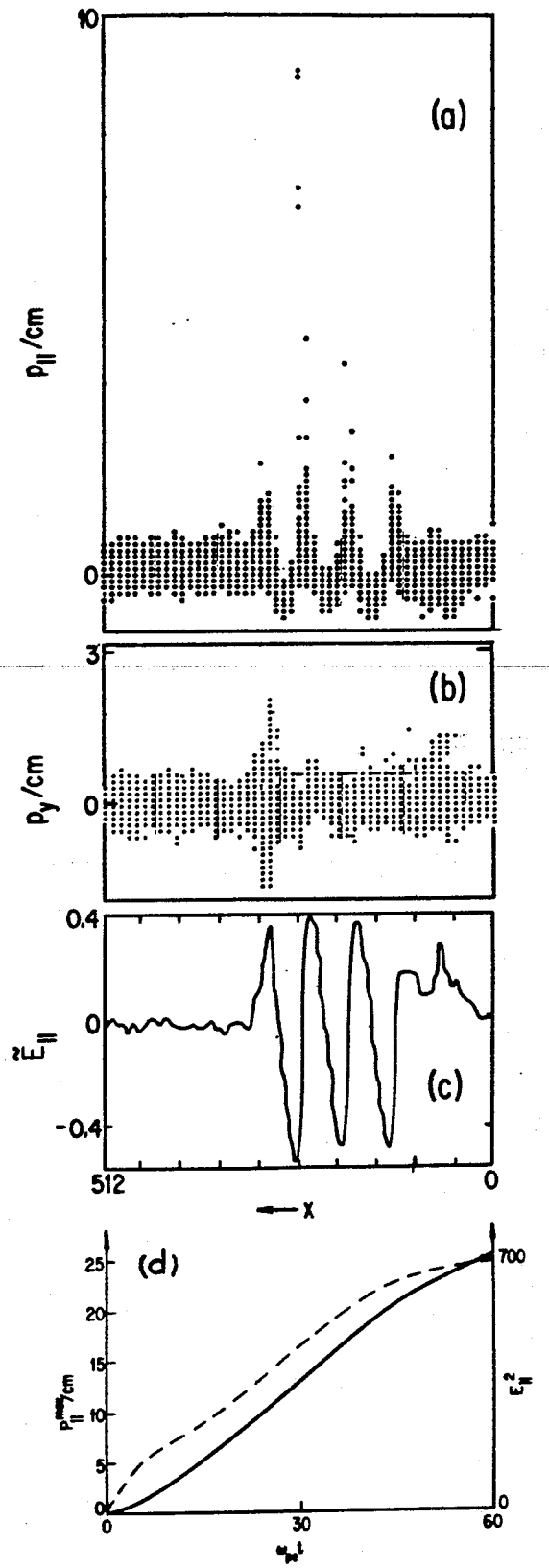
10
(a)
$p_{\parallel}$/cm
0
3
(b)
p_y/cm
0
0.4
0
$\tilde{E}_{\parallel}$
(c)
-0.4
512
0
X
25
(d)
700
20
15
10
5
0
$p_{\parallel}^{max}$/cm
$\mathcal{E}_{\parallel}^2$
0
30
60
$\omega_{pe}t$

FIG. 8

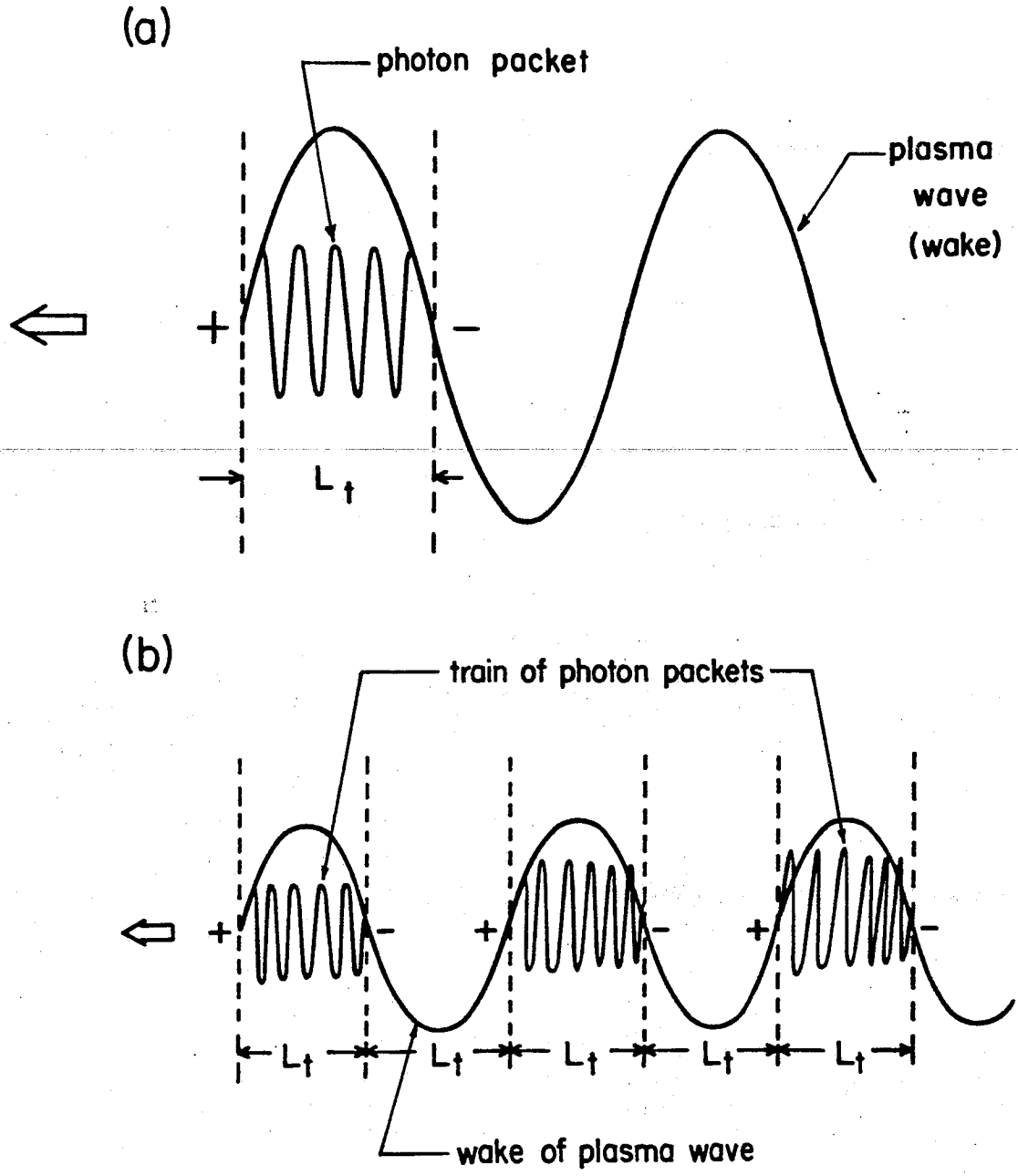
(a)
photon packet
plasma
wave
(wake)
+
−
L_t
(b)
train of photon packets
+
−
L_t
wake of plasma wave

FIG. 9

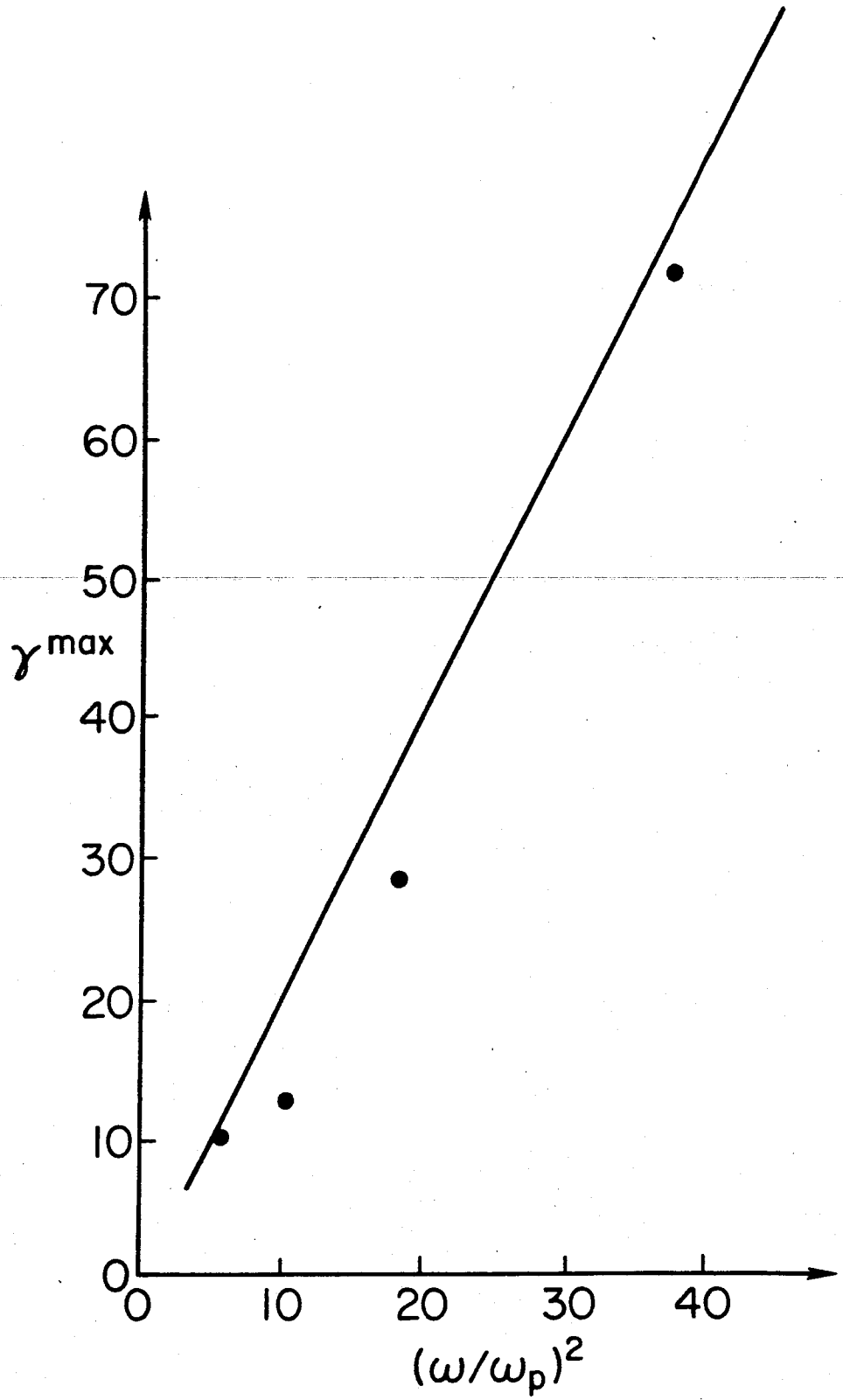

FIG. 10

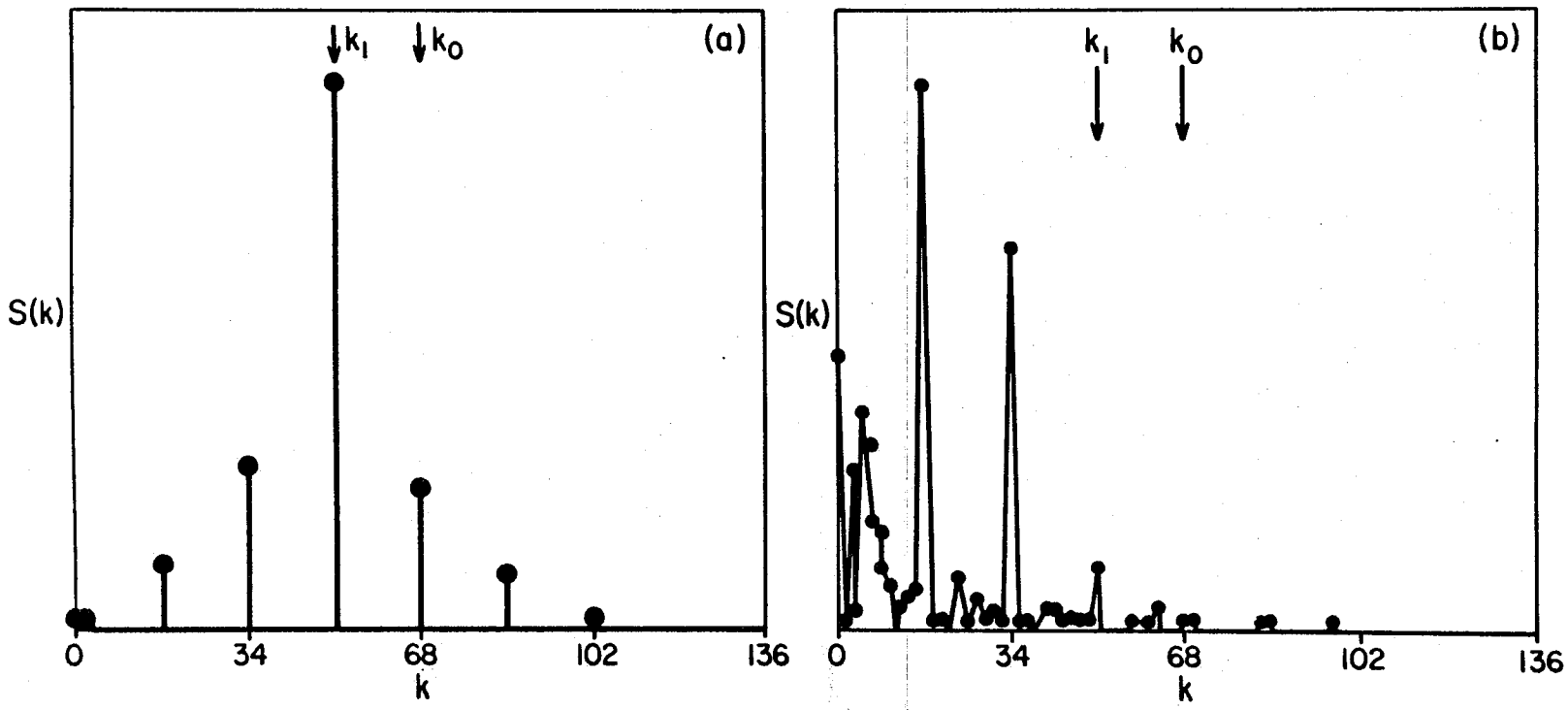

FIG. 11

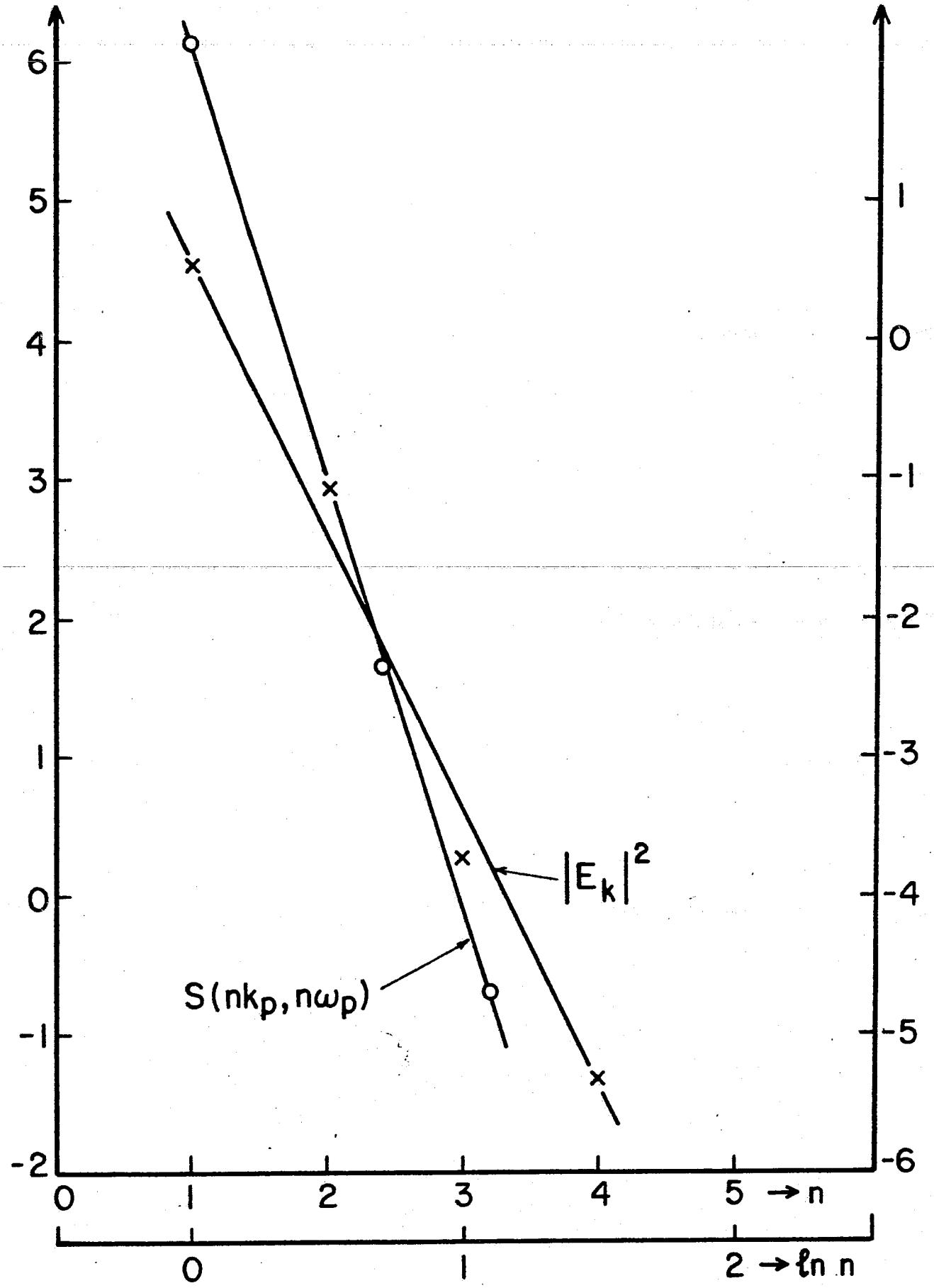

Fig, 12

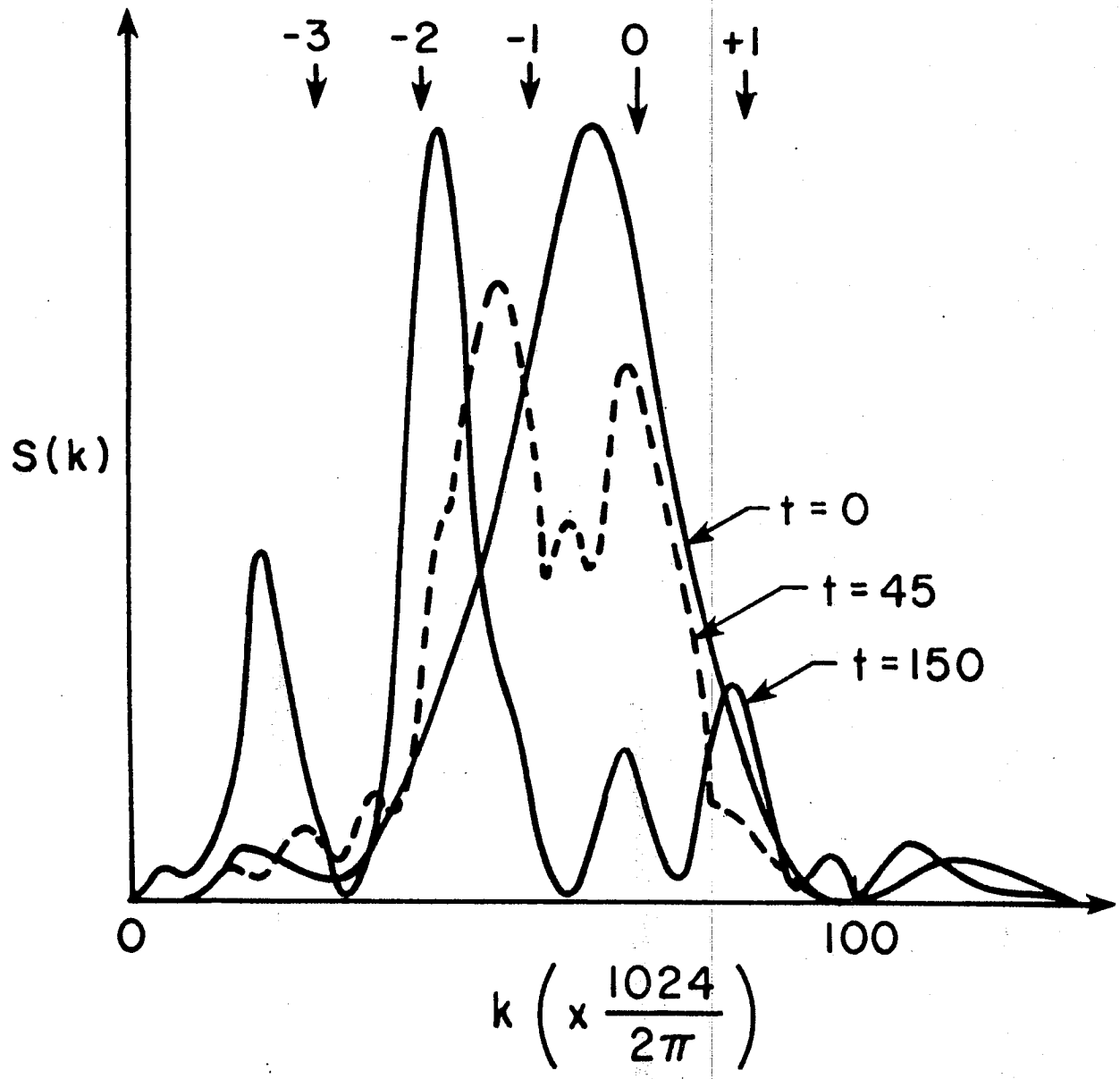

FIG. 13

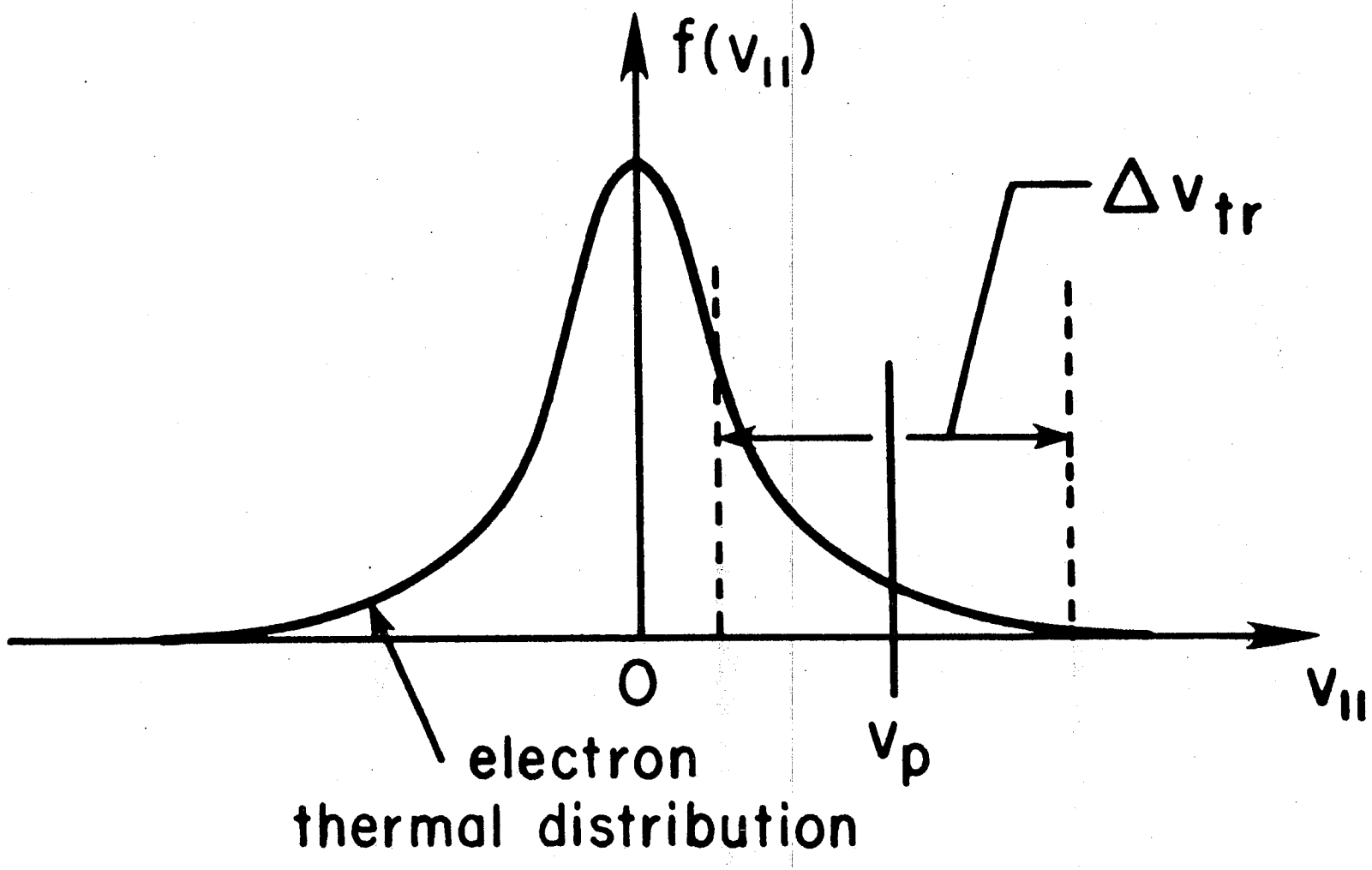

FIG. 14

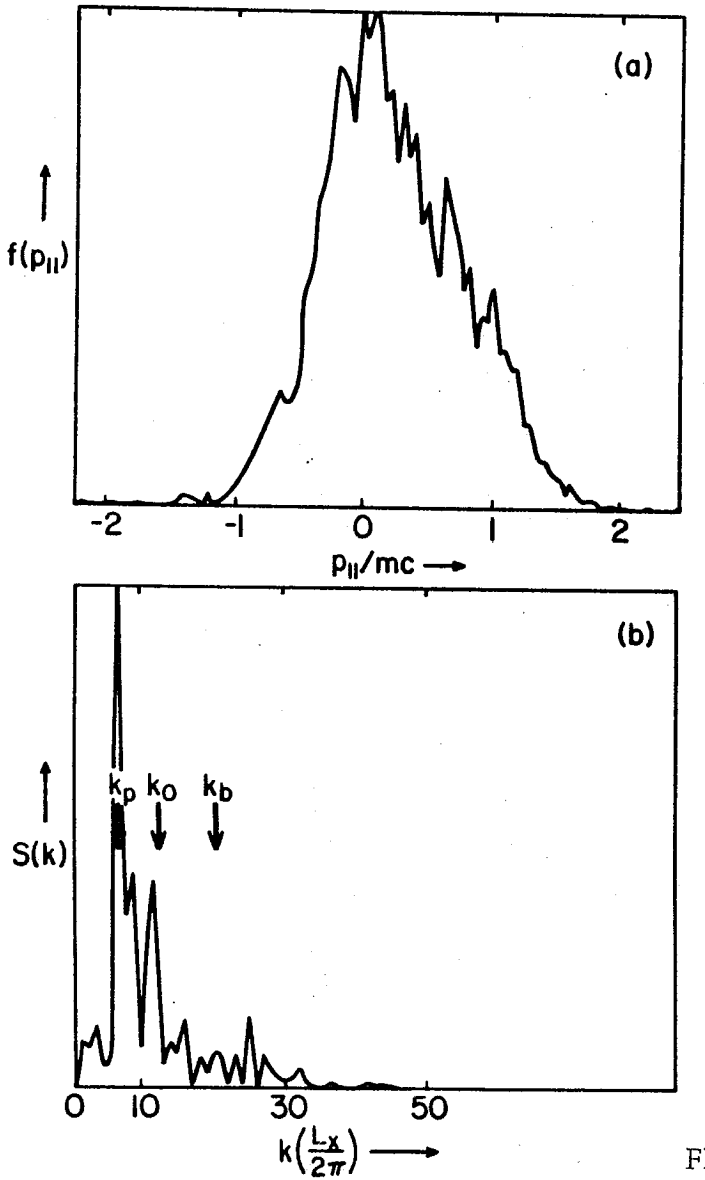
(a)
f(p_II)
-2
-1
0
1
2
p_II/mc
(b)
S(k)
k_p
k_o
k_b
0
10
30
50
k(L_x/2π)

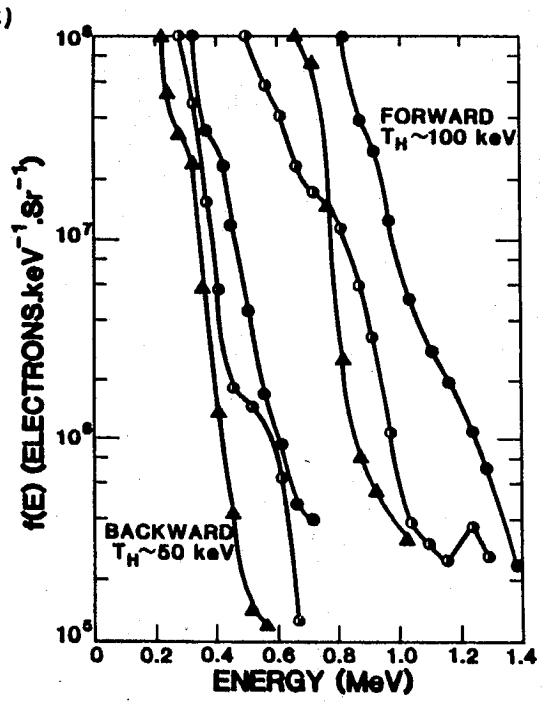
(c)
f(E) (ELECTRONS.keV⁻¹.Sr⁻¹)
FORWARD
T_H~100 keV
BACKWARD
T_H~50 keV
0
0.2
0.4
0.6
0.8
1.0
1.2
1.4
ENERGY (MeV)

FIG. 15

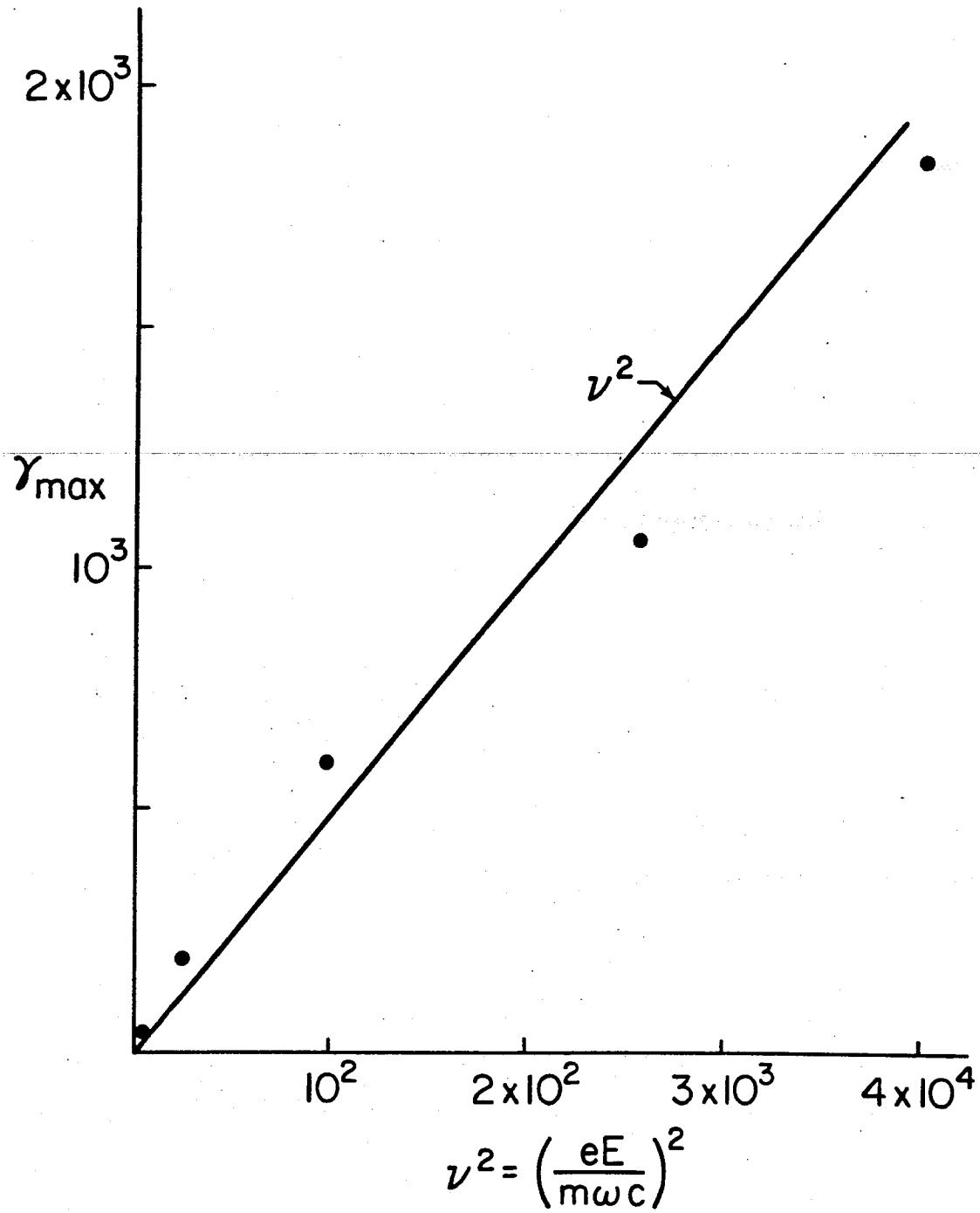

FIG. 16

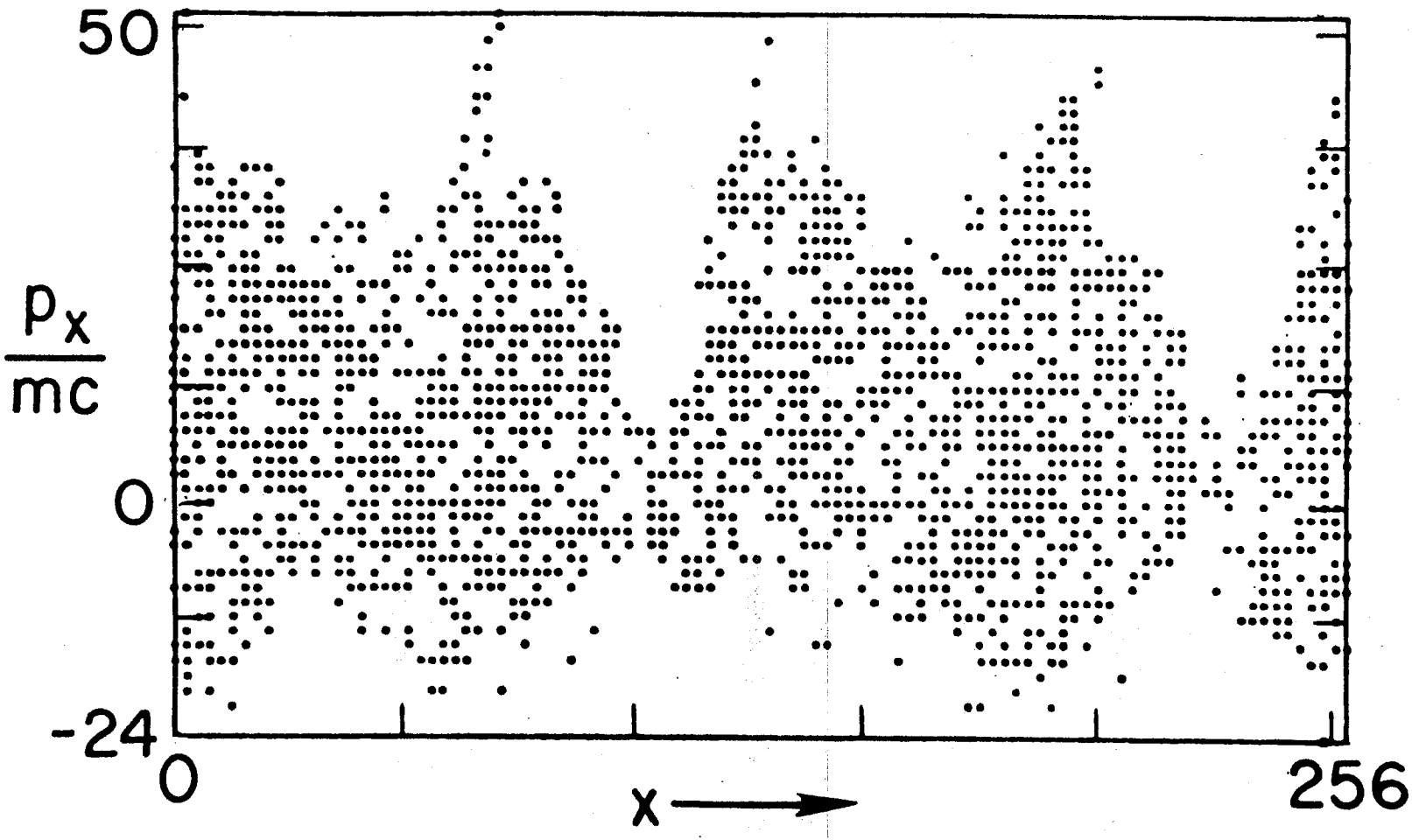

FIG. 17

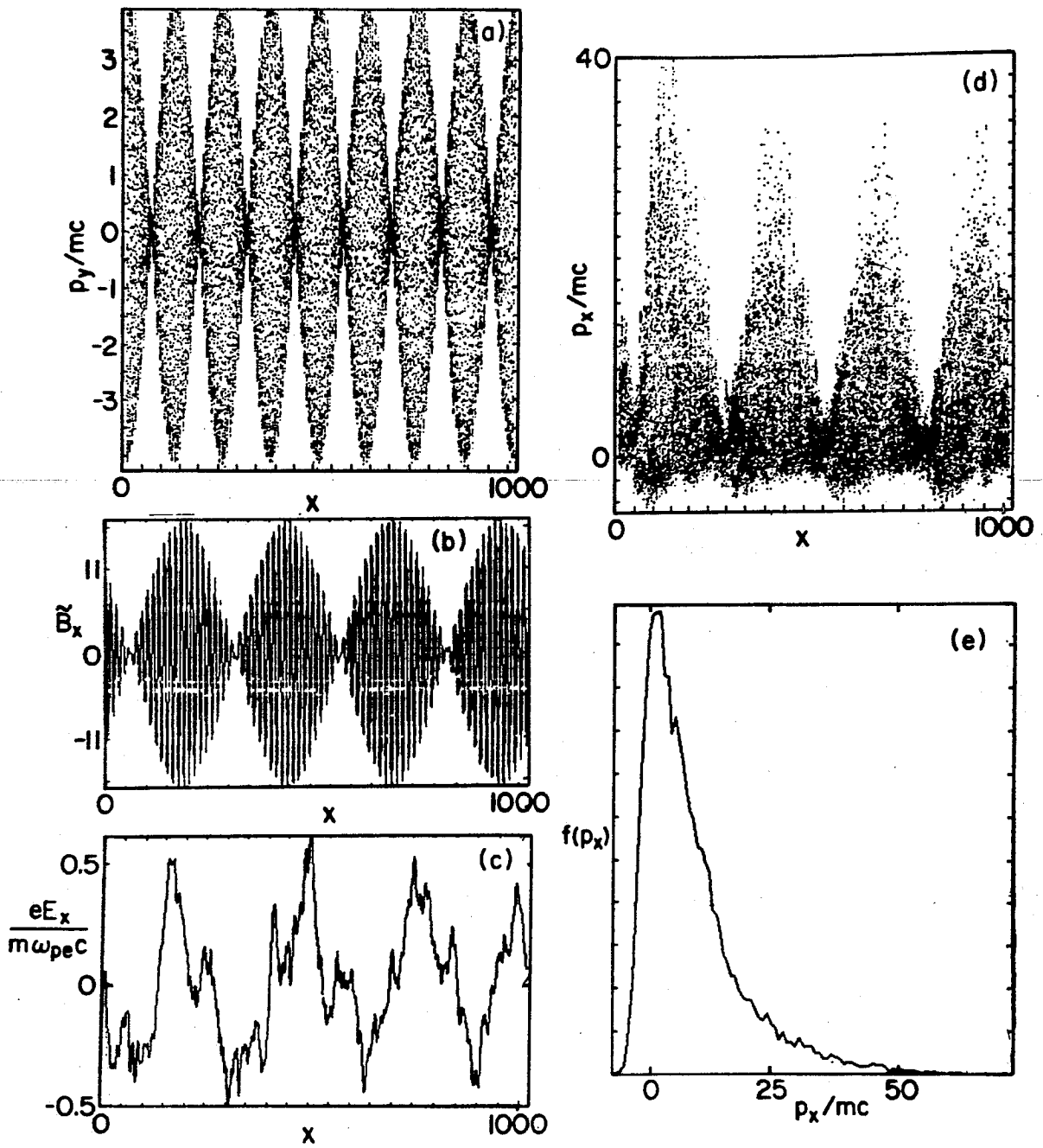
(a)
3
2
1
0
-1
-2
-3
p_y/mc
0
x
1000
(b)
11
0
-11
$\tilde{B}_x$
0
x
1000
(c)
0.5
0
-0.5
$\frac{eE_x}{m\omega_{pe}c}$
0
x
1000
(d)
40
0
p_x/mc
0
x
1000
(e)
$f(p_x)$
0
25
50
p_x/mc

FIG. 18

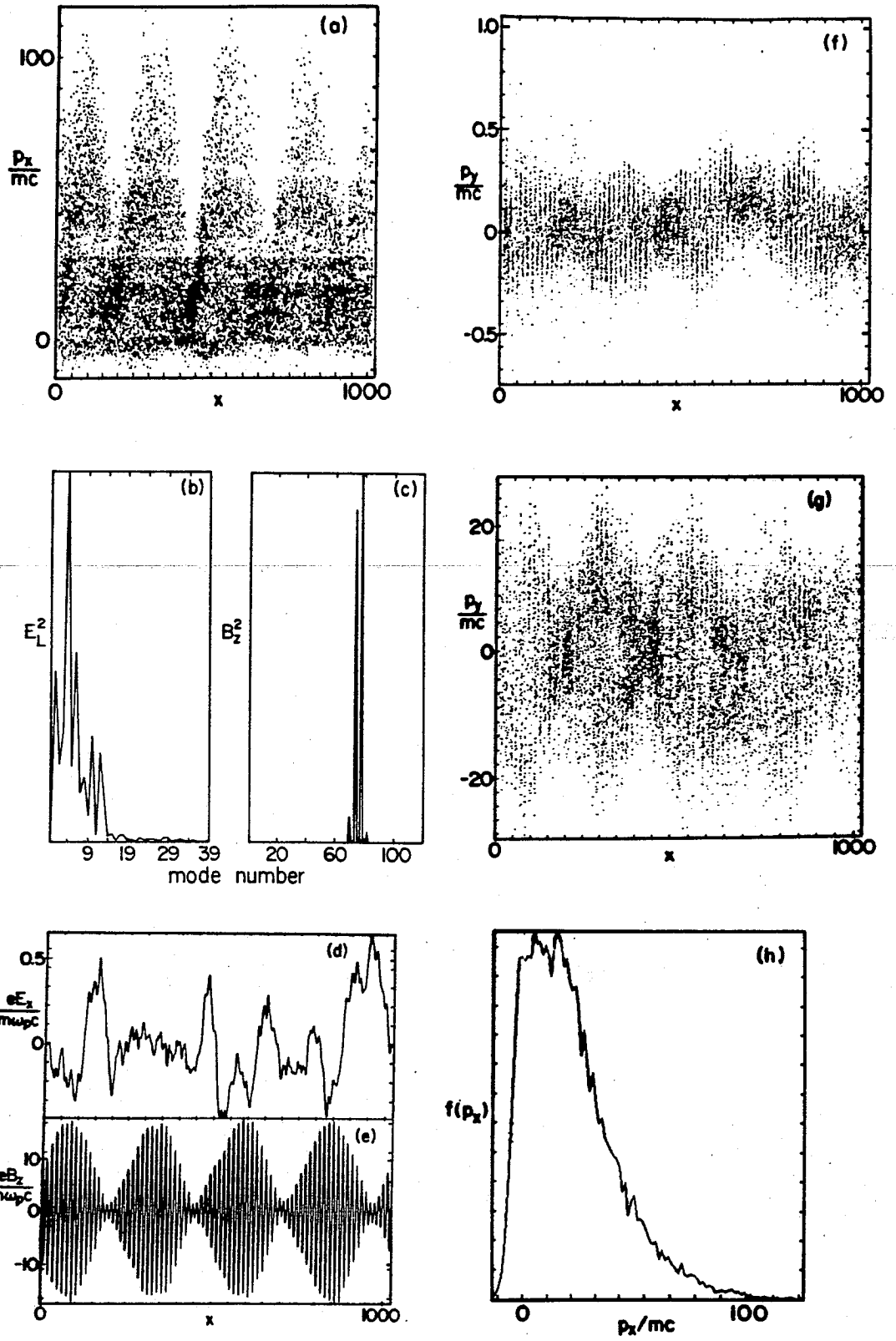
(a)
100
$\frac{p_x}{mc}$
0
0
x
1000
(f)
1.0
0.5
$\frac{p_y}{mc}$
0
-0.5
0
x
1000
(b)
E_L^2
9 19 29 39
(c)
B_z^2
20 60 100
mode number
(g)
20
$\frac{p_y}{mc}$
0
-20
0
x
1000
(d)
0.5
$\frac{eE_x}{m\omega_p c}$
0
(e)
10
$\frac{eB_z}{m\omega_p c}$
0
-10
0
x
1000
(h)
$f(p_x)$
0
100
p_x/mc

FIG. 19

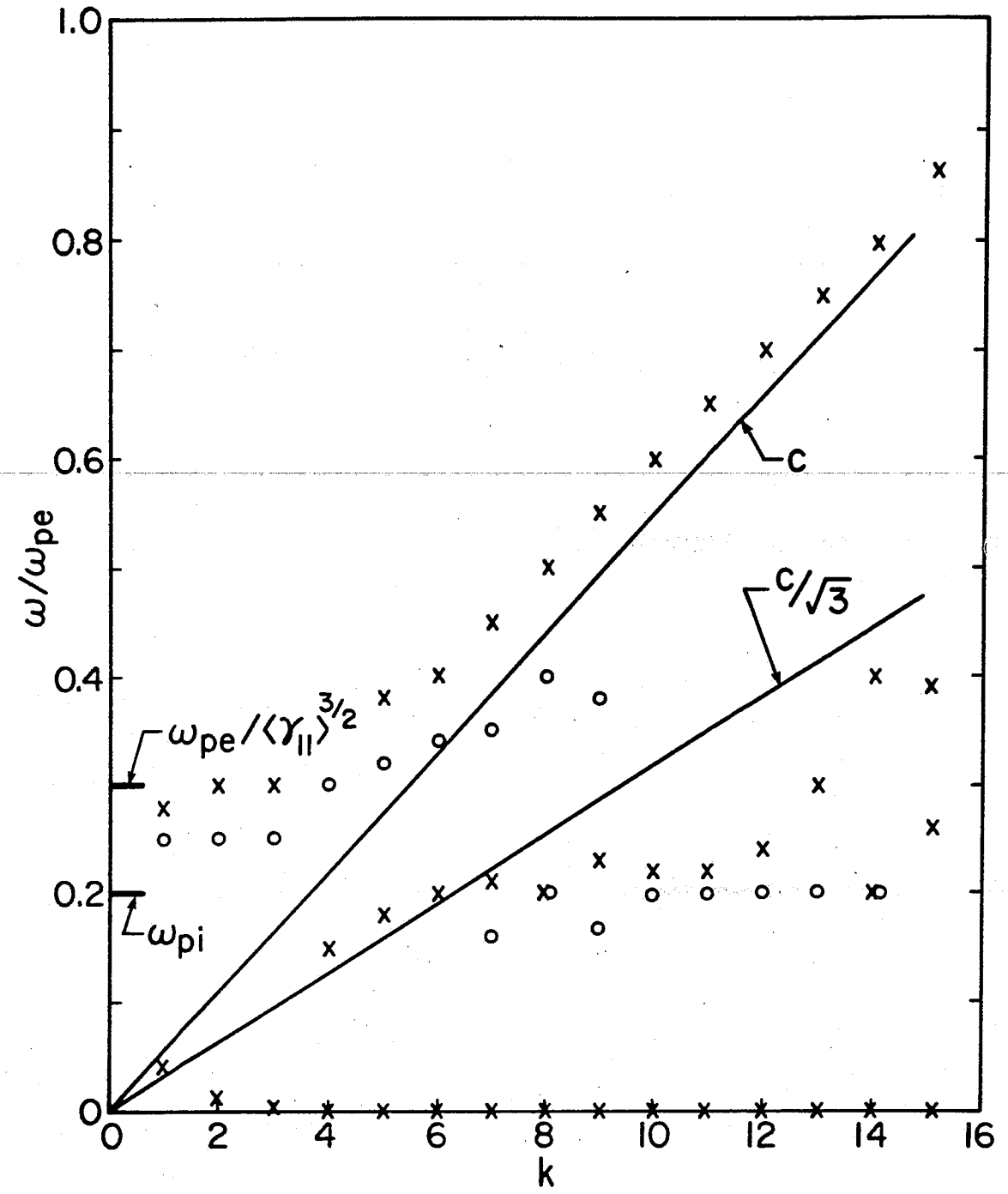

FIG. 20

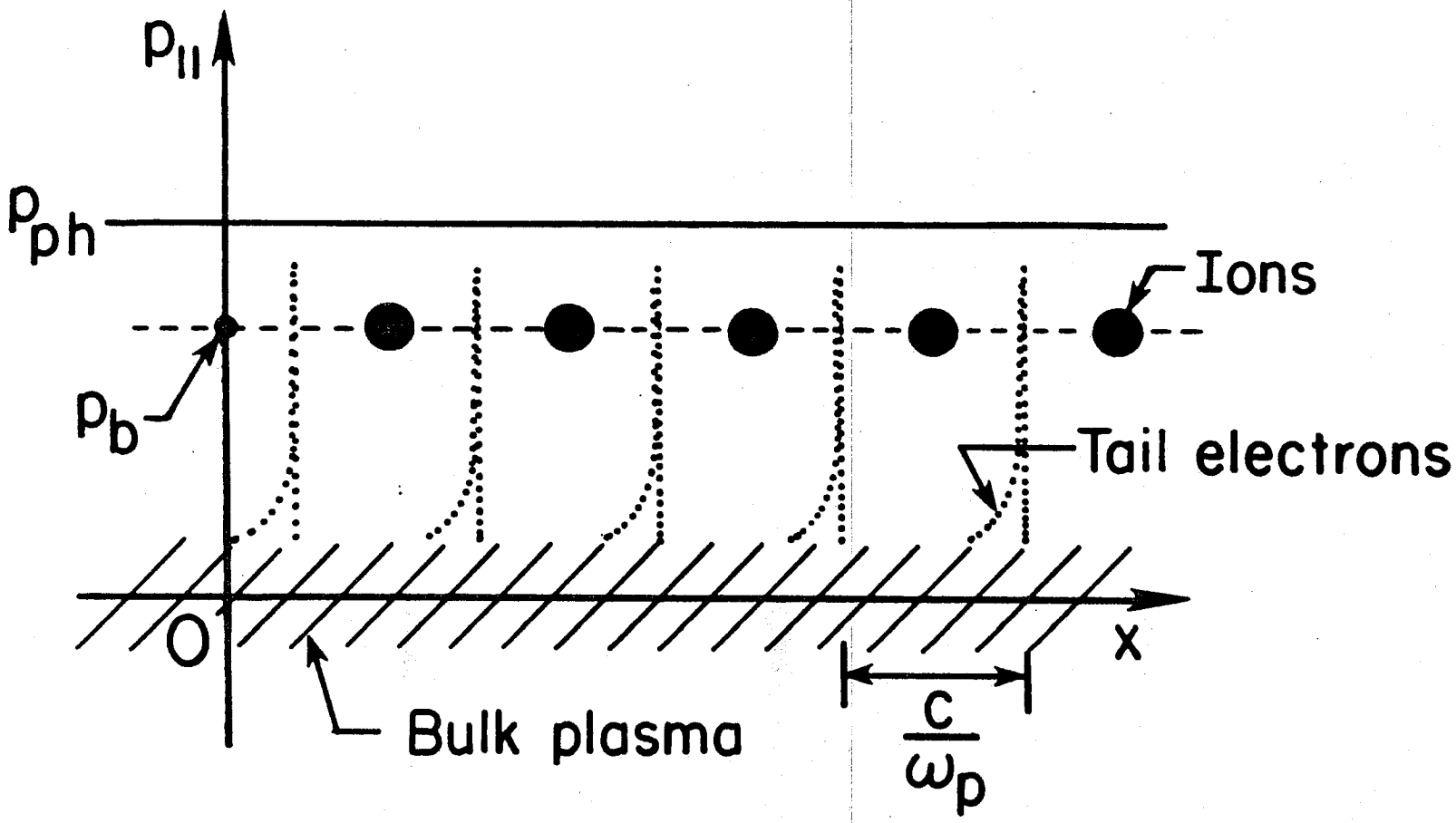
$p_{\parallel}$
p_{ph}
p_b
Ions
Tail electrons
O
x
Bulk plasma
$\frac{c}{\omega_p}$

FIG. 21

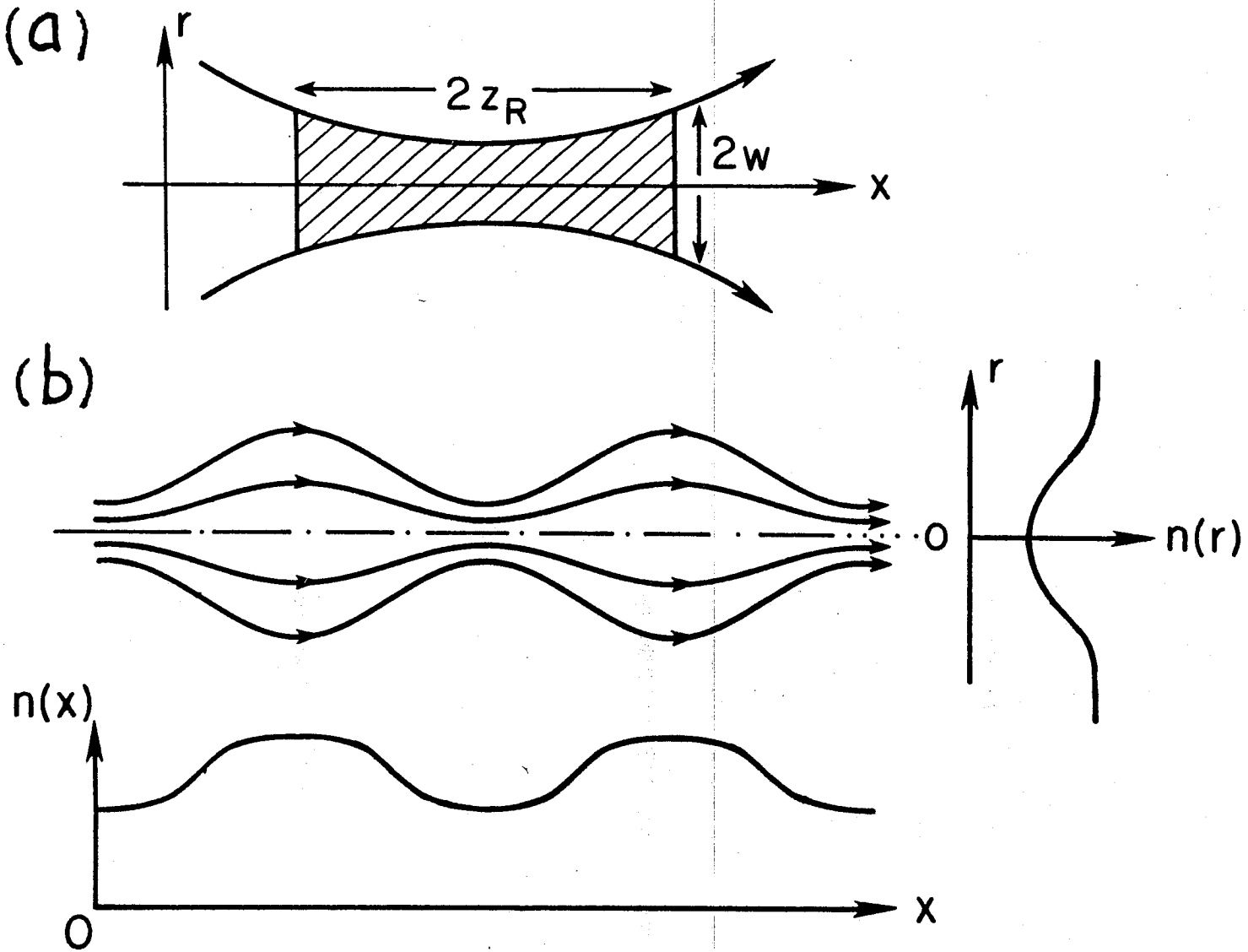

FIG. 22

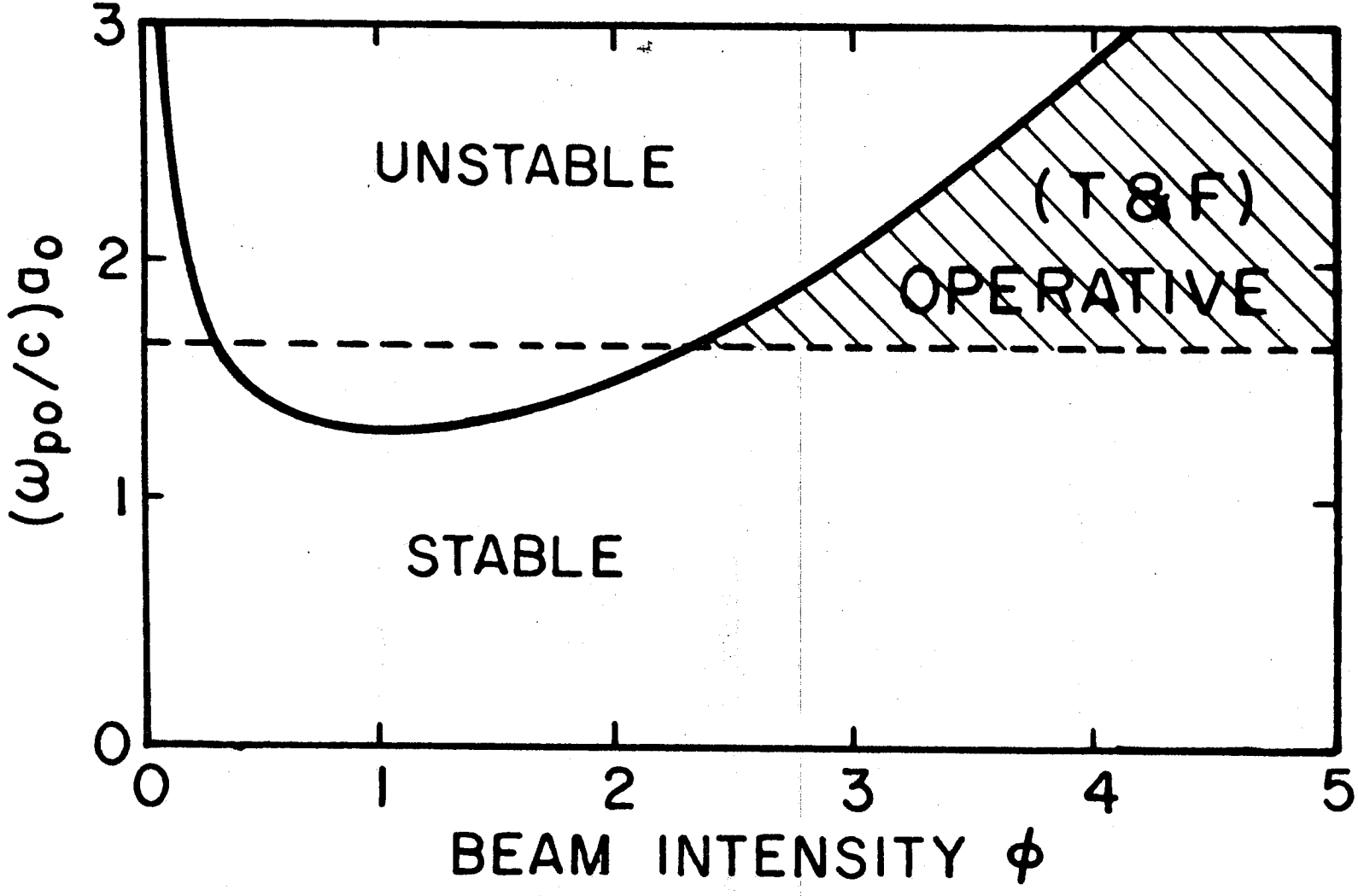
UNSTABLE
(T&F)
OPERATIVE
STABLE
$(\omega_{po}/c)a_o$
BEAM INTENSITY ϕ
0
1
2
3
4
5

FIG. 23

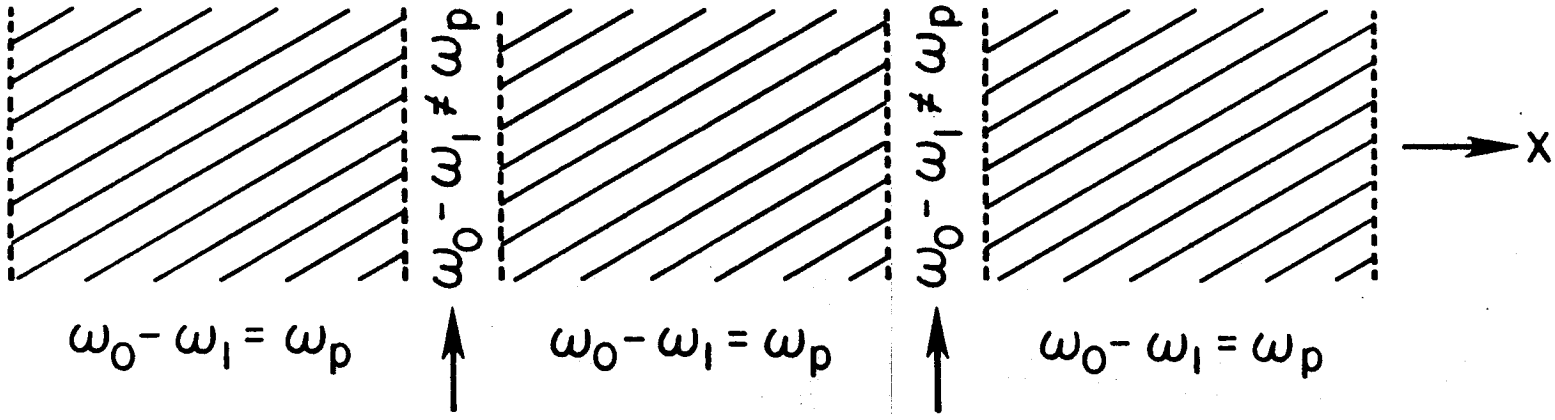
$\omega_0 - \omega_1 \neq \omega_p$
$\omega_0 - \omega_1 \neq \omega_p$
X
$\omega_0 - \omega_1 = \omega_p$
$\omega_0 - \omega_1 = \omega_p$
$\omega_0 - \omega_1 = \omega_p$
Here either wave phase advances or retards to adjust.

FIG. 24

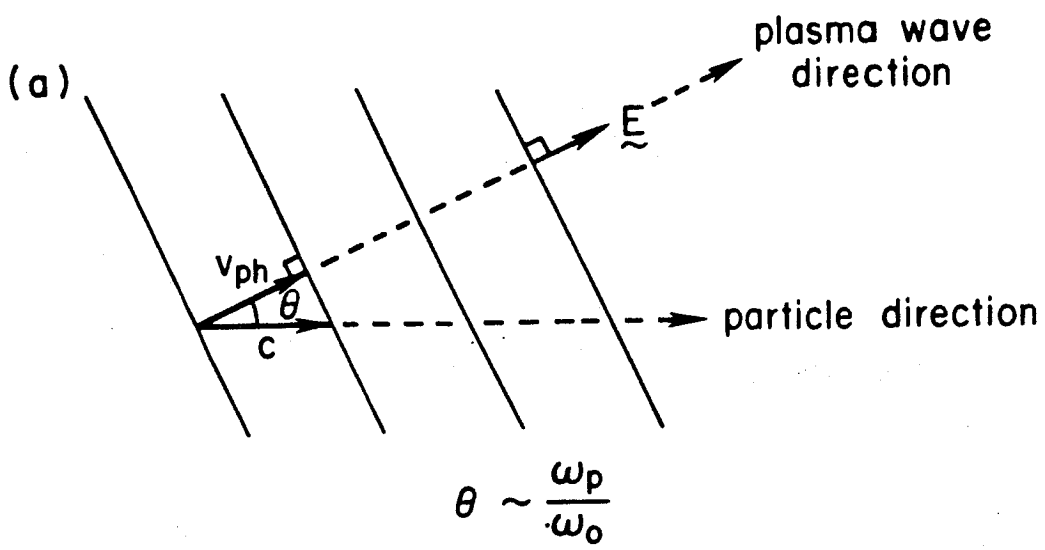

$$\theta \sim \frac{\omega_p}{\omega_o}$$

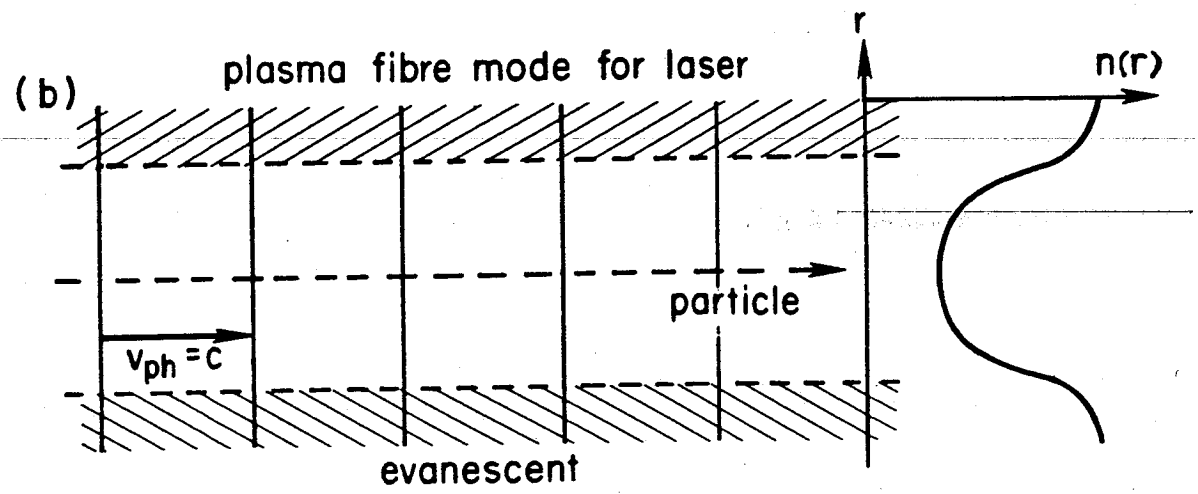

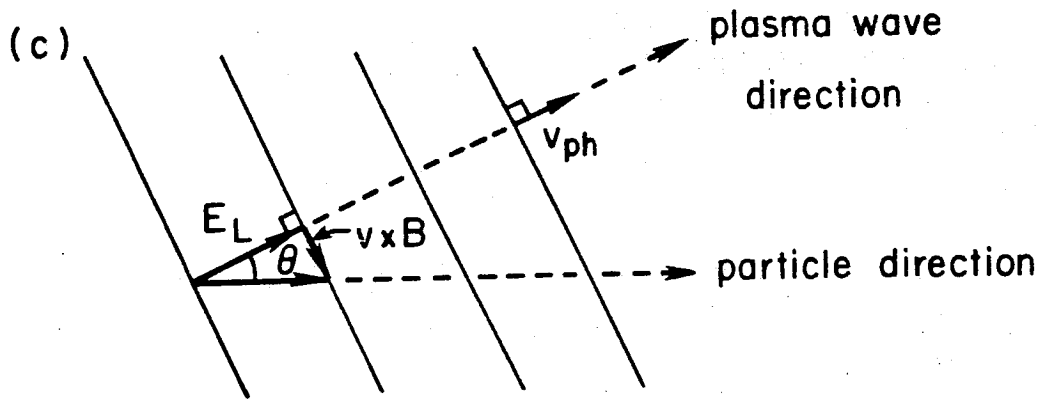

$$\frac{B}{E_L} \sim \frac{\omega_p}{\omega_o}$$

FIG. 25

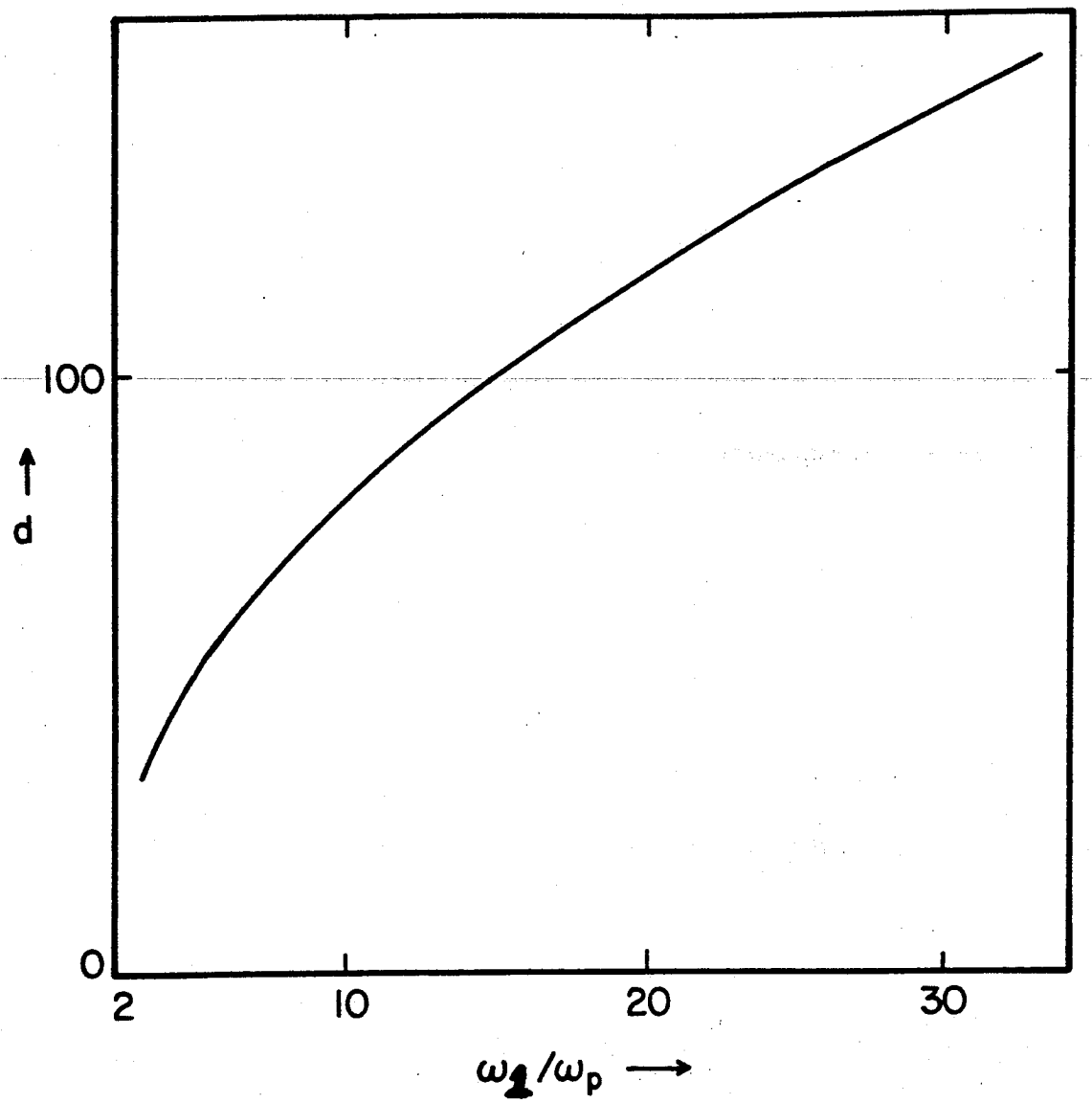

FIG. 26

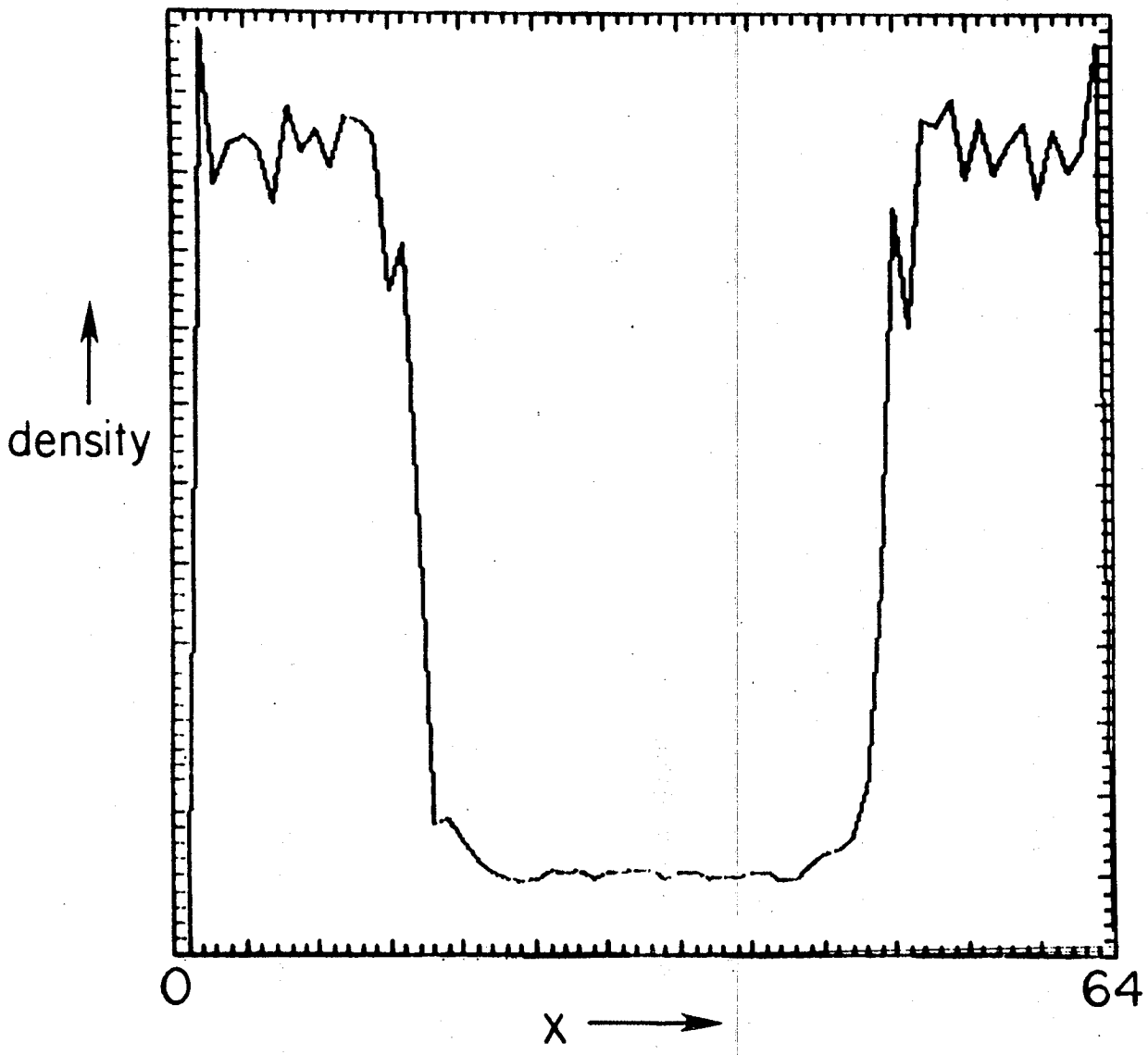

FIG. 27

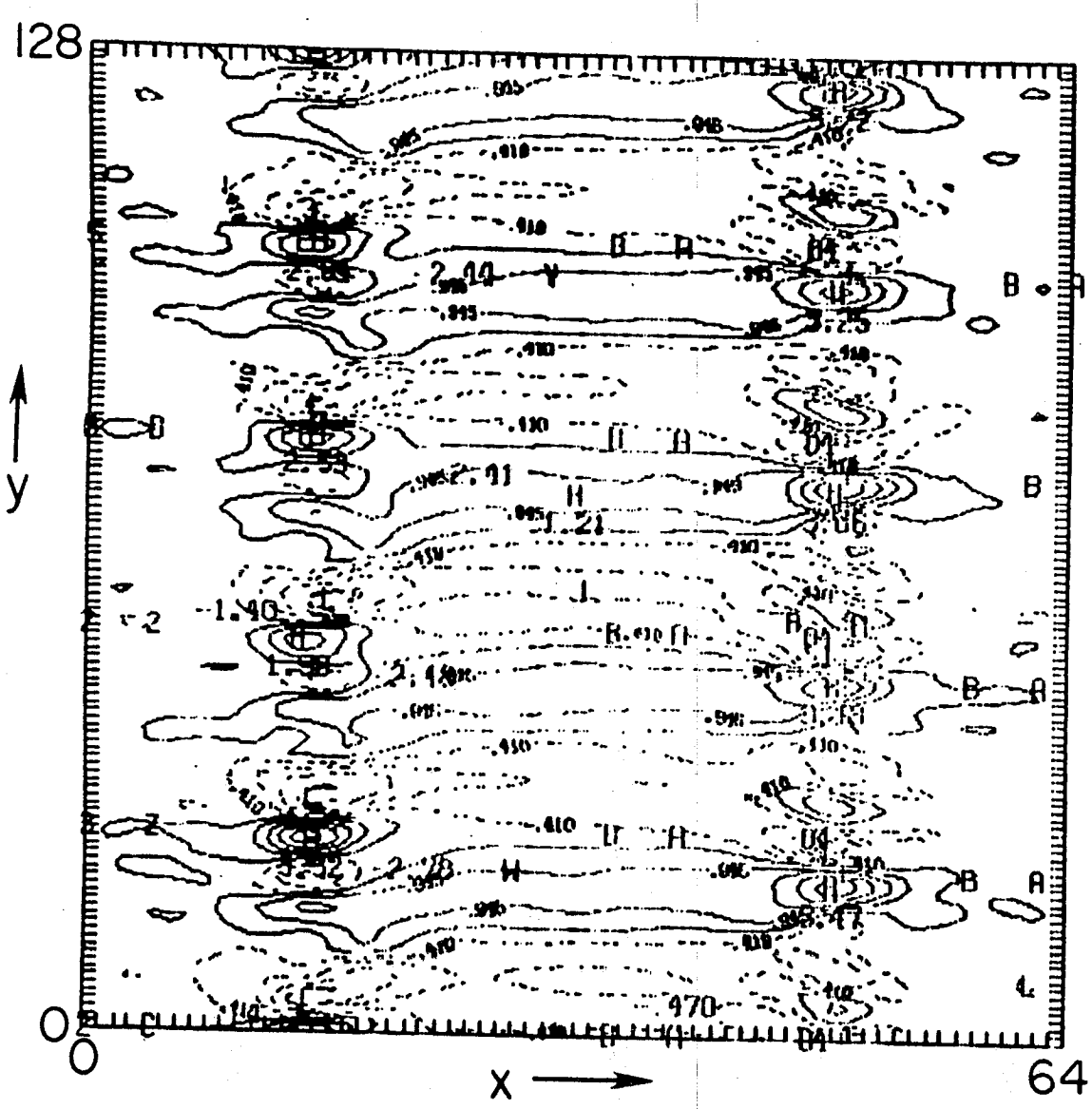

FIG. 28

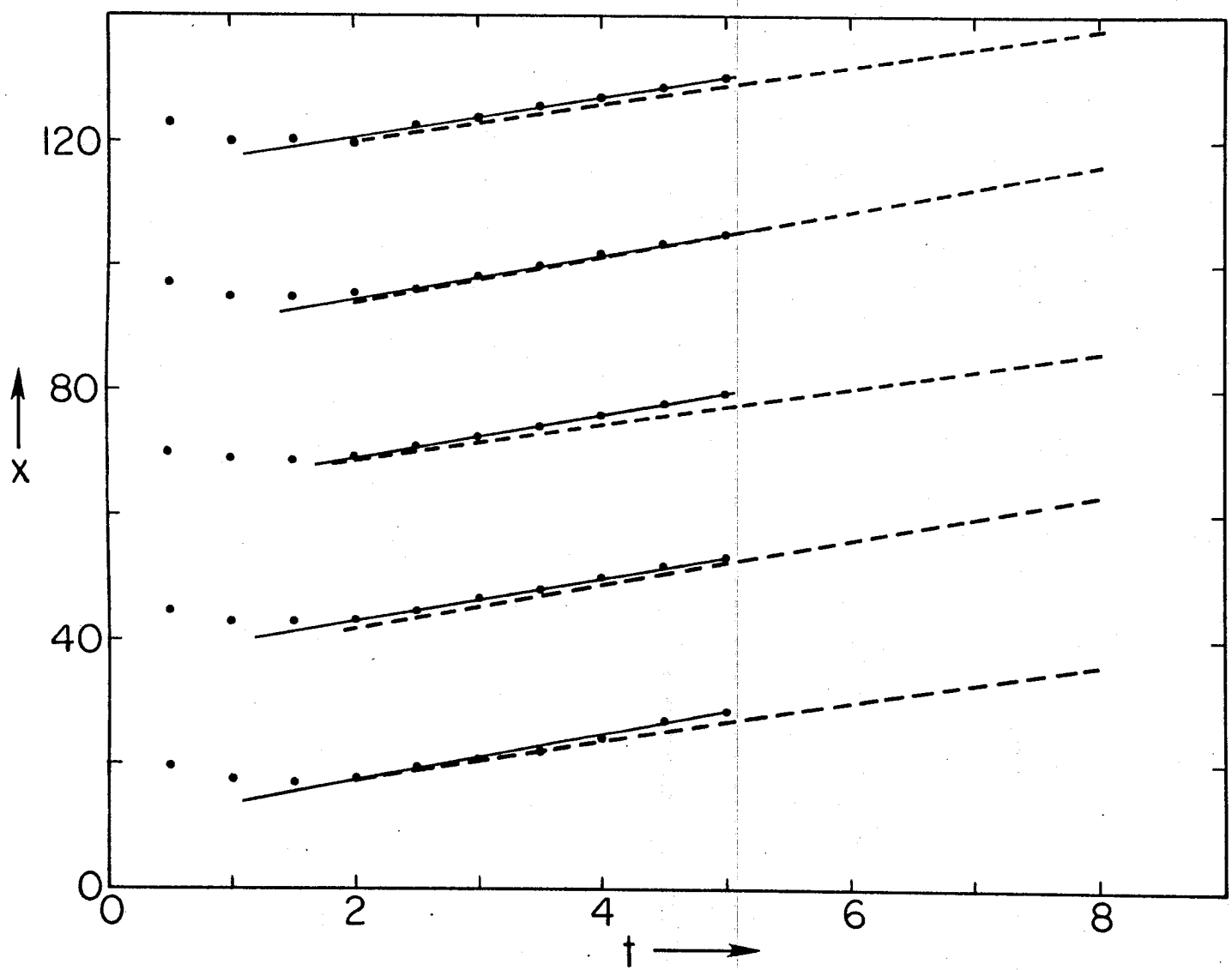

FIG. 29

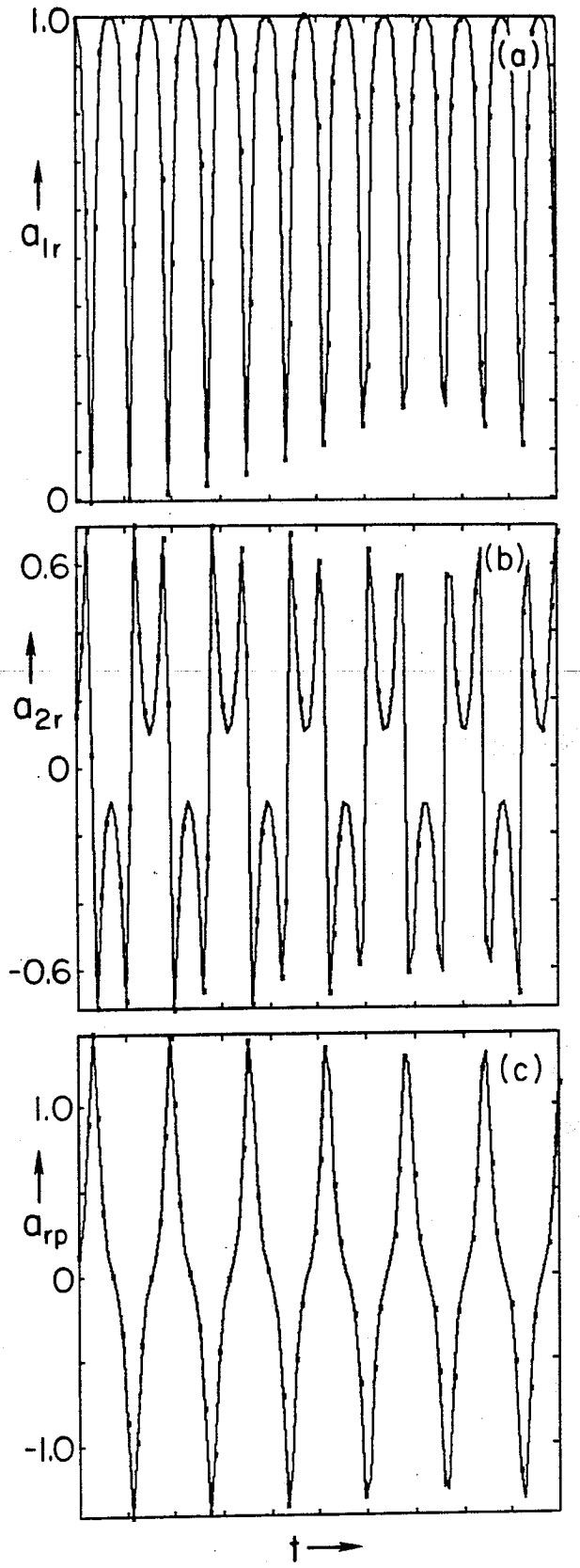

FIG. 30

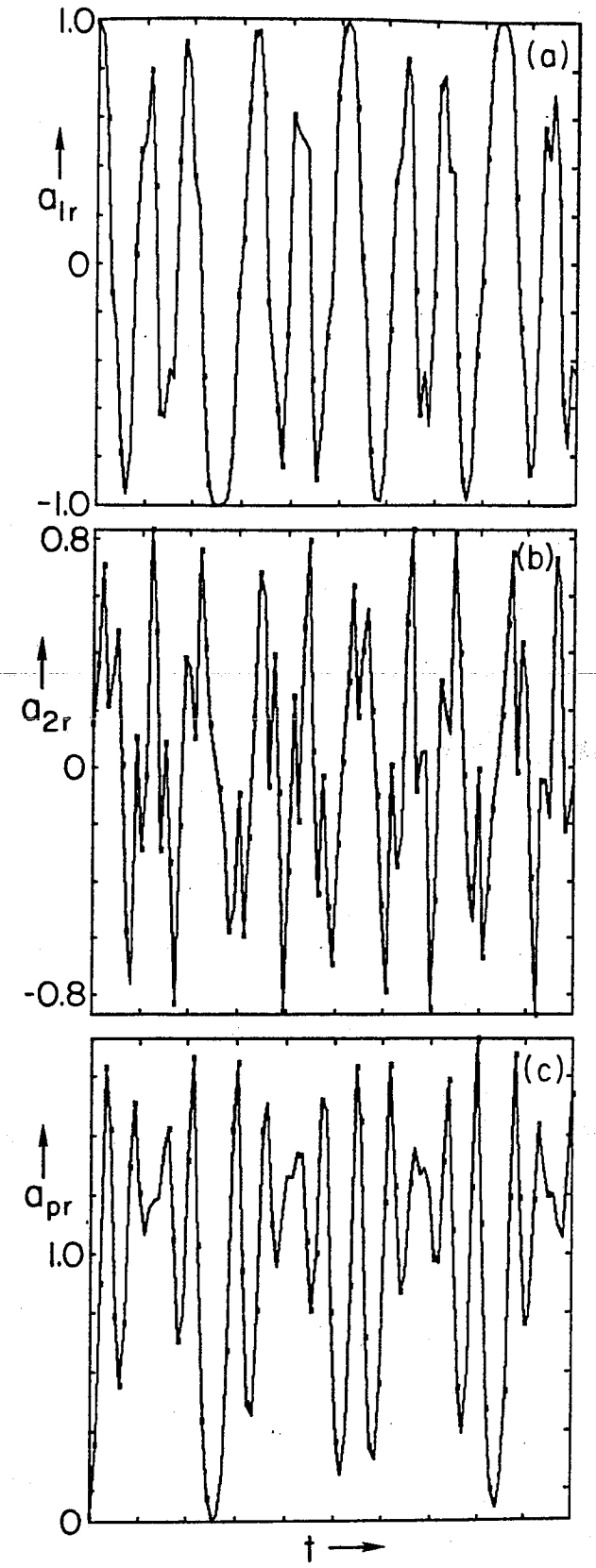

FIG. 31

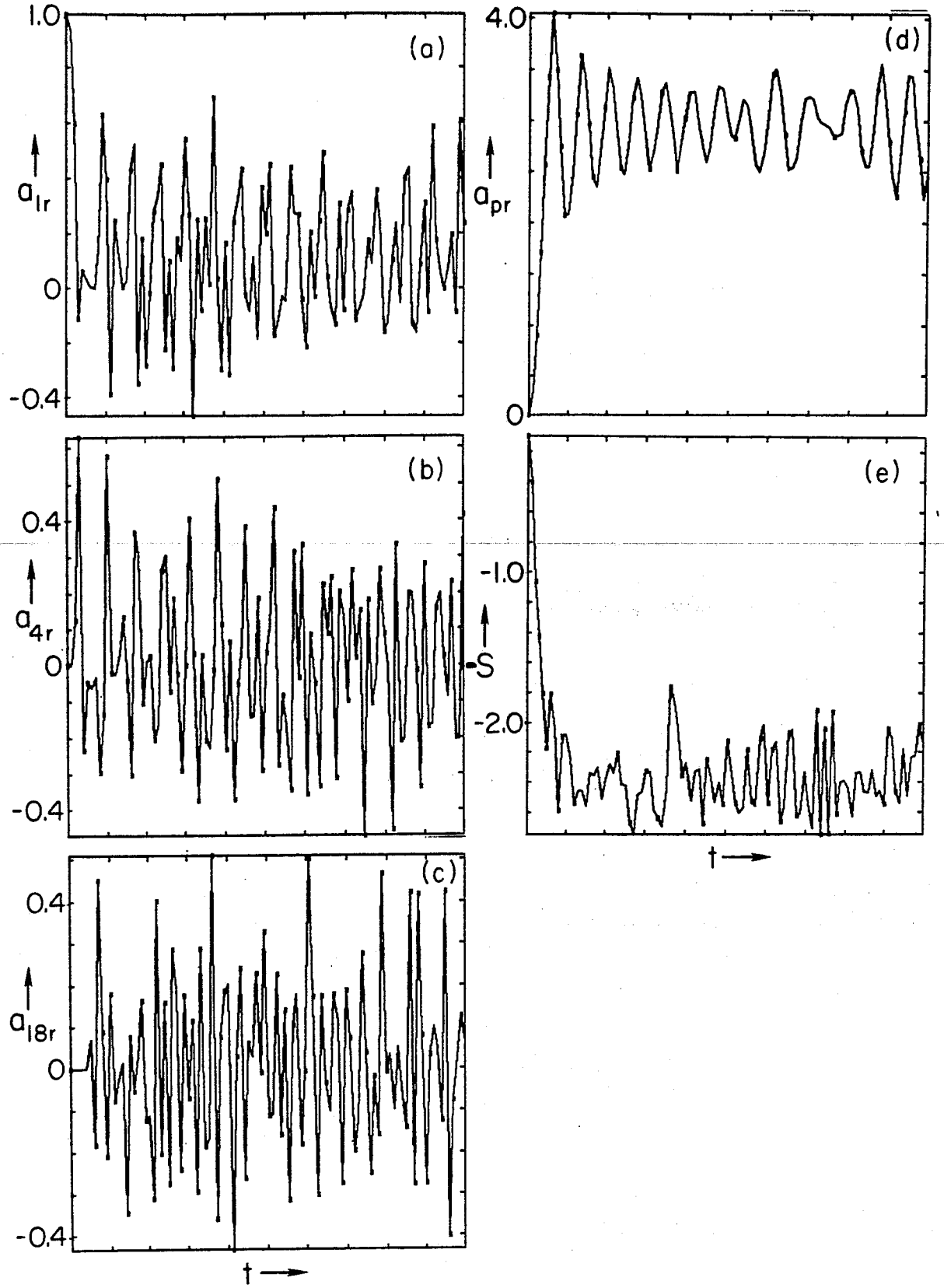

FIG. 32

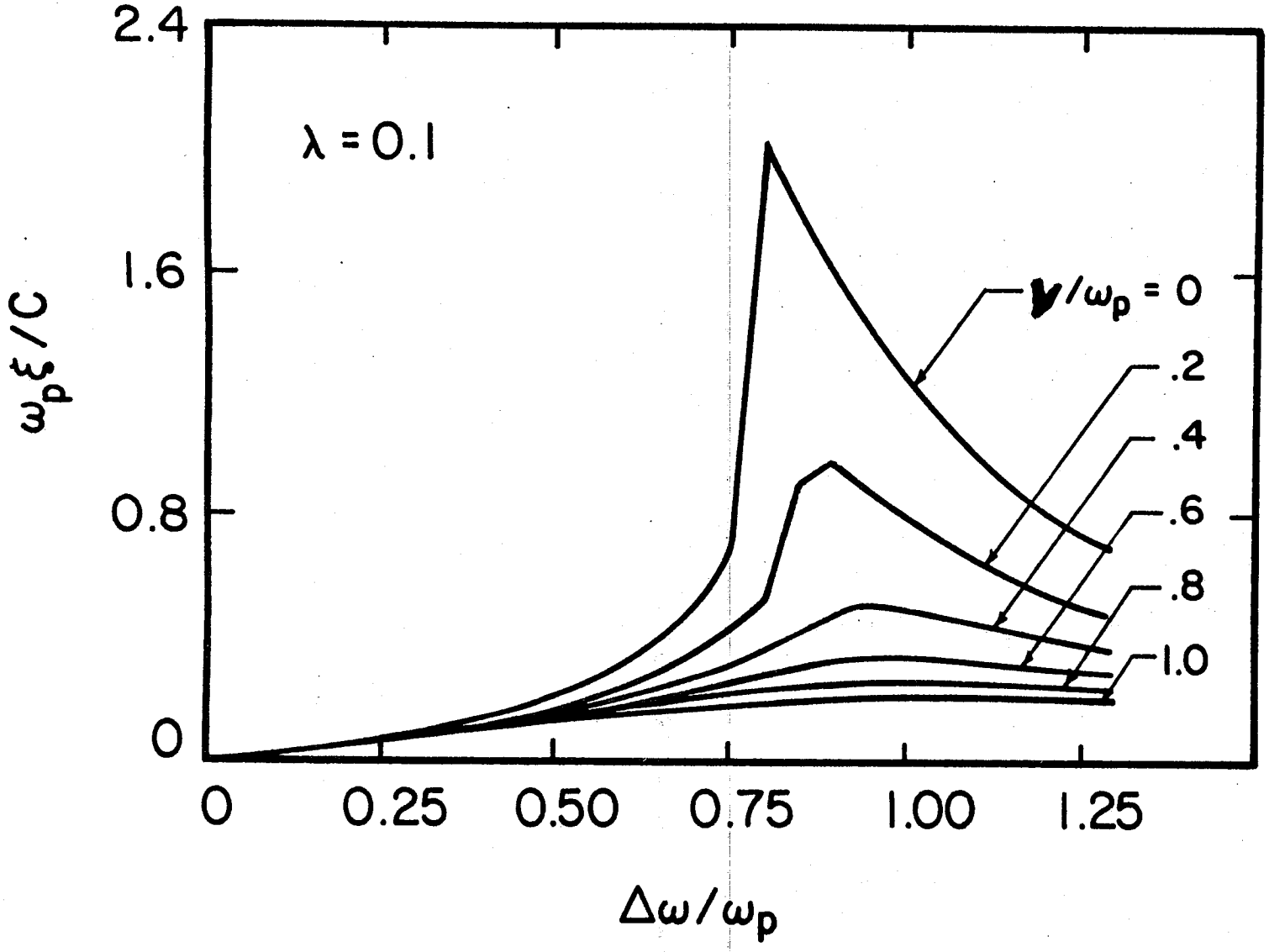

FIG. 33

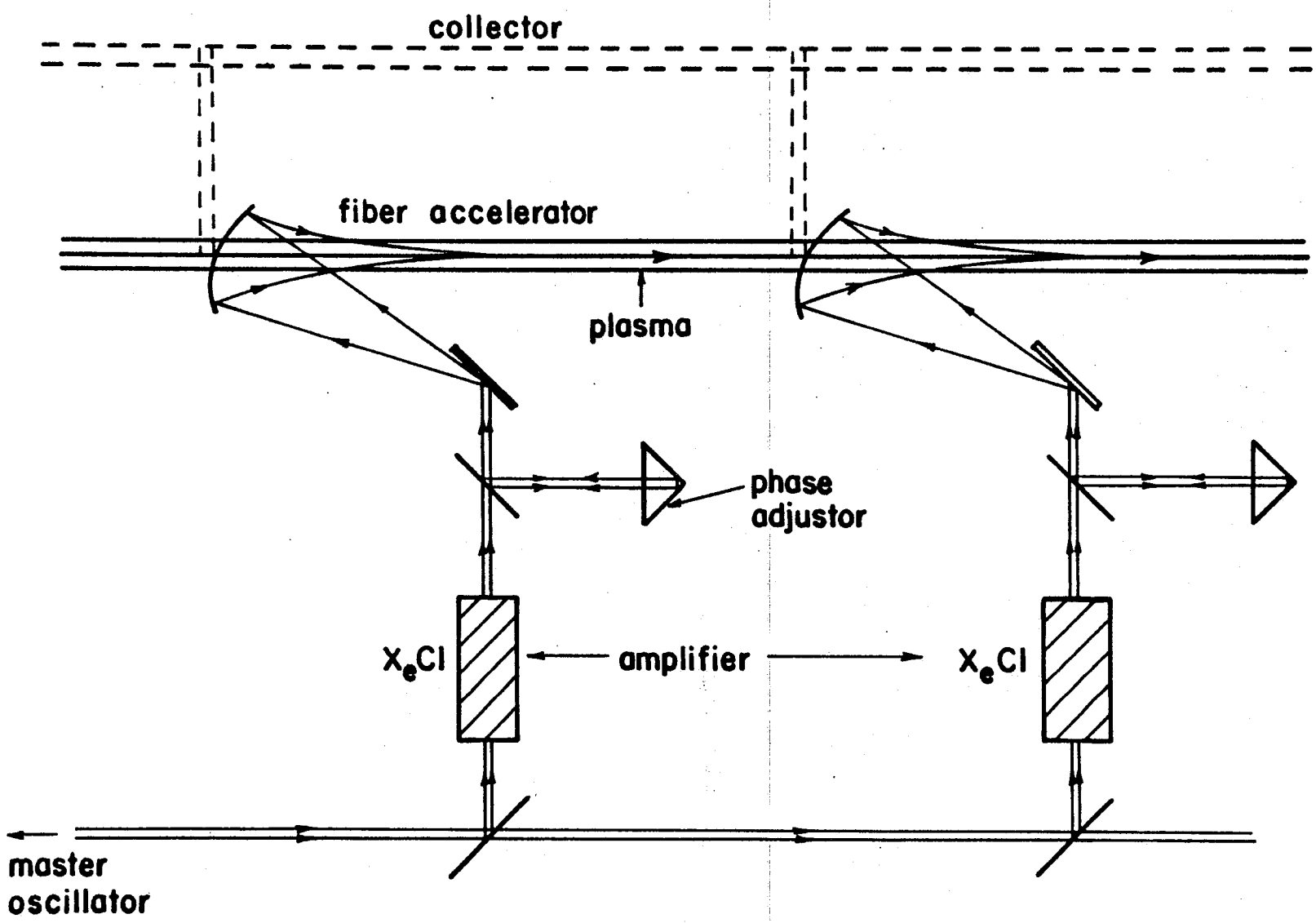
collector
fiber accelerator
plasma
phase
adjustor
X_eCl
amplifier
X_eCl
master
oscillator

FIG. 34

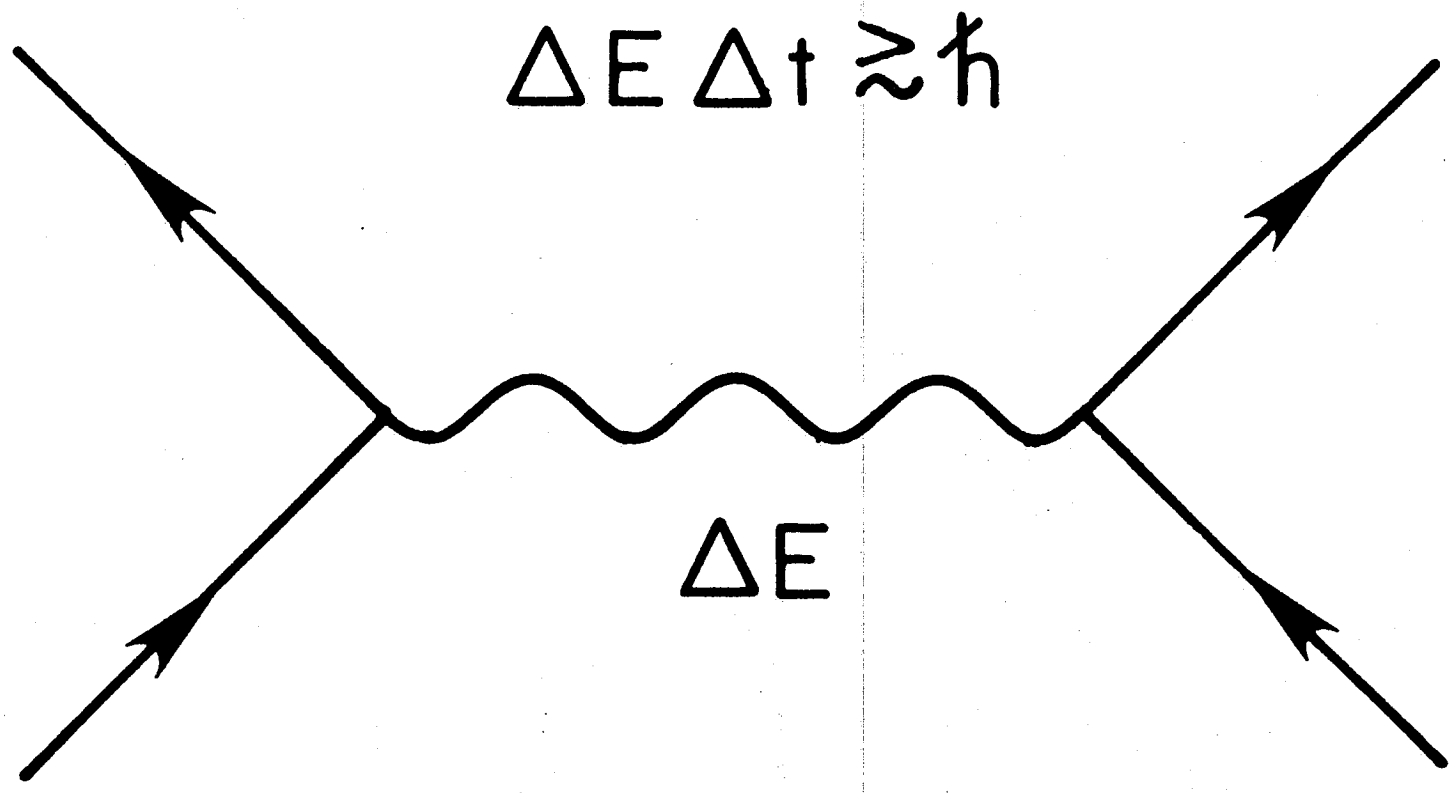

$$\sigma(\Delta E \to \infty) \propto \frac{1}{E_{cm}^2}$$

FIG. 35

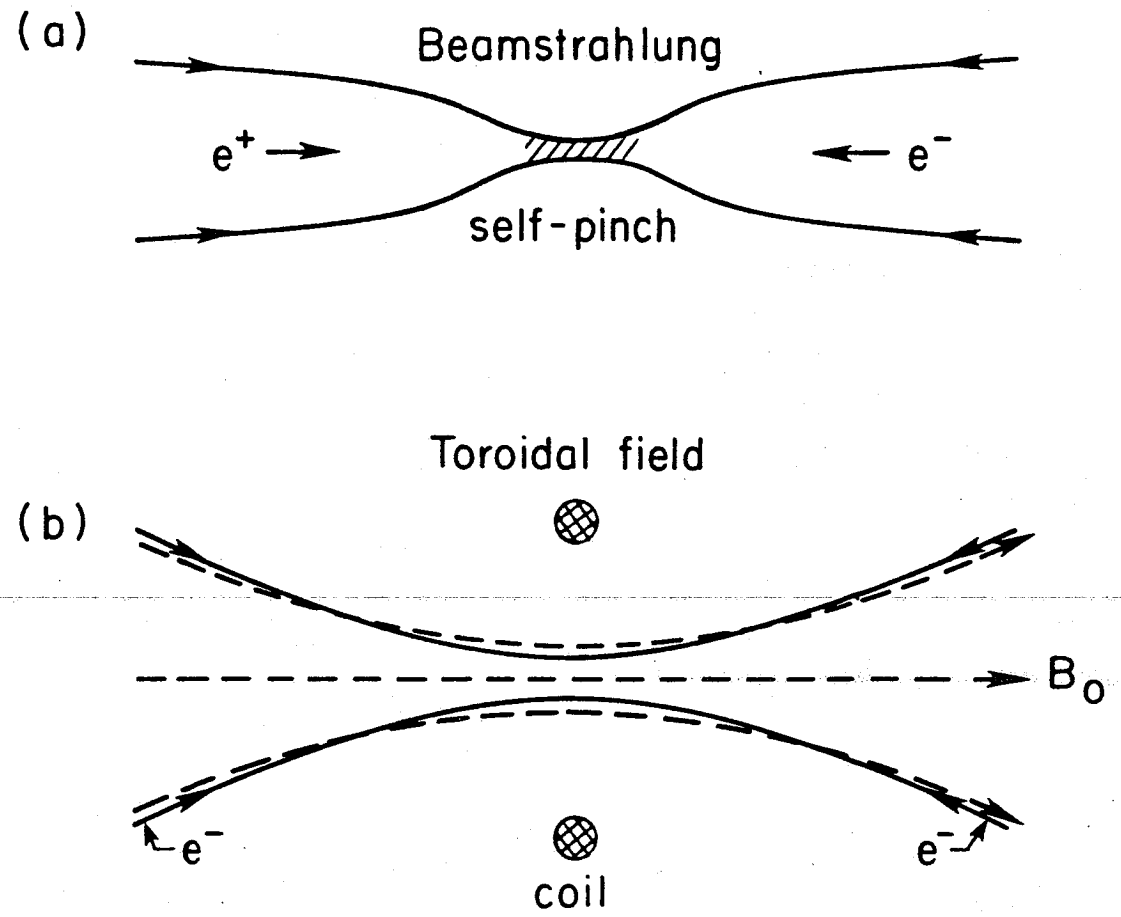
(a)
Beamstrahlung
e+
e-
self-pinch
Toroidal field
(b)
Bo
e-
e-
coil
(c)
e- Spin magnetization
e+
e-

FIG. 36

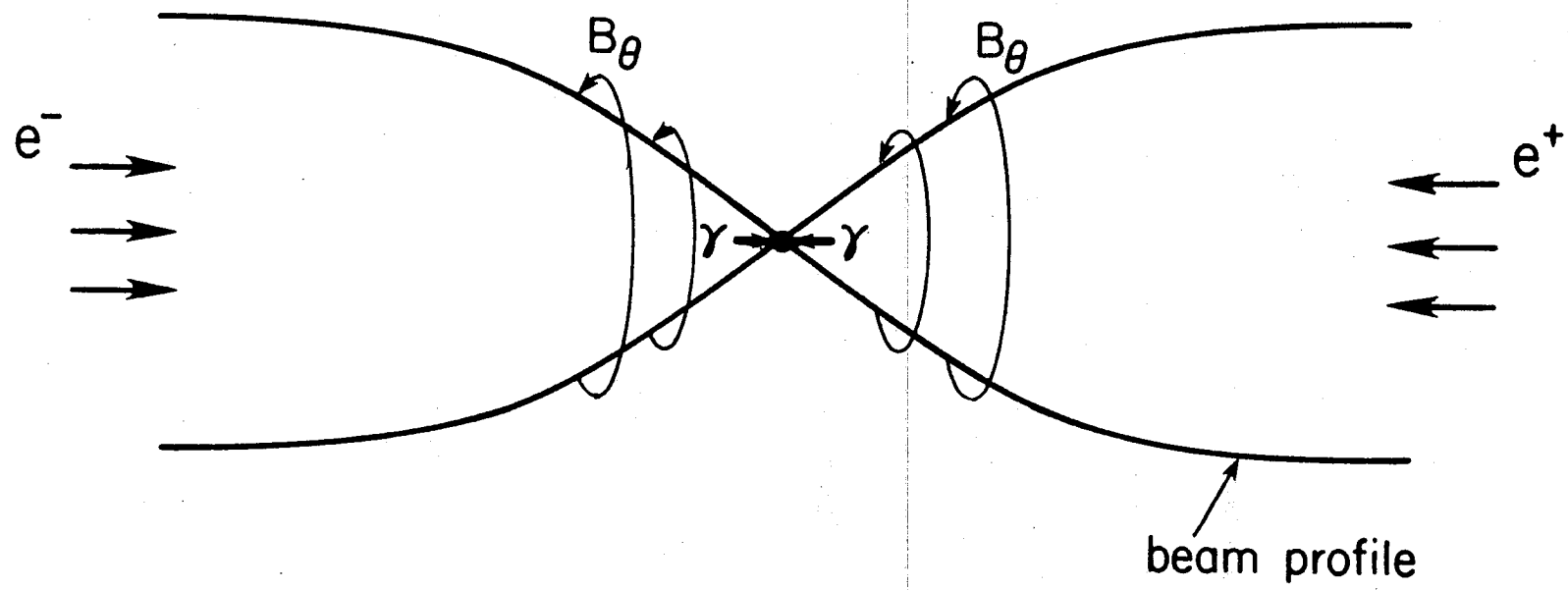

FIG. 37

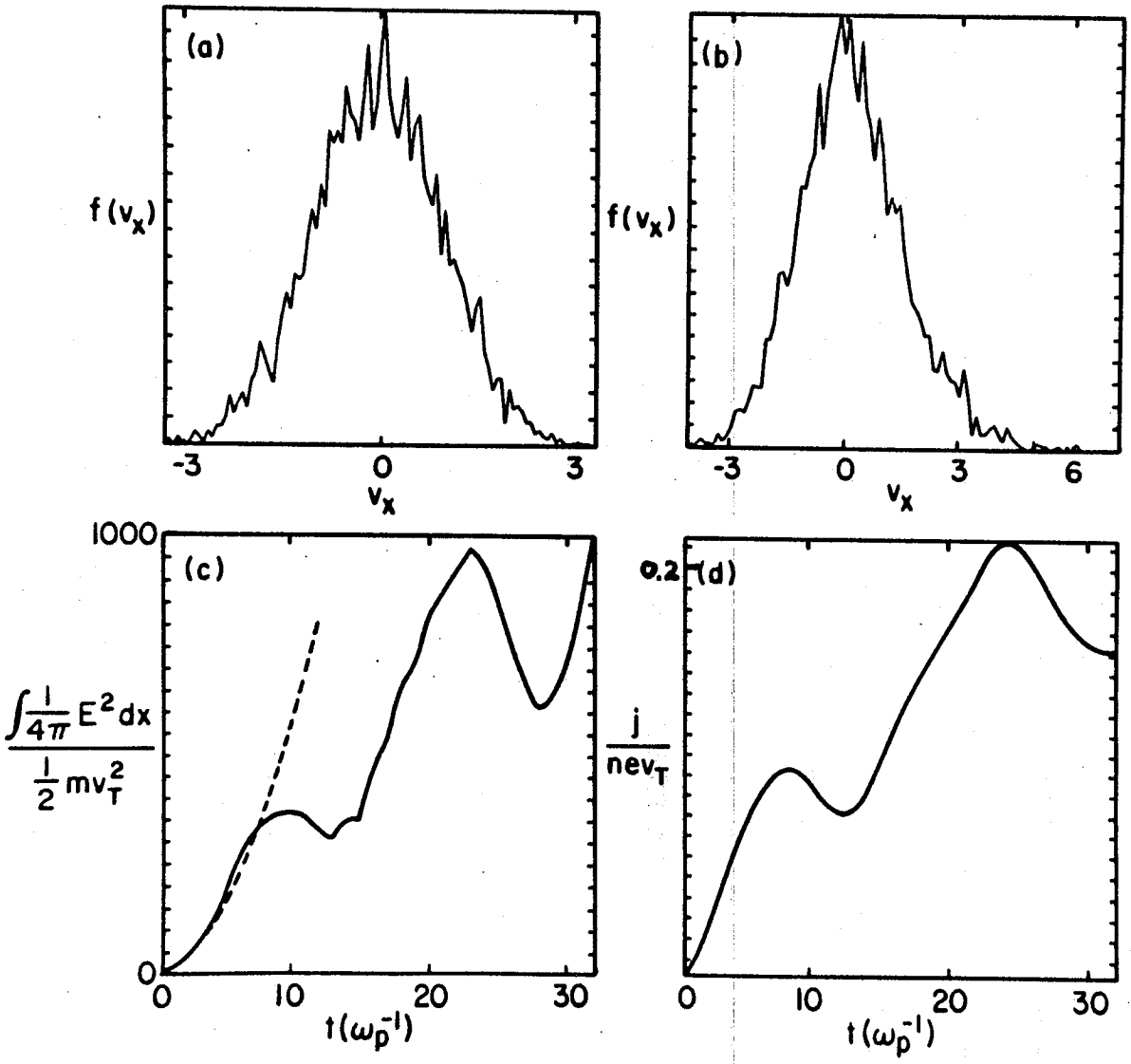
(a)
f(v_x)
-3
0
3
v_x
(b)
f(v_x)
-3
0
3
6
v_x
1000
(c)
∫(1/4π) E² dx / (1/2) m v_T²
0
0
10
20
30
t(ω_p⁻¹)
0.2
(d)
j / nev_T
0
10
20
30
t(ω_p⁻¹)

FIG. 38